PhD degree in Molecular Medicine

European School of Molecular Medicine (SEMM),

University of Milan and University of Naples "Federico II"

Faculty of Medicine

Settore disciplinare: BIO/10

Mechanisms mediating replication fork collapse and processing in checkpoint defective cells.

Arianna Colosio

IFOM-IEO Campus, Milan

Matricola n. R08896

Supervisor: Prof. Marco Foiani

IFOM-IEO Campus, Milan

Added Supervisor: Dr. Rodrigo Bermejo,

IBFG, Salamanca; IFOM-IEO Campus, Milan

Anno accademico 2012-2013

Table of contents

FIGURES INDEX

TABLE INDEX

LIST OF ABBREVIATIONS

2D gel Two dimensional agarose gel electrophoresis

BIR Break Induce Replication

BSA Bovine Serum Albumin

DSB Double Strand Break

EDTA Ethylen Diammino Tetraacetic Acid

HR Homologous Recombination

RT Room Temperature

O/N Over Night

SCJ Sister Chromatid Junctions

SDS Sodium Dodecyl Sulphate

SSA Single Strand Annealing

SSC Sodium Chloride Sodium Citrate

ssDNA Single Strand DNA

TBE Tris Borate EDTA

TE Tris EDTA

YPA Yeast extract Peptone Adenine

RFs Reversed forks

HJs Hollyday Junctions

bp base pairs

ARS Autonomous Replicating Sequence

ORC Orogin Recognition Complex

RNAP RNA polymerase

HU Hydroxyurea

1. ABSTRACT

An accurate DNA replication is essential to prevent genome instability events, such as mutations and chromosomal rearrangements that are hallmarks of neoplastic transformation and cancer onset. A dedicated branch of the DNA damage checkpoint maintains the integrity of replicating chromosomes by stabilising replication forks in the presence of genotoxic agents, thus ensuring cell viability. Upon fork collapse, budding yeast checkpoint mutants experiencing replication stress accumulate aberrant replication intermediates, such as gapped and hemireplicated molecules, as well as four-branched structures known as reversed forks. Aberrant replication intermediates are potentially harmful for the cells since they are thought to trigger unscheduled recombination events that cause genome rearrangements. In this PhD thesis, I examined checkpoint-dependent mechanisms controlling fork stability, and I provide *in vivo* evidence that positive supercoiling accumulating ahead of replication forks is the main mechanical force driving fork reversal. Thus, DNA topology is a critical determinant of replication fork stability *in vivo*. Furthermore, a 2D-gel screening for enzymatic activities involved in the metabolism of collapsed forks, revealed a novel role for the Sae2 and Dna2 endonucelases in replication intermediates processing.

2. INTRODUCTION

2.1 The yeast *Saccharomyces cerevisiae* cell cycle and the DNA damage checkpoint.

The cell cycle is an ordered succession of events that subsequently occur with the final goal of proliferation. During the cell cycle from a mother cell two daughter cells are generated, that possess all the information to repeat the process. Thus, during cell division, all cellular components must be duplicated and transmitted correctly to the newborn cell. The most important element is the genetic information, which must be accurately duplicated in a process called DNA replication. The two copies are then segregated carefully to the two daughter cells. DNA synthesis and chromosome segregation take place in two distinct phases of the cell cycle, the first during S-phase, while the latter occurs during mitosis (or M phase), where the cells physically divide in a process termed cytokinesis. Those two phases are separated by two additional gap phases, called G1 and G2, in which cells undertake all the metabolic reactions necessary for the next cell cycle stage (Figure 1). The cell cycle can be therefore divided in four phases: the G1, in which the synthesis of cytoplasmatic proteins takes place, the S-phase of DNA replication, the G2 phase, in which the preparation of the mitotic apparatus and the synthesis of the membrane proteins occur, and the final M phase, where chromosomes segregate and cells divide.

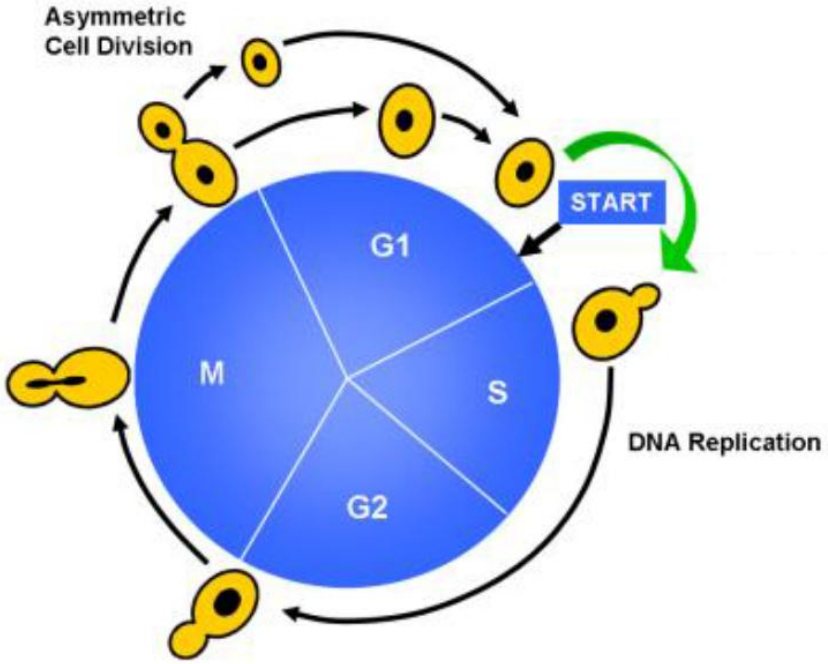

Figure 1. Schematic representation of the budding yeast mitotic cell cycle. *S. cerevisiae* cell cycle is divided into G1, S, G2 and M phases. DNA replication occurs during S-phase and at the end of the M phase the mother cell divides giving rise to two daughter cells. Each phase can be identified by analysing the cell morphology: G1 cells are characterized by an oval shape, from which at the beginning of the S-phase a bud emerges that becomes progressively elongated and grows until M-phase onset, where the division of the cells takes place.
(adapted from http://www.csb.ethz.ch/research/dynamic)

The duplication of the genetic material is a process crucial for cell life and it must be tightly regulated to prevent errors during replication or unbalanced segregation of the chromosomes that lead to mutations and chromosomal aberrations causing genetic diseases and cancer onset (Hartwell and Kastan, 1994). To preserve the integrity of the genome, cells have developed specific mechanisms of surveillance that control the order and timing of cell cycle transitions, orchestrating the cellular response to DNA damages and/or events that perturb replication, referred to as DNA damage checkpoint (Hartwell and Weinert, 1989; Elledge, 1996). The checkpoint pathways were initially

described as limited to the transduction of a signal required to arrest the cell cycle progression, thus providing time for the cells to repair DNA lesions (Hartwell and Weinert, 1989). However, the current believe is that the checkpoint acts as a much more complex response that cooperates with multiple cellular pathways to modulate the cellular physiology with the final objective to sustain cell viability and genome integrity (Branzei and Foiani, 2009; Labib and De Piccoli, 2011). The checkpoints pathway is very well conserved throughout eukaryotes and acts in different phases of the cell cycle: in late G1, in S and in G2/M.

2.2 DNA replication.

DNA replication, occurring in the S-phase of the cell cycle, is a semi-conservative process, since each strand of the double helix serves as a template for the synthesis of a complementary strand. Thus, the final product of this process are two identical double stranded helices, each of the two composed by a parental strand and a newly synthetised one.

In budding yeast DNA replication begins at specific chromosomal regions, named Origins of Replication. Each replication origin is specified by a conserved region of 100-200 base pairs (bp) named autonomous replicating sequence (ARS), which serves as binding site for the Origin Recognition Complex (ORC) that promotes the recruitment of additional factors that start

replication (Bell et al., 1993). Architectural studies revealed that each ARS is characterized by a modular structure of three elements essential for ARS functioning (Dubey et al., 1996): domain "A", consisting of 11-bp consensus sequence known as ACS (ARS consensus sequence), essential for activation and recognised by ORC; as well as domain "B", which is more variable and constitutes the region for DNA unwinding and domain "C", that contains sites for the binding of transcription factors (Bell et al., 1993). In contrast to yeast, replication origins in higher eucaryotes are not so well defined and they do not seem to require specific sequences for initiation. However, despite some differences, the mechanisms and the molecules ensuring a correct replication initiation have been conserved throughout evolution (Errico et al., 2010).

To duplicate their rather big genomes in a limited time, eukaryotic cells have developed mechanisms that allow the initiation of replication from multiple sites, leading to the establishment of several individual replicons that are activated during S-phase. This mechanism is finely regulated to guarantee that the duplication of each part of the genome occurs only once every round of cell cycle. This temporal regulation enabled the characterisation of the replication origins according to the time of their firing: "early replication origins" are activated in the early S-phase, while "late replication origins" are fired later (Raghuraman et al., 2001). Furthermore, some late origins might be activated exclusively under specific situations, such as the dormant replication origins, that are fired only in the presence of damages or, alternatively, they remain silent (Diffley and Labib, 2002).

In budding yeast, origin firing is a multi-step process, orchestrated by the cyclin dependent kinase Cdc28 and the B-type cyclins (Clbs) (Dutta et al., 1997). DNA synthesis requires the binding of the ORC complex to the origins of replication (Bell and Stillman, 1992). The ORC complex is composed by six proteins, named Orc1-6 and "marks" the origins, remaining attached to them during the entire cell cycle. This complex acts as an initiation factor to recruit additional proteins, such as Cdc6 (Cocker et al., 1996), the "origin loading factor" essential for the binding to the origin of the helicase Minichromosome Maintainance Complex (MCM). Those factors together with additional components such as Cdc45, form the "pre-replicative complex" (Santocanale and Diffley, 1996; Santocanale and Diffley, 1997). Pre-replicative complex formation depends on the inactivation at the end of mitosis of Clb-Cdc28 kinase and cannot occur until Clbs are degraded. Thus, it is permitted to occur once per cell cycle since Clb-Cdc28 triggers initiation and also prevents re-replication by blocking the assembly of new complexes. At the very end of G1 phase, Clb-Cdc28 kinase activation changes the conformation of the pre-replicative complex, forming the pre-initiation complex (Zou and Stillman, 1998). Then, protein kinase Cdc7/Dbf4 – dependent phosphorylation of the MCM complex is required to activate the origin and the MCM complex facilitates the loading of the initiation complex (Mimura and Takisawa, 1998), including primase and DNA polymerase α. The initiation complex forms in turn the replication bubble, allowing the unwinding of DNA mediated by the MCM complex (Asparicio et al., 1997) and replication can start.

Replication is mediated by a large protein complex called replisome (Yao and O'Donnell, 2010). Upon origin activation two replication forks are established.

Replicative helicases unwind the duplex generating the free template to duplicate and the ssDNA formed in this way is covered by RPA to stabilize it and protect it from breakage. Replication forks proceed bi-directionally into flanking DNA until they encounter forks emanated from proximal origins thus engaging replication termination.

DNA synthesis is carried out continuously in the leading strand primarily by polymerase ε (Pol ε) from a single initiation event, while it is discontinuous at the lagging strand, where it is initiated by the Pol-α primase complex, formed by the RNA polymerase and the DNA polymerase α that synthesize the RNA primers and a short DNA segment, extended by Pol δ, as a succession of Okazaky fragments (Hubscher and Seo, 2001; Kunkel and Burgers, 2008). This occurs due to the anti-parallel nature of the template and the catalytic ability of the DNA polymerases to synthetise DNA exclusively in the 5' to 3' direction. A primase activity is required to synthetise RNA primers at both leading and lagging strand. As mentioned, DNA replication is a potential source of genome instability, due to the possible misincorporation of nucleotides and because DNA polymerase α is vacant of a proofreading activity. Thus, on the leading strand, Pol α is displaced by the replication factor C (RFC), proliferating cell nuclear antigen (PCNA) and Pol ε, so that a processive polymerisation complex is assembled (Kunkel and Burgers, 2008). On the lagging strand, the complex composed by Pol α and the RNA primase generates frequent RNA primers and is subsequently displaced by Pol δ through RFC and PCNA polymerase switching mechanisms that favour a processive synthesis of DNA (Burgers, 2009). During synthesis on the lagging strand, DNA polymerases δ reaches the end of a previous Okazaky fragment, marginally displacing its end into a single stranded DNA flap structure that is subsequently removed.

Furthermore, the RNA portion present in each RNA-DNA segment at Okazaky fragments needs to be eliminated to form a linear DNA duplex. Okazaky fragment processing is crucial for cell duplication and proliferation (Figure 2).

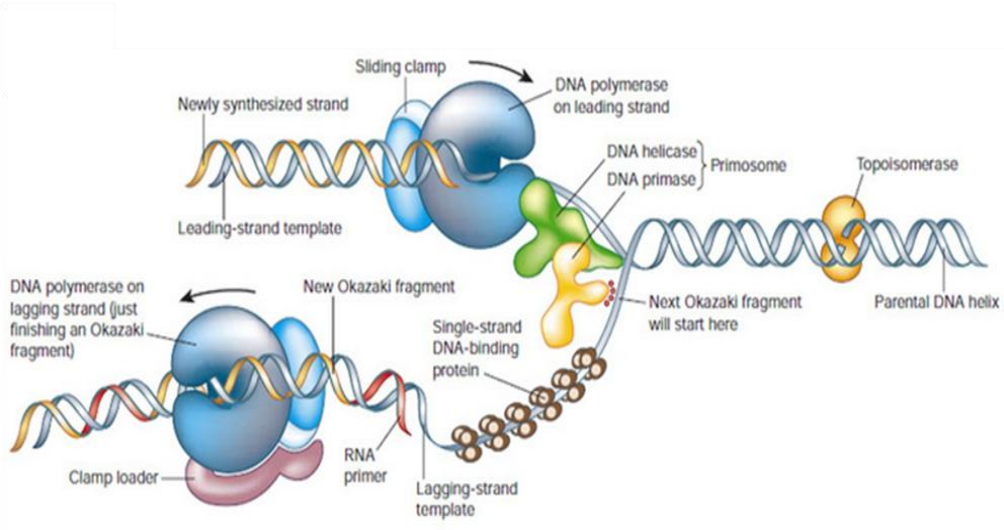

Figure 2. Schematic illustration of proteins acting at the fork during replication. Two DNA polymerases are actively synthesizing at the fork. Leading strand polymerase moves continuously to generate the daughter DNA molecule, whereas on the lagging strand the polymerase synthesizes DNA discontinuously, producing Okazaki fragments. Both polymerases attachment to the template is favored by accessory proteins, such as the sliding clamp and the clamp loader. DNA helicases are powered by ATP hydrolysis to open the DNA helix ahead of the replication fork, exposing ssDNA filaments for polymerases to copy. DNA topoisomerases facilitate DNA helix unwinding ahead of the fork branching point. In addition to the template, DNA polymerases require a pre-existing RNA end, provided by the primer segment, onto which to add the nucleotides. Primases produce a short RNA molecule onto which the DNA polymerase adds nucleotides. The ssDNA exposed at the fork is covered by single-strand DNA-binding protein RPA complexes (adapted from Cimprich and Cortez, 2008).

Multiple nucleases, including Dna2 and Exo1, are involved in Okazaky fragment processing (Bae et al., 2000; Sun et al., 2003). The current model

comprises different steps and strategies to remove primer RNA and create ligatable nicks (Bae et al., 2001), that can be summarised in the following steps: i) DNA-RNA synthesis by pol α–primase; ii) Elongation of the RNA-DNA primer after polymerase switching (pol α to pol δ with the help of PCNA) and extension of the primer by pol δ; iii) flap formation by displacement DNA synthesis by pol δ - the size of the flap determines further processing, with short flaps directly processed by Fen1, while long flaps processed by sequential action RPA-dependent of Dna2, which removes the majority of the flap, and Fen1 or other nucleases, such as Exo1 or pol δ, which create nicks at the remaining part of the flap; vi) sealing of the nicks by a ligase and formation of a continuous double stranded DNA.

2.3 The topology of replicating chromosomes.

Topological constraints related to DNA originate mainly from the fact that the two DNA strands in the double helix intertwine many times. Most of the DNA metabolic processes necessitating nucleic acid access require the untangling of the two strands. The simplest considerable scenario is a linear DNA molecule in which untangling can be obtained by free rotation of the DNA ends. However, nuclear DNA is constrained by topological domain barriers, so that relaxation by the free rotation of the ends is not possible. Examples of topological domains are represented by circular DNAs, such as the bacterial chromosome, that is a covalently closed structure, and by the chromatin loops attached to the nuclear cellular matrix organizing eukaryotic chromosomes.

The topological state of DNA influences different cellular processes, such as DNA replication and transcription. DNA replication requires the unwinding of the parental DNA filaments wrapped around each other in a double helix, so that each filament can be used as template for the synthesis of the new complementary strand by DNA polymerases. Replicative helicases unwind DNA generating as a consequence of the overwinding of the parental duplex in the unreplicated DNA regions in front of the replication fork. The torsional energy formed in this way accumulates as positive supercoiling (Figure 3a). Thus, positive supercoiling generated during DNA synthesis distributes along unreplicated DNA portions as helical overwinding, but its diffusion is precluded by topological barriers. The tension accumulated as positive

supercoiling ahead of the replication fork obstacles the progression of the fork, counteracting duplex unwinding by helicases. This scenario is complicated by topological transitions taking place if the replication fork can rotate at it branching point (Wang et al., 2002). In that case, positive supercoiling accumulated ahead of the replication fork can be distributed to the replicated DNA portions, generating intertwinings between the replicated duplexes, giving rise to crossings termed precatenanes (Figure 3b).

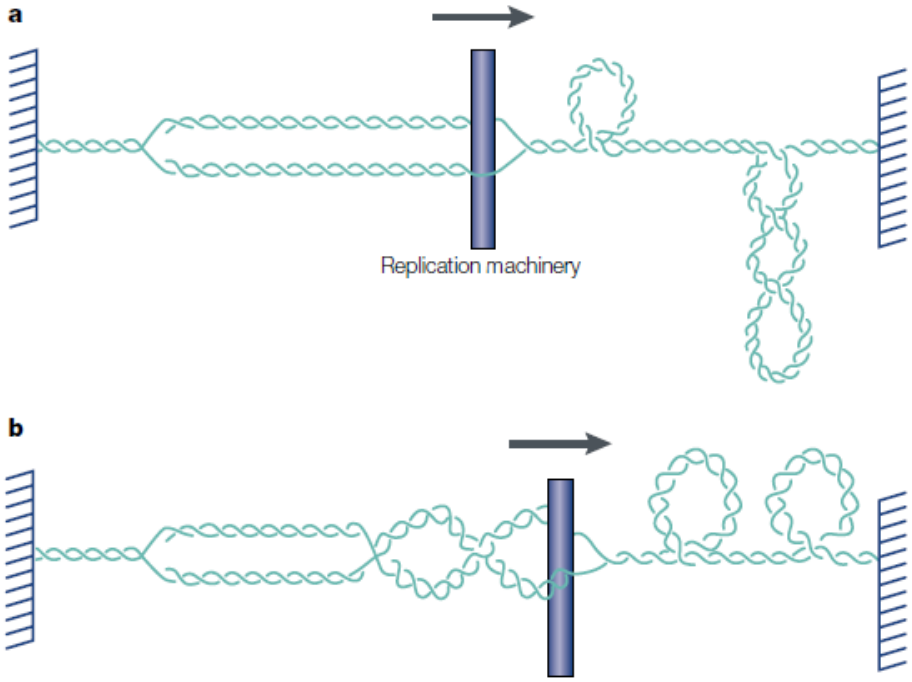

Figure 3. Topological problems associated to replication. The replication machinery is depicted as a blue rod and discontinuous bars represent topological domain barriers, such as sites of attachment of the nuclear membrane with chromatin. The topological transitions at replication forks depend on whether the replication machinery can rotate or not along the helical axis. (a) If the replication machinery is immobile, positive supercoiling accumulates ahead of the replication fork. (b) If the replication machinery is permitted to rotate along the helical axis, then this turning permits the distribution of positive supercoiling to the region behind the fork, leading to the intertwining of the duplicated DNA helices (from Wang et. al, 2002).

Similarly, transcription by RNA polymerase (RNAP) affects the topological state of chromosomes. An RNAP machinery prevented from rotation around the helix forces the DNA rotation while proceeding, thus generating positive and negative supercoiling ahead and behind the transcription bubble (Figure 4A) (Liu and Wang, 1987). Alternatively, if RNAP would rotate constrains will not be formed, but the nascent RNA would entangle around the duplex (Figure 4B).

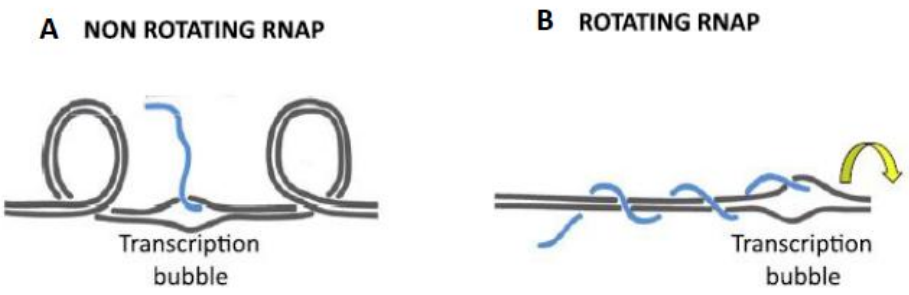

Figure 4. Topological problems associated to transcription. Similarly to what described for replication, the topology of transcription differs depending on whether the transcription machinery is permitted to rotate or not around DNA axis. An immobile RNAP generates positive and negative supercoiling in front and behind the transcription bubble, respectively (A). Rotation of the transcription machinery would twist nascent RNA around the DNA template behind the transcription bubble (B) (adapted from Bermejo et al., 2012).

The local changes in DNA topology described have functional consequences on different cellular processes and therefore cells have developed a specialized subset of nucleases, called DNA topoisomerases (Wang, 2002; Champoux, 2001), that finely regulate the degree of supercoiling in the cell. DNA topoisomerases resolve topological constrains by introducing temporary cleavages in the DNA backbone that are resealed at the end of the process. In

this reaction, the formation of a gap is coordinated with the passage of a single helix or an entire duplex through it, therefore changing the DNA topology and relaxing the domains.

There are two families of DNA topoisomerases, type I and type II, which catalyse single or double strand DNA breakage, respectively. Type I topoisomerases, differently from type II, do not require ATP hydrolysis for their activity and are further subdivided into IA and IB subfamilies. Enzymes belonging to the IA group are characterized by a so called "enzyme-bridging" mechanism that involves the passage of one strand through its opposite (Tse and Wang, 1980) and their activity is directed towards negatively supercoiled DNA, while type IB uses a "strand rotation" mechanism that involves the free rotation of the duplex strands (Stewart et al., 1998). Type IB enzymes can relax both positive and negative supercoils. Type II topoisomerases hydrolyse ATP and both type IIA and IIB mediate the passage of the entire duplex through a double stranded gap of the same or a different DNA molecules (Roca et al., 1996). Beside the relaxation of positive and negative supercoils, this category of enzymes can also decatenate dsDNA entanglements, such as DNA precatenanes (Wang et al., 2002).

S. cerevisiae Top1, a type IB enzyme, and Top2, a type IIA enzyme, can sustain the progression of the replication machinery (Kim and Wang, 1989; Bermejo et al., 2007). Top1 and Top2 travel with replication forks during DNA synthesis, likely coordinating positive supercoiling and precatenanes relaxation (Bermejo et al., 2007). In budding yeast Top1 is dispensable for cell viability, while Top2 inactivation causes cells death (Wang et al., 1996). Of notice,

contemporary inactivation of both topoisomerases precludes DNA replication (Bermejo et al., 2007).

2.4 The replication checkpoint stabilizes stalled replication forks.

An accurate completion of DNA replication is crucial to maintain genome integrity. However, during S-phase, different endogenous and exogenous factors can interfere with replication fork progression, generating replication stress. Replication stress can be described as a situation in which different impediments cause replication forks to slow down and stall. Topological constraints (Bermejo et al., 2012), DNA lesions (Paulovich et al., 2006), clashing with transcription (Bermejo et al., 2011), oncogene over-expression (Di Micco et al., 2006) and depletion of dNTPs pool (Zhao et al., 2001) have been described as causes of replication stress. Mechanistic insight on how the DNA damage checkpoint acts to preserve genome integrity upon replication stress comes mainly from the model organism *Saccharomyces cerevisiae* (Perego et al., 2000). Cells experiencing replication stress induced by genotoxic agents activate a dedicated branch of the DNA damage checkpoint, termed replication checkpoint or S-phase checkpoint, that stabilises stalled replication forks promoting the functional integrity of the replication machinery (Lucca et al., 2004; Cobb et al., 2005). When the replication stress is overcome, checkpoint proficient cells are able to resume DNA synthesis (Lopes et al., 2001). ssDNA accumulating at stalled replication forks due to uncoupling between DNA unwinding by helicases and the progression of DNA

polymerases triggers checkpoint activation upon replication inhibition (Sogo et al., 2002). ssDNA can also be generated by Exo1 exonucleolytic activity (Cotta-Ramusino et al., 2005), as well as by other unidentified factors (Branzei and Foiani, 2009). The checkpoint response is mediated by a complex cascade of evolutionary conserved proteins that can be divided into sensors, mediators and effectors (Longhese et al., 2003). Two parallel pathways respond to different kind of genotoxic stresses: the ATM/Tel1 kinase is activated by the presence of DSBs, while the ATR/Mec1 activity is mainly responsible for cell survival upon treatment with agents that interfere with the progression of replication forks, such as the replication inhibitor hydroxyurea (HU). Extended ssDNA patches exposed upon replication inhibition are coated by RPA (replication protein A) (Sogo et al., 2002), which recruits the apical checkpoint kinase Mec1/ATR associated to Ddc2 (Zou and Elledge, 2003). Once activated, Mec1 phosphorylates Mrc1, a structural component of the replication fork, required for replisome stabilisation and transduction of the checkpoint signal (Katou et al., 2003). Mrc1, in turn, mediates Rad53 effector kinase activation (Alcasabas et al., 2001), that hyper-autophosphorylates and gets fully activated to reach its targets (Pelliccioli and Foiani, 2005), thus promoting cell survival and genome integrity. Of notice, Rad53 is essential for the checkpoint response upon fork blockage in the presence of genotoxic agents (Foiani et al., 2000). There is evidence indicating that Rad53 and Mec1 are involved in replisome stability upon replication stress, thus preventing forks collapse (Desany et al., 1998).

The S-phase checkpoint so activated can accomplish different functions (Figure 5). Initially it delays the progression through mitosis by modifying key cell cycle regulators, so preventing premature segregation of partially

replicated chromosomes (Krishnan et al., 2004; Putnam et al., 2010). Furthermore, it up-regulates dNTP pools, thus counteracting mutagenic events and favouring genome integrity (Chabes et al., 2003). Checkpoint activation also represses late/dormant origins firing through not yet fully understood mechanisms, thus limiting the number of replication forks susceptible to destabilization (Tercero and Diffley, 2001; Lopes et al., 2001). In addition, the checkpoint pathway modulates the DNA repair.

Replication fork stabilization is thought to be the most relevant function for cell viability in conditions inducing replication stress (Tercero et al., 2003). Replication forks are intrinsically fragile structure prone to accumulate breaks since during replication they expose ssDNA, which is fragile and prone to prime unscheduled recombination events (Johnson and O'Donnell, 2005; Branzei and Foiani, 2010).

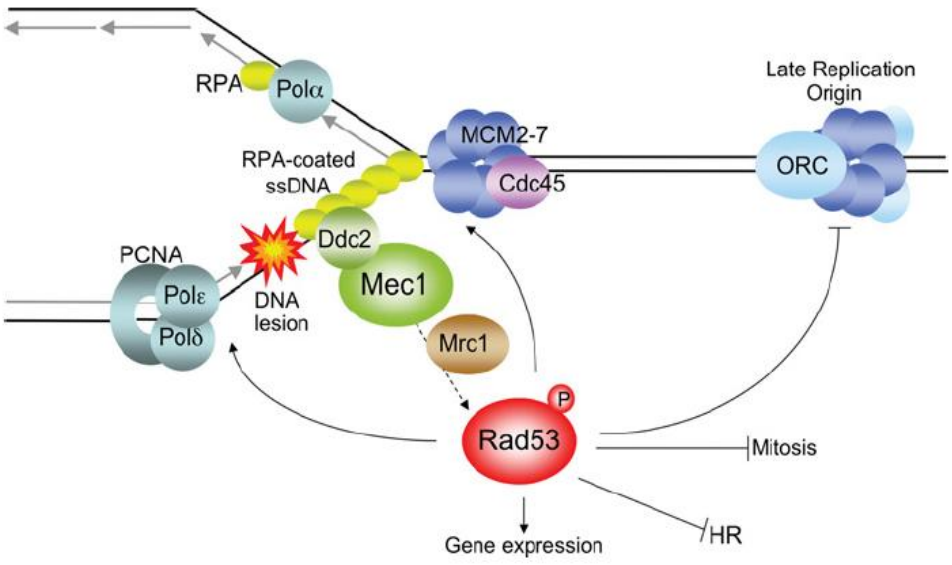

Figure 5. Schematic cartoon of S-phase checkpoint response signalling and functions. When replication forks stall, for instance due to dNTPs pool depletion, helicase and polymerases uncouple, generating ssDNA, which is covered by RPA complexes. The presence of RPA brings Mec1, through its with Ddc2, to the stalled

forks. The checkpoint signal reaches effector kinase Rad53 through the adaptor function of Mrc1. Rad53, once activated, acts at different levels: it is responsible for replication fork stability, it prevents premature entry in mitosis and inhibits both late origins firing and unscheduled homologous recombination events (adapted from Segurado and Tercero, 2009).

In checkpoint defective mutants, such as *rad53* cells, failure to stabilize stalled replication forks and consequent detachment of replisome proteins from fork DNA is retained as the main cause of lethality after exposure to the replication inhibitor hydroxyurea (Lopes et al., 2001; Sogo et al. 2002; Segurado and Diffley, 2008). Replication fork breakdown and dissociation of replisome factors is referred to as fork collapse. Collapsed forks are extremely harmful structures, since they can be engaged in structural changes and prime chromosomal rearrangements.

A hallmark of fork collapse in checkpoint mutant is the accumulation of reversed forks, which can be observed by electron microscopy. Reversed forks are formed through re-annealing of nascent strands to generate four way junctions named “chicken feet” (Sogo et al., 2002). Reversed forks counteract the resumption of DNA synthesis and therefore are thought to represent terminal events contributing to the loss of viability of these mutants (Figure 6). Furthermore, collapsed forks undergo additional pathological transitions, accumulating ssDNA-gapped and hemi-replicated molecules due to nucleolytic processing (Cotta-Ramusino et al., 2005; Sogo et al., 2002) that favours unscheduled recombination events (Myung et al, 2002) and further nucleolytic cleavages, contributing to the accumulation of DNA breaks and priming chromosomal rearrangements (Branzei and Foiani, 2009).

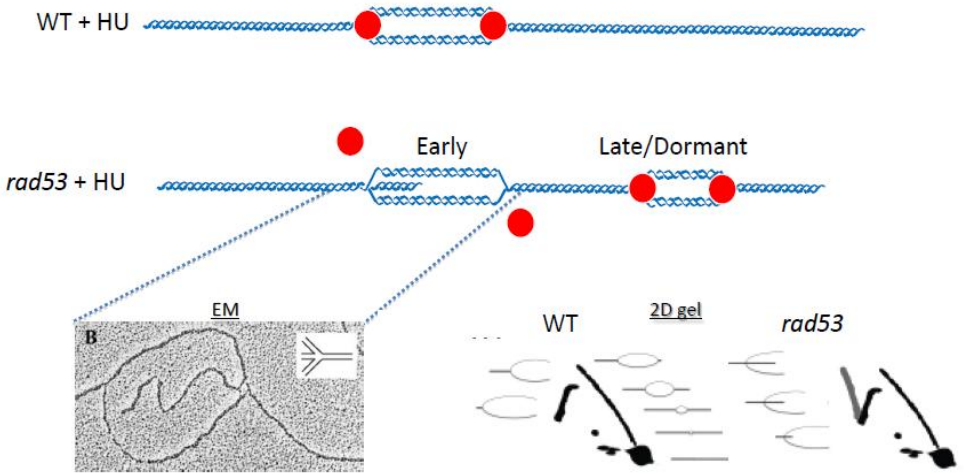

Figure 6. Replication fork collapse in checkpoint mutants. Red dots represent the replisome. See text for details. Reversed forks visualised by electron microscopy (Sogo et al., 2002) are shown, as well as schematic representations of 2D gel patterns in wild type (WT) and *rad53* cells. Canonical replication intermediates and reversed forks, migrating along a spike signal, are depicted.

2.5 Homologous recombination factors and replication fork protection.

Recent evidence suggests that homologous recombination proteins play a crucial role in the protection of stalled replication forks independently from their most characterized function in the HR-mediated repair pathways (Costanzo, 2011). In addition to their role in repairing ssDNA gaps and DSBs, recombination components might contribute to fork stability mainly by two mechanisms: first, protecting the fork from extensive nuclease resection; second, promoting forks restart. Little is known on the role of HR factors during replication and most of the current knowledge focuses on their function in DNA repair pathways. However, it has been reported that during bacterial DNA replication, nascent strands are transiently engaged by HR factors at damaged forks to restart DNA synthesis (Courcelle et al., 1999) and HR factors protect the new filaments from endonucleolytic cleavage, thus counteracting chromosomes fragmentation (Chow et al., 2004). Recent studies show that vertebrate RAD51 and BRCA2 are recruited to arrested forks (Hashimoto et al., 2010; Schlacher et al., 2011; Sirbu et al, 2011). These factors have been proposed to limit the length of ssDNA gaps left behind the replisome and are extended by Mre11 in an attempt to favour post-replicative repair (Costanzo, 2011). Intriguingly, BRCA2 and RAD51 exert this function independently from DSBs repair pathways, supporting the idea that they might besides potentially repairing lesions arising at stalled forks, directly promote fork stability (Aze et al., 2013).

An important function attributed to HR proteins is to restart blocked replication forks in the presence of impediments that affect replisome progression (Michel et al., 2007). In *E. coli*, arrested replication forks can be resumed by a recombination-dependent error-free pathway (Michel et al., 2004), that allows cells to reload a functional replisome at collapsed forks (Kogoma et al., 1997). This mechanism occurs sequentially through recombination proteins (such as RecA) dependent fork remodelling into an intermediate structure bound by the PriA. This transition permits the re-loading of the replisome (Sandler et al., 2000). The key intermediate generated during this process is a regressed fork, structurally similar to the HJs forming during homologous recombination, that can be restored by regressing the reversion or by endonucleolytic activities (McGlynn and Lloyd 2000; Courcelle et al., 2003). In eukaryotes mechanisms that rebuilt the replisome have been recently proposed.

In *Schizosaccharomyces pombe* recombination factors restart forks arrested at artificial replication fork barriers independently of the formation of DSBs (Lambert et al., 2010). Accordingly, a recent study in human cells suggests that Rad51 promotes replication fork restart after stalling due to HU treatment and this role is distinct from the DSB repair (Petermann et al., 2010).

In *S. cerevisiae* replication fork restart have been described to occur through a pathway that mediates DNA synthesis from a single DSB end, called break-induced replication (BIR) (Llorente et al., 2008). This pathway is exclusively Rad52-dependent and could promote fork repair starting from a one-ended break, in a "one-ended recombination event". The homologous duplex is invaded by the free end, forming a D-loop structure that becomes an unidirectional replication fork, thus re-starting DNA synthesis (Paques et al., 1999). For efficient restart, the BIR pathway requires most of HR pathway

genes as well as DNA polymerases and components of the replicative helicases (Lydeard et al. 2010). However, the replication apparatus built by the BIR pathway is highly mutagenic. Thus, the lethality arising from DSBs is rescued at the expense of genetic stability (Deem et al. 2011).

Different lines of evidence support a role for *S. cerevisiae* recombination proteins in processes coupled with replication. Recombination genes mutants are sensitive to drugs that impede replication fork progression, such as HU (Hartman and Tippery, 2004), suggesting that those factors are required for an appropriate cellular response to fork stalling. This observation is in agreement with recent data showing that cells defective in Rad52 or Rad51 recombination proteins function accumulate small ssDNA gaps at and behind replication forks, indicating a role for those factors in promoting continuous DNA synthesis (Hashimoto et al., 2010). Furthermore, Rad52 foci numbers increase in mutants of replication factor genes (Lisby et al., 2001) and Rad52 sustains the viability of these mutants (Symington et al., 1998). This evidence indicates that recombination factors could be either necessary to protect DNA from degradation or to resume replication. However, in some circumstances homologous recombination factors might be deleterious for replication, if not properly regulated. For instance, Rad52 foci formation is observed only in checkpoint deficient cells when experiencing replication stress (Lisby et al., 2004), suggesting that under this conditions a functional checkpoint inhibits recombination factors-mediated fork processing, likely avoiding the transition from stalled to collapsed forks. Intriguingly, upon ablation of recombination factors, aberrant structures are not detected at replication forks (Lopes et al., 2001). These data suggest that yeast recombination factors act at stalled replication forks, although their function is still unclear.

In higher eukaryotes, inactivation of recombination factors causes lethality at the initial steps of development (West et al., 2003), hinting at a crucial role for those proteins in protecting genome integrity. As mentioned, the function of HR factors in repairing DSBs and protecting the replication fork are separable in mammals (Petermann et al., 2010; Schlacher et al., 2011), suggesting that specialised homologous recombination machineries could be devoted to both fork protection and fork restart, while others might mediate the DSBs repair. Current data support the notion that recombination factors play important roles at stalled forks and that they might directly contribute to forks stability (Lambert et al., 2007; Peterman et al. 2010). However, mechanistic insight on their contribution to replication is lacking.

2.6 The multiple roles for DNA nucleases in protecting genome stability.

DNA nucleases are key enzymes that influence many aspects of the DNA metabolism, on a wide variety of substrates according to their specificity. As mentioned before, DNA experiences different exogenous and endogenous environmental stresses that can modify its structure, potentially leading to genome instability. Unusual structures arising during recombination or replication must be properly resolved to avoid alterations in the DNA sequence or chromosomal rearrangements. To execute this task, cells have developed a high number of nucleases that function in different cellular processes, either alone or in complexes, metabolising DNA intermediates that arise during unperturbed or aberrant DNA replication. As previously mentioned (see section 1.2), during replication a specific subset of nuclease activities is involved in nascent strands proof-reading, thus avoiding nucleotide misincorporation, while others are engaged in the removal of flaps forming during lagging strand synthesis. The latter function involves Exo1 and Dna2, two nucleases that counteract reversed forks in cells experiencing replication stress, in *S. cerevisiae* and *S. pombe*, respectively (Cotta-Ramusino et al., 2005; Hu et al., 2012).

Other nucleases deal with the presence of DNA damages. The HR-mediated DSB repair pathways are well characterised in budding yeast. DSB repair starts with the recognition of lesions that can be then processed to generate RPA-

coated ssDNA, which stimulates the activation of the DNA damage checkpoint response and DNA repair by homologous recombination error free pathway. During the initial stages of repair, lesions are nucleolytically processed into intermediate structures by a 5' strand degradation that generates 3' ssDNA overhanging tails, in a process called 5'-3' resection (Paques et al., 1999; Mazon et al., 2010). As mentioned, ssDNA coated by RPA complexes contributes to DNA damage checkpoint signalling by recruiting and activating the Mec1/ATR checkpoint kinase (Zou et al., 2003). DSB processing begins with a first step of resection mediated by the conserved Mre11-Rad50-Xrs2/Nbs1 (MRX/N) complex that together with endonuclease Sae2/CtIP catalyses a limited removal of oligonucleotides from the 5'strand (Zhu et al., 2008; Mimitou et al., 2008). Further extensive resection relies on the activity of other nucleases, such as the 5'-3' exonuclease Exo1 or, alternatively, the endonuclease/helicase Dna2 in concert with the STR complex, composed by Sgs1-Top3-Rmi1 (Mimitou et al., 2009). This second step of resection generates long stretches of ssDNA that constitute nucleofilaments engaged in homology search strand invasion reactions mediated by Rad51 and Rad52 (Bianco et al., 1998). Interestingly, the activity of nucleases is not limited to DNA ends processing, but also in facilitating the engagement of additional factors to the lesion. For instance, Mre11 is required to recruit the repair factors to the break (Shim et al., 2010). The coordinated activities of these nucleases are crucial since mutants carrying their contemporary ablation fail to perform homologous recombination repair (Zhu et al., 2008; Mimitou et al., 2008).

Noteworthy, nucleases are characterized by a certain degree of "plasticity", as they can play different roles in multiple pathways. For instance, a novel role for *S. cerevisiae* Mre11 and Sae2 nucleases in preventing the accumulation of

cruciform structures at terminal forks approaching a DSB has recently emerged (Doksany et al, 2009). Impairment of Mre11 or Sae2 function leads not only to the accumulation of aberrant replication intermediates, but also results in further fork processing by yet unidentified nucleases.

Other categories of nucleases deal with the presence of more complex DNA structures, such as branched molecules (i.e. DNA junction structures or flaps), that can form in multiple cellular processes, such as DNA synthesis or recombination repair (Schwartz and Heyer, 2011). For example, late steps of DSB repair by HR require the physical resolution of the connection established between sister chromatids by four-way joint molecules, named Holliday junctions. These structures are physiological intermediates of DSB repair and are resolved by a subset of structure selective nucleases (SSEs) that are highly conserved through evolution (Figure 7).

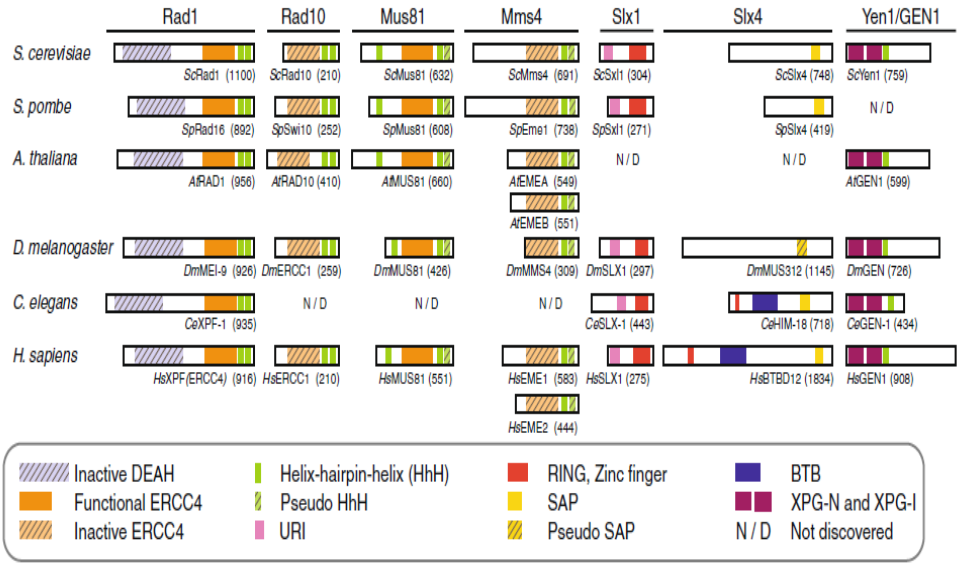

Figure 7. Schematic representation of the domains conservation and architectural features of structure selective nucleases. Domains are identified as written in the key box, N/D, not discovered. (from Schwartz and Heyer, 2010).

Some SSEs preferentially recognise four branched structures and therefore are named HJ resolvases. Interestingly, reversed forks resemble HJs and therefore might represent potential targets for those enzymes. The first nuclease described as HJ resolvase in *S. cerevisiae* was Mus81 (Boddy et al., 2001). Budding yeast Mus81 cleaves Holliday Junctions *in vitro* (Fricke et al., 2005), although it posses specificity also for other types of DNA junctions that can form during the processing of stalled or collapsed forks, as well as nicked HJs, D-loops and 3'flaps (Osman and Whitby, 2007). Accordingly, budding yeast cells lacking Mus81 are sensitive to drugs that cause fork stalling, such as HU (Blanco et al., 2010). Moreover, Mus81 mutants show chromosomal rearrangements (Smith et al., 2004). The role for Mus81 in the maintenance of genome stability was linked to stalled forks cleavage as part of the adaptation to prolonged replication arrests (Osman and Whitby, 2007). Supporting this idea, Mus81 is required to restart blocked replication forks in human cells experiencing replication stress. In this context Mus81 converts potentially harmful structures in intermediates suitable for repair by HR (Hanada et al., 2006; Hanada et al., 2007). However, in some contexts, Mus81-dependent cleavage replication fork can favour unscheduled HR events and trigger genome instability. *S. pombe* Mus81 is inhibited through phosphorylation by the checkpoint kinase Cds1 in response to replication stress (Kai et al., 2005). Accordingly, recent data show that human MUS81 specifically cleaves reversed forks also in checkpoint deficient cells experiencing oncogene over-expression, thus triggering genome instability (Neelsen et al., 2013). Thus, Mus81-mediated processing is crucial for the maintenance of genome stability and this function seems to be conserved among different organisms.

Budding yeast Mus81 activity in the resolution of HJs partially overlaps *in vivo* with the one of a second resolvase named Yen1 (Tay et al., 2010; Blanco et al.,

2010). Accordingly, *mus81Δyen1Δ* double mutants are more sensitive than the singles mutants to agents that disturb fork progression (Tay et al., 2010; Blanco et al., 2010). Furthermore, MUS81 and GEN1, the human homologue of yeast Yen1, cooperate in chromosomes segregation in the absence of BLM helicase and concomitant depletion of these resolvases leads to chromosome abnormalities (Wechsler et al., 2011). However, Mus81and Yen1 are not the only nucleases in yeast that show specificity towards structures arising at replication forks. Mus81 shares preference for branch replication fork-like substrates with another SSE named Slx4 (Fricke et al., 2003). Slx4 processes aberrant structures arising upon fork stalling at replication fork barriers (Kaliraman et al., 2002) and it seems to function as a platform in the recruitment of specific factors to replication-associated lesions (Rouse, 2009). Slx4 is targeted by the DNA damage checkpoint promoting the formation of dimers with Slx1 in response to replication blocks and DSBs (Flott et al., 2007). Furthermore, Slx4 also interacts with Rad1-Rad10, another structure specific endonucleases complex, involved in DNA repair (Flott et al., 2007). This interaction occurs independently from Slx1 and facilitates the removal of the non-homologous tails during HR (Toh et al., 2010).

These data indicate the presence of a complex network of nucleases that can be regulated by the checkpoint response according to the different cellular requirements. These nucleases can play a wide range of roles in genome integrity maintenance, through their association with multiple partners and due to their different substrate specificities.

3. MATERIAL AND METHODS

3.1 *S. cerevisiae* strains.

Strains are listed in Table 1. All the strains used are isogenic derivatives of W303-1A (Thomas and Rothstain, 1989). Deletion strains were generated using PCR-base gene disruption strategy (Wach et al., 1994), while *rad53* mutants were constructed integrating a *rad53-K227A*-KanMX4 cassette into the *RAD53* locus. All the strains used for the experiments were mating type *a*.

Table 1. Genotypes of the strains used in this study.

Strain	Number	Genotype	Reference
wt	CY7028	*MATa ADE2+ CAN1+, ura3-1, his3-11, leu2-3,112, trp1-1, RAD5+, DUN1::DUN1-3HA-TRP1*	Lab collection
rad53	CY7031	*MATa ADE2+ CAN1+, ura3-1, his3-11, leu2-3,112, trp1-1, RAD5+, DUN1::DUN1-3HA-TRP1, rad53K227A Kan-r*	Lab collection
exo1Δ	CY10342	*MATa ADE2+ CAN1+, ura3-1, his3-11, leu2-3,112, trp1-1, RAD5+, DUN1::DUN1-3HA-TRP1, exo1::HIS*	This study
rad53exo1Δ	CY10343	*MATa ADE2+ CAN1+, ura3-1, his3-11, leu2-3,112, trp1-1, RAD5+, DUN1::DUN1-3HA-TRP1, rad53K227A Kan-r, exo1::HIS*	This study
wt Inc	CY7812	*MATa-inc, hmldelta::ADE1, hmrdelta::ADE1 ade1-100, ade2-1, ura3,trp1-1, leu2-3, leu2-112, his3-11, his3-15, can1-100, GAL, PSI+ ade3::GAL::HO Δ chrIII [41800-41839] ::HOsite INC::HPH, BAR1::TRP*	Lab collection
wt Cut	CY7814	*MATa-inc, hmldelta::ADE1, hmrdelta::ADE1 ade1-100, ade2-1, ura3, trp1-1, leu2-3, leu2-112, his3-11, his3-15, can1-100, GAL, PSI+ ade3::GAL::HO Δ chrIII [41800-41839] ::HOsite::HPH,*	Lab collection

		BAR1::TRP	
rad53 Inc	CY10102	*Mat<u>a</u>-inc, hmldelta::ADE1, hmrdelta::ADE1 ade1-100, ade2-1, ura3, trp1-1, leu2-3, leu2-112, his3-11, his3-15, can1-100, GAL, PSI+ ade3::GAL::HO Δ chrIII [41800-41839] ::HOsite INC::HPH, BAR1::TRP, rad53K227A Kan-r*	Lab collection
rad53 Cut	CY8385	*Mat<u>a</u>-inc, hmldelta::ADE1, hmrdelta::ADE1 ade1-100, ade2-1, ura3, trp1-1, leu2-3, leu2-112, his3-11, his3-15, can1-100, GAL, PSI+ ade3::GAL::HO Δ chrIII [41800-41839] ::HOsite::HPH, BAR1::TRP, rad53K227A Kan-r*	Lab collection
wt Inc *exo1Δ*	CY11584	*MAT<u>a</u>-inc, hmldelta::ADE1, hmrdelta::ADE1 ade1-100, ade2-1, ura3,trp1-1, leu2-3, leu2-112, his3-11, his3-15, can1-100, GAL, PSI+ ade3::GAL::HO Δ chrIII [41800-41839] ::HOsite INC::HPH, BAR1::TRP, exo1::HPH*	This study
wt Cut *exo1Δ*	CY11586	*MAT<u>a</u>-inc, hmldelta::ADE1, hmrdelta::ADE1 ade1-100, ade2-1, ura3, trp1-1, leu2-3, leu2-112, his3-11, his3-15, can1-100, GAL, PSI+ ade3::GAL::HO Δ chrIII [41800-41839] ::HOsite::HPH, BAR1::TRP, exo1::HPH*	This study
rad53 Inc exo1Δ	CY11585	*Mat<u>a</u>-inc, hmldelta::ADE1, hmrdelta::ADE1 ade1-100, ade2-1, ura3, trp1-1, leu2-3, leu2-112, his3-11, his3-15, can1-100, GAL, PSI+ ade3::GAL::HO Δ chrIII [41800-41839] ::HOsite INC::HPH, BAR1::TRP, rad53K227A Kan-r, exo1::HPH*	This study
rad53 Cut exo1Δ	CY11587	*Mat<u>a</u>-inc, hmldelta::ADE1, hmrdelta::ADE1 ade1-100, ade2-1, ura3, trp1-1, leu2-3, leu2-112, his3-11, his3-15, can1-100, GAL, PSI+ ade3::GAL::HO Δ chrIII [41800-41839] ::HOsite::HPH, BAR1::TRP, rad53K227A Kan-r , exo1::HPH*	This study
top2-1top1Δ	CY10344	*MAT<u>a</u> ADE2+ CAN1+, ura3-1, his3-11, leu2-3,112, trp1-1, RAD5+, DUN1::DUN1-3HA-TRP1, top2-1*	This study
rad53 top2-1top1Δ	CY10347	*MAT<u>a</u> ADE2+ CAN1+, ura3-1, his3-11, leu2-3,112, trp1-1, RAD5+, DUN1::DUN1-3HA-TRP1, rad53K227A Kan-r, top2-1*	This study
pYesGAL	CY11589	*MAT<u>a</u> ADE2+ CAN1+, ura3-1, his3-11, leu2-3,112, trp1-1, RAD5+, DUN1::DUN1-3HA-TRP1, pYes2*	This study
pYesGALTop2	CY11593	*MAT<u>a</u> ADE2+ CAN1+, ura3-1, his3-11, leu2-3,112, trp1-1, RAD5+, DUN1::DUN1-3HA-TRP1, rad53K227A Kan-r, pYes2*	This study
rad53pYes GAL	CY11597	*MAT<u>a</u> ADE2+ CAN1+, ura3-1, his3-11, leu2-3,112, trp1-1, RAD5+, DUN1::DUN1-3HA-TRP1, pYcpTop2-*	This study

		Gal1	
rad53pYes GALTop2	CY11601	*MATa ADE2+ CAN1+, ura3-1, his3-11, leu2-3,112, trp1-1, RAD5+, DUN1::DUN1-3HA-TRP1, rad53K227A Kan-r, pYcpTop2-Gal1*	This study
wt GAL1	CY12285	*MATa ADE2+ CAN1+, ura3-1, his3-11, leu2-3,112, trp1-1, RAD5+, DUN1::DUN1-3HA-TRP1, pYcp-Gal1*	This study
wt GAL1TOP1	CY12286	*MATa ADE2+ CAN1+, ura3-1, his3-11, leu2-3,112, trp1-1, RAD5+, DUN1::DUN1-3HA-TRP1, pYcpTop1-Gal1*	This study
rad53GAL1	CY12287	*MATa ADE2+ CAN1+, ura3-1, his3-11, leu2-3,112, trp1-1, RAD5+, DUN1::DUN1-3HA-TRP1, rad53K227A Kan-r, pYcp-Gal1*	This study
rad53 GAL1TOP1	CY12288	*MATa ADE2+ CAN1+, ura3-1, his3-11, leu2-3,112, trp1-1, RAD5+, DUN1::DUN1-3HA-TRP1, rad53K227A Kan-r, pYcpTop1-Gal1*	This study
rad53mus81Δ	CY10916	*MATa ADE2+ CAN1+, ura3-1, his3-11, leu2-3,112, trp1-1, RAD5+, DUN1::DUN1-3HA-TRP1, rad53K227A Kan-r, mus81::HPH*	This study
rad53mus81Δ exo1Δ	CY10917	*MATa ADE2+ CAN1+, ura3-1, his3-11, leu2-3,112, trp1-1, RAD5+, DUN1::DUN1-3HA-TRP1, rad53K227A Kan-r, exo1::HIS, mus81::HPH*	This study
mus81Δ	CY10914	*MATa ADE2+ CAN1+, ura3-1, his3-11, leu2-3,112, trp1-1, RAD5+, DUN1::DUN1-3HA-TRP1, mus81::HPH*	This study
mus81Δexo1Δ	CY10915	*MATa ADE2+ CAN1+, ura3-1, his3-11, leu2-3,112, trp1-1, RAD5+, DUN1::DUN1-3HA-TRP1, exo1::HIS, mus81::HPH*	This study
rad53yen1Δ	CY10908	*MATa ADE2+ CAN1+, ura3-1, his3-11, leu2-3,112, trp1-1, RAD5+, DUN1::DUN1-3HA-TRP1, rad53K227A Kan-r, yen1::NAT*	This study
rad53yen1Δ exo1Δ	CY10912	*MATa ADE2+ CAN1+, ura3-1, his3-11, leu2-3,112, trp1-1, RAD5+, DUN1::DUN1-3HA-TRP1, rad53K227A Kan-r, exo1::HIS, yen1::NAT*	This study
yen1Δ	CY10907	*MATa ADE2+ CAN1+, ura3-1, his3-11, leu2-3,112, trp1-1, RAD5+, DUN1::DUN1-3HA-TRP1, yen1::NAT*	This study
yen1Δexo1Δ	CY10909	*MATa ADE2+ CAN1+, ura3-1, his3-11, leu2-3,112, trp1-1, RAD5+, DUN1::DUN1-3HA-TRP1, exo1::HIS, yen1::NAT*	This study
yen1Δexo1Δ mus81Δ	CY10911	*MATa ADE2+ CAN1+, ura3-1, his3-11, leu2-3,112, trp1-1, RAD5+, DUN1::DUN1-3HA-TRP1, exo1::HIS, yen1::NAT, mus81::HPH*	This study
yen1Δmus81Δ	CY10910	*MATa ADE2+ CAN1+, ura3-1, his3-11, leu2-3,112, trp1-1, RAD5+,*	This study

		DUN1::DUN1-3HA-TRP1, yen1::NAT, mus81::HPH	
exo1Δmus81Δ	CY10915	*MATa ADE2+ CAN1+, ura3-1, his3-11, leu2-3,112, trp1-1, RAD5+, DUN1::DUN1-3HA-TRP1, mus81::HPH, exo1::HIS*	This study
exo1Δyen1Δ	CY10909	*MATa ADE2+ CAN1+, ura3-1, his3-11, leu2-3,112, trp1-1, RAD5+, DUN1::DUN1-3HA-TRP1, yen1::NAT, exo1::HIS*	This study
rad53slx1Δ exo1Δ	CY12289	*MATa ADE2+ CAN1+, ura3-1, his3-11, leu2-3,112, trp1-1, RAD5+, DUN1::DUN1-3HA-TRP1, rad53K227A Kan-r, exo1::HIS, slx1::HIS*	This study
rad53slx1Δ exo1Δyen1Δ	CY12290	*MATa ADE2+ CAN1+, ura3-1, his3-11, leu2-3,112, trp1-1, RAD5+, DUN1::DUN1-3HA-TRP1, rad53K227A Kan-r, exo1::HIS, slx1::HIS, yen1::NAT*	This study
rad53slx1Δ exo1Δmus81Δ	CY12291	*MATa ADE2+ CAN1+, ura3-1, his3-11, leu2-3,112, trp1-1, RAD5+, DUN1::DUN1-3HA-TRP1, rad53K227A Kan-r, exo1::HIS, slx1::HIS, mus81::HPH*	This study
rad53slx1Δ exo1Δmus81Δ yen1Δ	CY12292	*MATa ADE2+ CAN1+, ura3-1, his3-11, leu2-3,112, trp1-1, RAD5+, DUN1::DUN1-3HA-TRP1, rad53K227A Kan-r, exo1::HIS, slx1::HIS, mus81::HPH, yen1::NAT*	This study
rad53rad1Δ	CY11938	*MATa ADE2+ CAN1+, ura3-1, his3-11, leu2-3,112, trp1-1, RAD5+, DUN1::DUN1-3HA-TRP1, rad53K227A Kan-r, rad1::NAT*	This study
rad53rad1Δ exo1Δ	CY11939	*MATa ADE2+ CAN1+, ura3-1, his3-11, leu2-3,112, trp1-1, RAD5+, DUN1::DUN1-3HA-TRP1, rad53K227A Kan-r, exo1::HIS, rad1::NAT*	This study
rad53sae2Δ	CY11669	*MATa ADE2+ CAN1+, ura3-1, his3-11, leu2-3,112, trp1-1, RAD5+, DUN1::DUN1-3HA-TRP1, rad53K227A Kan-r, sae2::HPH*	This study
sae2Δ	CY11672	*MATa ADE2+ CAN1+, ura3-1, his3-11, leu2-3,112, trp1-1, RAD5+, DUN1::DUN1-3HA-TRP1, sae2::HPH*	This study
sae2Δexo1Δ	CY11671	*MATa ADE2+ CAN1+, ura3-1, his3-11, leu2-3,112, trp1-1, RAD5+, DUN1::DUN1-3HA-TRP1, exo1::HIS, sae2::HPH*	This study
rad53exo1Δ sae2Δ	CY11670	*MATa ADE2+ CAN1+, ura3-1, his3-11, leu2-3,112, trp1-1, RAD5+, DUN1::DUN1-3HA-TRP1, rad53K227A Kan-r, exo1::HIS, sae2::HPH*	This study
rad53mre11Δ	CY11877	*MATa ADE2+ CAN1+, ura3-1, his3-11, leu2-3,112, trp1-1, RAD5+, DUN1::DUN1-3HA-TRP1, rad53K227A Kan-r, mre11::NAT*	This study
mre11Δ	CY12254	*MATa ADE2+ CAN1+, ura3-1, his3-11, leu2-3,112, trp1-1, RAD5+, DUN1::DUN1-3HA-TRP1, mre11::NAT*	This study

mre11Δexo1Δ	CY12256	*MATa ADE2+ CAN1+, ura3-1, his3-11, leu2-3,112, trp1-1, RAD5+, DUN1::DUN1-3HA-TRP1, mre11::NAT, exo1::HIS*	This study
rad53mre11Δ exo1Δ	CY11878	*MATa ADE2+ CAN1+, ura3-1, his3-11, leu2-3,112, trp1-1, RAD5+, DUN1::DUN1-3HA-TRP1, rad53K227A Kan-r, exo1::HIS, mre11::NAT*	This study
dna2-1	CY11836	*MATa ADE2+ CAN1+, ura3-1, his3-11, leu2-3,112, trp1-1, RAD5+, DUN1::DUN1-3HA-TRP1, dna2-1*	This study
exo1Δdna2-1	CY11837	*MATa ADE2+ CAN1+, ura3-1, his3-11, leu2-3,112, trp1-1, RAD5+, DUN1::DUN1-3HA-TRP1, dna2-1, exo1::HIS*	This study
rad53dna2-1	CY11788	*MATa ADE2+ CAN1+, ura3-1, his3-11, leu2-3,112, trp1-1, RAD5+, DUN1::DUN1-3HA-TRP1, rad53K227A Kan-r, dna2-1*	This study
rad53exo1Δ dna2-1	CY11789	*MATa ADE2+ CAN1+, ura3-1, his3-11, leu2-3,112, trp1-1, RAD5+, DUN1::DUN1-3HA-TRP1, rad53K227A Kan-r, exo1::HIS, dna2-1*	This study
rad52Δ	CY10672	*MATa ADE2+ CAN1+, ura3-1, his3-11, leu2-3,112, trp1-1, RAD5+, DUN1::DUN1-3HA-TRP1, rad52::HPH*	This study
rad53rad52Δ	CY10675	*MATa ADE2+ CAN1+, ura3-1, his3-11, leu2-3,112, trp1-1, RAD5+, DUN1::DUN1-3HA-TRP1, rad53K227A Kan-r, rad52::HPH*	This study
rad51Δ	CY10905	*MATa ADE2+ CAN1+, ura3-1, his3-11, leu2-3,112, trp1-1, RAD5+, DUN1::DUN1-3HA-TRP1, rad51::NAT*	This study
rad53rad51Δ	CY10906	*MATa ADE2+ CAN1+, ura3-1, his3-11, leu2-3,112, trp1-1, RAD5+, DUN1::DUN1-3HA-TRP1, rad53K227A Kan-r, rad51::NAT*	This study

3.2 Growing media for *Saccharomyces cerevisae* cells.

3.2.1 Complete medium.

Yeast extract	10g
Peptone	20g

H_2O	up to 1000 ml

(Added glucose/other sugars at 2% final concentration before using).

3.2.2 Minimum medium.

Misturozzo (Thr, Phe, Ile, Lys, Arg, Tyr, Ini, Ade)	16 ml
YNB 10X	40 ml
H_2O	up to 600 ml

(Added glucose/other sugars at 2% final concentration before using).

(Other amino acids can be added before using at the final concentration of 25mg/ml).

3.2.3 YNB (Yeast Nitrogen Base).

YNB (Difco)	6.7 g
H_2O	up to 1000 ml

3.2.4 Sporulation medium (VB).

Na Acetate	13.6 g
KCl	1.9 g
NaCl	1.2 g
$MgSO_4$	0.35 g
Agar	15 g
H_2O	up to 1000 ml

3.2.5 Solid medium.

Add agar at the final concentration of 2% to the right media.

3.3 List of buffers.

Buffer G2 (digestion buffer): 800 mM guanidine HCl, 30 mM Tris-Cl pH 8.0, 30 mM EDTA pH 8.0, 5% Tween-20, 0.5% Triton X-100.

Buffer QBT (equilibration buffer): 750 mM NaCl, 50 mM MOPS pH 7.0, 15% Isopropanol, 0.15% Triton X-100.

Buffer QC (wash buffer): 1.0 M NaCl, 50 mM MOPS pH 7.0, 15% Isopropanol.

Buffer QF: (elution buffer) 1.25 M NaCl, 50 mM Tris-Cl pH 8.5, 15% Isopropanol.

Denaturing solution (Blot#1): NaOH 0.5 M, NaCl 1.5 M.

Blot#2: 1 M $AcNH_4$, 0.02 M NaOH.

NIB Buffer: Glycerol 17%, MOPS 50 mM, K-acetate 150 mM, $MgCl_2$ 2 mM, Spermidine 500 mM, Spermine 150 mM, pH 7.2**.**

SSC 20 X: NaCl 3M, Sodium citrate 0.3M, pH 7.5.

TAE: Tris Acetate 0.04 M, EDTA 0.001M.

TBE: Tris base 89 mM, Boric acid 89 mM, EDTA 2mM.

TE: Tris-HCl 10 mM, EDTA 1 mM, pH 7.4.

Washing solution I: SSC 2X, SDS 1%.

Washing solution II: SSC 0.1X, SDS 0.1%.

FACS Buffer solution: TrisHCl 200 mM, NaCl 200 mM, $MgCl_2$ 80 mM.

3.4 Growth conditions, cell cycle arrest and drug treatment.

For FACS and 2D gel analysis, strains were grown at the reported temperatures in YPDA medium (unless indicated) over night to reach a density of $1x10^7$ cells/ml in the morning. Cells synchronisation in G1 phase was achieved by addition of 4 μg/ml α-factor to the cultures. G1 arrest efficacy was evaluated by cellular morphology and the release was performed by a first centrifugation of the cells, washing with fresh YPD, second round of centrifugation and re-suspension of the cells in fresh medium in the presence or not of HU (concentrations used described according to the experiment).

3.5 Amplification of deletion cassettes by PCR.

To delete genes, specific deletion cassettes (different markers) were constructed by PCR.

PCR reaction mix:

100 μl Dynanzyme buffer 10X

100 μl dNTPs (20 mM)

10 μl cassette template specific for marker (10ng/μl)

20 μl Primer reverse (20 mM)

20 μl Primer forward (20 mM)

10 μl Dynanzyme

740 µl ddH_20

Total final volume: 1000 µl

PCR conditions:

3’ 94°C

30’’ 94°C, 30’’ 42°C 1’30’’ 72°C (x 8 cycles)

30’’ 94°C, 30’’ 58°C, 1’30’’ 72°C (x 30 cycles)

7’ 72°C

PCR products were analysed on a 1% agarose/TAE gel and resuspended in TE 1X to a final concentration of 1 µg/µl. DNA was precipitated adding 1/10 Sodium Acetate (NaAc) 3 M and 2.5 volume of iced EtOH 100% and centrifuging (10 minutes, maximum speed, equal to 13 200 rpm, 4°C). Pellets were washed with 1 ml of EtOH 70% and re-centrifuged (2 minutes, max speed, 4°C), dried and re-suspended in sterile TE 1X to reach a final concentration of 1 µg/µl. Different DNA quantities were then used for transformations from this stock solution.

3.6 High efficiency Lithium Acetate (LiAc) yeast transformation.

To generate gene deletion mutants, a high efficiency LiAc transformation protocol as described (Gietz et al., 2007) was used.

Strains to be transformed were grown in 50 ml YPDA in flasks over night and diluted to $5x10^6$ cells/ml. Cells were centrifuged (4000 rpm, 3 minutes, RT) and pellets were washed with 25 ml of sterile water. Cells were centrifuged again, resuspended in 1 ml of LiAC/TE (0.1 LiAc / TE 1X) and transferred to a 1.5 ml Eppendorf sterile tube. Cells were centrifuged (max speed, 15 seconds, RT) and pellets were resuspended in a final volume of 500 μl LiAc (0.1 M). Cells were vortexed to get an homogenous suspension and 50 μl were aliquot in sterile 1.5 ml Eppendorf tubes and used for each transformation. Single strand DNA from salmon sperm testes was used as carrier. Before adding the ssDNA to the transformation mixtures, it was boiled at 95°C for 5 minutes. Cells were centrifuged (max speed, 15 seconds, RT) and the transformation mix was added in the following order:

240 μl polyethylene glycol - PEG 4000 (50% water)

36 μl LiAC 1 M

10.5 single stranded DNA (9.5 μg/ml)

X μl DNA (usually 1-5 μl from 1 μg of the PCR product of deletion)

73.5-X μl DNA sterile water

360 μl: total final volume.

Transformations reaction were vortexed for one minute until the cell pellets were completely mixed and incubated for 40 minutes at 42°C. After the heat shock, cells were centrifuged (6000 rpm, 15 seconds), transformations mix were discarded and cells were resuspended in 200 μl sterile water and plated with sterile rods to distribute the cells on the selective plates. In case of clonat, kanamicyn and hygromycin markers, after the heat shock and the discard of the transformations mixture, cells were resuspended in 5 ml YPDA and grown

for around 4 hours before plating, thus giving them the time to develop the resistance against the antibiotics. The plates were incubated at the permissive temperature for growth and analysed by colony PCR for deletions.

3.7 Colony PCR (Polymerase chain reaction).

Approximately 1 μl of cells were collected with a yellow tip and resuspended in 3 μl 20 mM NaOH in a PCR tube. The solutions so prepared were then boiled at 99°C for 10 minutes and kept at 4°C. For the PCR reaction, the following mix was added to each boiled solution:

2.5 μl dNTPs (20 mM)

0.625 μl Oligo forward (20 μM) (specific for gene deletion)

0.625 μl Oligo reverse (20 μM) (specific for gene deletion) / 0.625 μl Oligo marker reverse (20 μM) (specific for marker)

2.5 μl Dynanzyme buffer 10X

25 μl final volume

The PCR conditions used were the followings:

5’ 95°C

1’ 95°C, 1’ 55°C, 1’ 72 °C (for 35 cycles)

7’ 72 °C

PCR products were analysed on a 1% agarose/TAE gel.

3.8 HU sensitivity spot assay.

Cells were grown in YPDA at 28°C (unless differently stated, as in the case of temperature sensitive *dna2-1*strains) on "96 multi-well plates" over night to reach stationary phase. 10 fold serial dilutions were made and plated on YPDA medium or YPDA containing HU at the indicated concentrations. Plates were then incubated at 28 °C (unless differently indicated).

3.9 FACS analysis.

Cellular DNA content can be determined by FACS or fluorescence activated cell sorter. FACS analysis was performed using a Beckton Dickinson fluorescence activated cell analyzer, as described by Foiani et al., 2000. 2 ml of $1X10^7$ culture cells was centrifuged, blocked with 1 ml of 70% ethanol (EtOH) /Tris 250 mM pH 7.6 and incubated for 1 hour at room temperature (or, alternatively, stored at 4 °C). Cells were then centrifuged for 1 minute at max speed and resuspended in 500 μl of 50 mM Tris HCl pH 7.5 containing 50 μL of Rnase A (10 mg/ml) for one hour at 37°C, to degrade RNA. Then, cells were centrifuged and resuspended in 500 μl of FACS buffer solution (TrisHCl 200 mM/NaCl 200 mM/ $MgCl_2$ 80 mM) containing 50 μL of Propidium Iodide (0.5 mg/ml) for staining. 200 ml of cell suspension was added to 1 ml TrisHCl 50 mM pH 7.6, sonicated to separate the cells for 8 seconds at 25% and used for FACS analysis. The remaining cells were stored at -20°C for further analysis.

3.10 Neutral/Neutral 2D gel electrophoresis procedure.

Bidimensional DNA electrophoresis developed by Brewer and Fangnam (1987) is a technique that allows the analysis of the intermediates of replication arising in a specific DNA fragment. When a DNA portion is replicated, it assumes structures that differ by mass and shape. 2D gel technique allows the separation and the identification of branched DNA molecules according to their mass and shape complexity, so that different signals can generate on a second dimension gel run (Figure 8). The monomer spot signal corresponds to DNA fragments in which DNA is un-replicated. When an active origin of replication fires bi-directionally inside the fragment, bubbles shaped structures with increased mass are generating, as the fork proceed toward the end of the fragment. In case the replication origin is not precisely positioned in the center of the analyzed DNA region, one fork of the bubbles will exit the fragment before the other, generating a Y-shaped structure. A second scenario that generates Y-shaped structures is when the fragment is passively replicated, so that a replication fork enters from one extremity. Depending on their dimension, Y-shaped molecules migrate along the small Y's or the big Y's arc. However, in checkpoint *rad53* mutants HU treated, small Y's signal corresponds to the processing by endonucleolytic activities of the stalled fork. X-shaped molecules, such as four branched structures usually forming during recombination processes, migrate along the spike axes. As explained in details in the results section, checkpoint *rad53* mutants HU treated accumulate four way junction molecules, called fork reversals, that migrate as a diffuse cone signal, generated by the presence of a mixed population of cruciform intermediates of replication spanning from fully duplicated molecules to structures of lower mass generated by nucleases resection activity. In the

absence of *EXO1* nuclease processing, *rad53* mutants accumulate reversed forks of constant mass, that migrate as X-shape intermediates along the spike axes. All the 2D-gel experiments shown in the present PhD thesis were repeated at least twice and the DNA was digested with NcoI restriction enzyme, unless differently indicated.

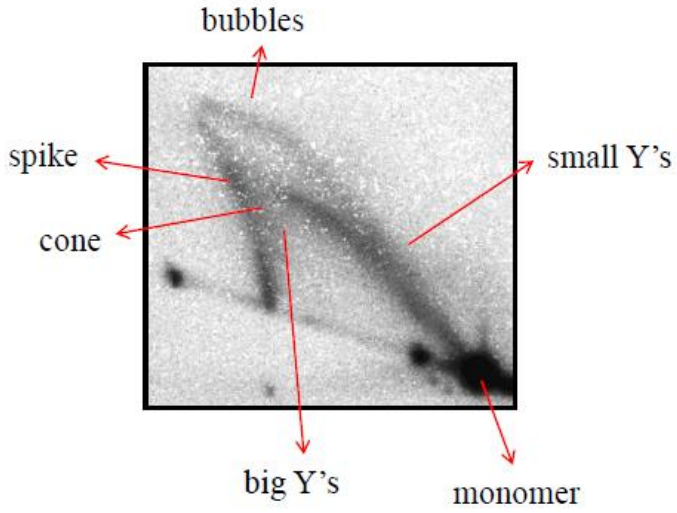

Figure 8. Image of the replication intermediates detectable by 2D gel analysis. Replication intermediates arising in *rad53* cells experiencing replication stress are indicated by red arrows. See text for details.

3.10.1 DNA extraction and *in vivo* psoralen crosslinking.

During the time course, 200 ml of $1x10^7$ cells culture were collected for each of the time points selected for the 2D gel analysis. 2 ml of Sodium Azide 10% were added to the samples that were kept in ice. At the end of the experiment, the collected samples were centrifuged (5000 rpm, 5 minutes, 4°C), supernatants were discarded and then pellets were washed once with 20 ml of ice-cold water.

Then, the psoralen crosslink procedure was performed. Psoralens efficiently intercalate in the double strand DNA and upon irradiation with ultraviolet (UV) light (366 nm) form covalent crosslinks between pyrimidines of opposite strands. Psoralen derivatives easily penetrate the membranes of living cells and Trimethylpsoralen (TMP) is the most commonly used for *in vivo* crosslinking of DNA (Wellinger and Sogo, 1998). Pellets were re-suspended in 5 ml of ice-cold water and transferred into 6 - wells plates. The plates were kept in ice during all the cross-linking procedure. Four cycles of the following passages were performed:

1. 300 μl of psoralen solution (0.2 mg/ml Trioxalen, SIGMA in 100% Ethanol, stored at -20 °C and keep in dark, dissolved by stirring) were added to each well containing the cells and mixed carefully with cut blue tips. Plates were covered with aluminum to avoid contact with light and incubated for 5 minutes at dark.

2. Samples were then irradiated for 10 minutes in a Stratalinker (Stratagene) with 365 nm bulbs at a distance of 2-3 centimeters from the bulbs.

3. Steps 1 and 2 were repeated for three times (one hour total time of the crosslinking procedure, 5 minutes at dark and 10 minutes of irradiation, each cycle).

Samples were transferred from the 6- wells-plates into 50 ml Falcon tubes and each well was then washed twice with 5 ml of ice-cold water to collect all the cells and avoid loss of material. Cells were centrifuged (4000 rpm, 3 minutes) and the dry pellets were stored at -20°C until genomic DNA extraction.

3.10.2 DNA extraction procedure with the Qiagen genomic Kit.

Cells were re-suspended into 5 ml of cold NIB buffer (nuclear isolation buffer) and kept in ice. An equal amount of glass beads was added to the pellets re-suspended in NIB. Falcon tubes were vortexed for 30 seconds at maximum speed and kept in ice after each round of mechanical break. This procedure was repeated for 15 cycles. Cells were collected into JA 25.50 tubes and the beads were washed with 5 ml of NIB buffer (twice). Then, after centrifugation (8000 rpm, 10 minutes, 4°C), pellets were re-suspended in 5 ml of buffer G2. 100 µl of RNAse A (10mg/ml) were added and samples were incubated in a water bath for at least 30 minutes at 37°C, mixing gently sometimes.

After 30 minutes, 100 µl of Proteinase K (20mg/ml) were added and samples were incubated for 1 hour at 37°C, mixing sometimes. Lysates were centrifuged (5000 rpm, 5 minutes, 4°C) and supernatants were diluted in 5 ml of equilibration buffer (QBT). Then supernatants were loaded on Qiagen Tip 100 G anion exchange columns, pre-equilibrated with 4 ml of buffer QBT. Columns were washed twice with 7.5 ml of buffer QC and eluted in corex glass tubes with 5 ml of buffer QF previously warmed at 50°C. DNA was precipitated adding 3.5 ml of isopropanol at RT and centrifuging (25 minutes, 4°C, 8000 rpm) in a Beckman JS 13.1 swing out rotor. Supernatants were collected in clean corex tubes and kept O/N at -20°C to favor the precipitation of residual DNA. The following day those supernatants were re-centrifuged and it was proceed as for the pellets (see above). Pellets were dried and DNA was re-suspended into 150 µl of sterile TE 1X, that was left O/N in agitation. Genomic DNA preparations were stored at 4° C.

3.10.3 DNA digestion.

10 μg of the DNA was digested O/N with the restriction enzymes required. Digestion times longer than 18 hours were avoided due to star activity. The digestion reactions were added 1/8 of the digestion volume of Potassium Acetate 2.5 M and 1 volume of isopropanol (RT). Tubes were inverted several times and centrifuged (10 minutes, max speed, RT). Pellets were washed with 500 μl of EtOH 75%, dried on velvet papers and re-suspended in 20 μl TE1X for at least 1 hour. Before loading, 5μl of loading dye 20X were added to the samples.

3.10.4 DNA electrophoresis.

During a first dimension gel run, the DNA digested fragments are separated according to their mass, in conditions that minimize the contribution of shape to the mobility (low agarose concentration, low voltage, no ethidium bromide).

First dimension gel (0,35% agarose, Low EEO, US Biological in TBE 1X, NO ethidium bromide) was poured at 4°C (it takes approximately 30 minutes to solidify). 20 μl of loading dye 6X were loaded into the wells to check their integrity. The wells were then washed with TBE 1X buffer to remove the dye and the samples were loaded alternating empty lanes to avoid cross contamination after excision of singular lanes for the second dimension run. 25 μ1 of 1 Kb marker were loaded in the first and in the last well of the gel. First dimension was run at RT, 50 V, at time dependent on the size of the DNA fragment analyzed (for 3.4 Kb fragment, around 19 hours are required for a

good separation, while for a 5 kb fragment 21 hours are recommended). Subsequently, the first dimension gel was stained with ethidium bromide (0.3 μg/ml) for 30 minutes and the lanes were separated by cut and so that each gel lines included the linear and the replicated size of the fragment of interest.

The gel slides were then placed in the second dimension gel, rotated at 90° with respect to the direction of the first dimension. The gels for the second dimension are run in conditions that maximize the effect of shape complexity: high agarose concentration (0.9%), high voltage (250 Volts) and with ethidium bromide addition (0.3 μg/ml). Second dimension gels were poured at RT and run at 4°C in TBE 1X buffer containing ethidium bromide (0.3 μg/ml), until the linear DNA line was 1 cm distance from the end of the gel. Then gels were cut up starting from that point 10 cm slides. DNA was de-crosslink by irradiating 10 minutes with 265 nM UV lamps.

3.10.5 Southern blot.

Prior to blotting, second dimension gels were treated as follows: 5 minutes in 0.25 M HCl and then washed with RX water to obtain depurination; 20 minutes in 0.5 M NaOH, 1.5 M NaCl to denature and 20 minutes in 1 M AcNH4, 0.02 M NaOH to neutralize. Gene screen neutral transfer membranes (Perkin Elmer) were equilibrated in SSC 10X for at least one hour and gels were blotted O/N using SSC 10X solution. Then, DNA was fixed to the membrane by UV cross linking using a Stratalinker (Stratagene).

3.10.6 Hybridization procedure.

The membranes were subjected to hybridization with a specific radiolabeled probe. 50 ng of purified DNA probe was labeled with 50 μCi of 32P dCTP using a prime kit (Prime-a-Gene labeling system, Promega). During the preparation of the radiolabelled probe, the membranes were rinsed prehybridized with 50 ml of Hybridisation solution 1X (SIGMA) for at least 30 minutes at 65°C in a rotating tube. The probe was boiled 10 minutes at 99°C and added to 20 ml of pre-hybridization mix. Hybridization was prolonged at 65°C O/N. Filters were then washed twice for 15 minutes with washing solution I (500 ml 2X SSC, 1% SDS) at 65°C and twice for 15 minutes each with washing solution II (500 ml 0.1 X SSC, 0.1% SDS) at 42°C. Signals were detected using a Phosphorimager Molecular Storm 820.

4. RESULTS

The aim of my PhD project was the analysis of the determinants that drive the replication fork collapse in checkpoint mutants, such as *rad53*, under replication stress conditions. As described in the introduction, when replication forks collapse, the replisome detaches from the template DNA at the replication fork and the nascent strands re-anneal together by homology base-pairing, generating the so-called reversed forks (RFs) (Sogo et al., 2002). Reversed forks are four-way junctions, which resemble Holliday junctions (HJs), intermediate structures generating during the homologous recombination repair pathway (Symington and Gautier, 2011). Reversed forks are a potential source of genome instability since they are processed by nucleolytic activities into hemireplicated and gapped molecules containing ssDNA stretches (Sogo et al., 2002), that preclude the completion of replication and cause replication forks loss of functionality (Pelliccioli and Foiani, 2005). In addition, these enzymatic reactions facilitate the engagement of reversed forks in unscheduled homologous recombination events, favoring gross chromosomal rearrangements and loss of genetic information (Cobb et al., 2005). In checkpoint mutants these events can account for the loss of viability in the presence of genotoxic agents, such as the replication inhibitor hydroxyurea (Sogo et al., 2002). To study how the checkpoint preserves the integrity of the replication forks, I used the budding yeast *Saccharomyces cerevisiae* as a model system. The kinase deficient *rad53-K227A* mutants, from now on *rad53*, bear a single amino acid substitution sufficient to render cells checkpoint deficient (Fay et al., 1997). *rad53* cells are highly sensitive to the replication

inhibitor hydroxyurea that induces replication stress by depleting deoxy-ribonucleotide (dNTPs) pools.

The identity and mechanism of action of the factors involved in fork stabilization are still obscure, thus the aim of the present work is to elucidate them. In particular, the main questions we asked were: (1) Does the topology of the replicating chromosomes influence replication fork stability? (2) Which is the identity of the endonucleases that resect collapsed forks? (3) Does the homologous recombination pathway play any role in reversed forks formation and/or replication fork stability?.

4.1 Visualizing reversed forks *in vivo*.

Reversed forks are cruciform structures that, as other replication intermediates, can be visualized by electron microscopy (EM) and neutral/neutral two dimensional gel electrophoresis (2D gels) techniques (Sogo et al., 2002; Cotta-Ramusino et al., 2005). My first aim was to set appropriate 2D gels experimental conditions for the detection of fork reversal events. Thus, I conducted a pilot experiment following the conditions described by Cotta-Ramusino and colleagues (2005), which had demonstrated that the endonuclease Exo1 counteracts fork reversals in *S. cerevisiae*. I arrested *rad53* and *rad53exo1Δ* mutants in G1 and I released them in the presence of 200 mM hydroxyurea, taking samples for 2D-gel analysis at 90 and 120 minutes after release. Accordingly with the report cited above, *rad53* mutants accumulated reversed forks that migrate as a diffuse cone signal, arising by a mixed population of cruciform replication intermediates ranging from fully duplicated

molecules to structures of lower mass generated by Exo1-dependent resection events (Figure 9). Upon *EXO1* deletion *rad53* mutants accumulate X-shaped intermediates of equal mass, resembling the X-shaped sister chromatid junctions observed in wild type cells, previously interpreted as hemicatenaned sister chromatids (Lopes et al., 2001; Cotta-Ramusino et al., 2005) (Figure 9).

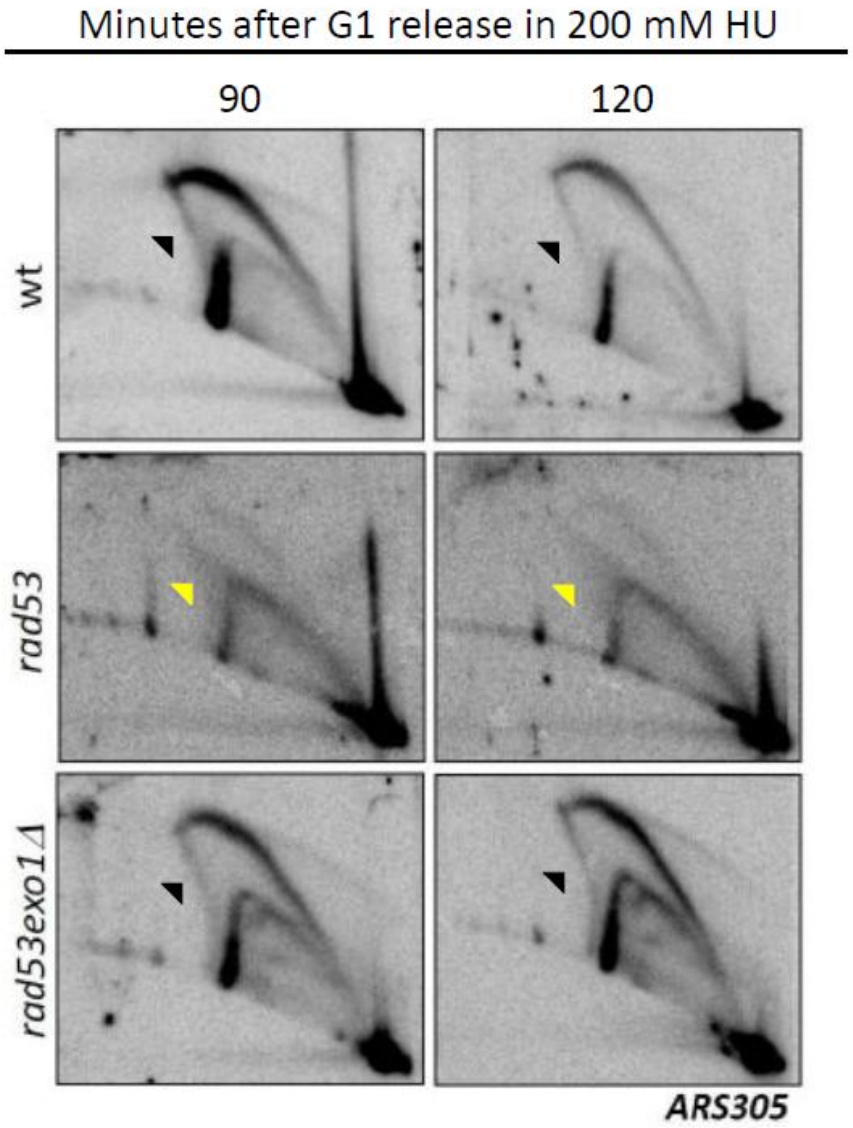

Figure 9. Replication intermediates in wt, *rad53* and *rad53exo1Δ* cells following HU treatment in the absence of psoralen crosslink. 2D gel analysis of replication intermediates accumulating in the *ARS305* region in wt, *rad53* and *rad53exo1Δ* cells 90 and 120 minutes after release from an α-factor induced G1 block into S-phase in

the presence of 200 mM HU. Black arrowheads indicate the position of unresected X-shaped intermediates, while the yellow ones of the cone signal.

In order to better preserve the topological transitions occurring at replication forks, I conducted 2D-gel experiments, stabilising replication intermediates by *in vivo* psoralen crosslinking (Figure 10A) (Lopes et al., 2001; Doksani et al., 1999). *rad53* mutants showed a cone signal, corresponding to Exo1-resected reversed forks, at all the time points analysed (Figure 10A). In contrast, *rad53exo1Δ* mutants accumulated fully duplicated X-shaped molecules that migrated along a spike (Figure 10A). This signal can be interpreted as un-resected reversed forks, as supported also by electron microscopy data (Lopes et al., 2001). In wt and *exo1Δ* cells replication origins fired, as indicated by the bubbles and big Y's signals, but cruciform intermediates did not accumulate (Figure 10A).

Therefore, stabilising replication intermediates *in vivo* by psoralen treatment allowed us to preserve reversed fork cruciforms in *EXO1*-deleted *rad53* mutants, different from the X-shaped hemicatenated junctions that were not observed in wt cells (see figure 9). Thus, the transition in the 2D-gel signals from a cone signal (correspondent to resected RFs) to a spike signal (correspondent to intact RFs) reflects the lack of reversed forks structures processing *in vivo*.

Intriguingly, under these experimental conditions and at late time points (180 minutes), we noticed the accumulation of branched intermediates with lower mass, that form a prominent signal along the small Y's-arc in *rad53exo1Δ* mutants (Figure 10A). This signal could be interpreted as the product of

nucleolytic branch cleavages at the collapsed forks (see Figure 22) and it was previously observed in other checkpoint deficient cells (Doksani et al., 2009).

rad53 mutants are sensitive to HU concentrations much lower than 200 mM (Pike et al., 2003). I carried out the 2D-gel analysis treating the cells with 25 mM HU to analyse if fork reversal also takes place in checkpoint mutants at lower concentrations of the drug (Figure 10B). Of notice, both *rad53* and double mutant *rad53exo1Δ* accumulated X-molecules migrating along the spike signal to an equal extent (Figure 10B), while intermediates migrating in the cone signal were almost not visible. This experiment suggests that Exo1 has a minor contribution to reversed fork processing at lower HU concentrations, although reversed forks still form in checkpoint defective mutants.

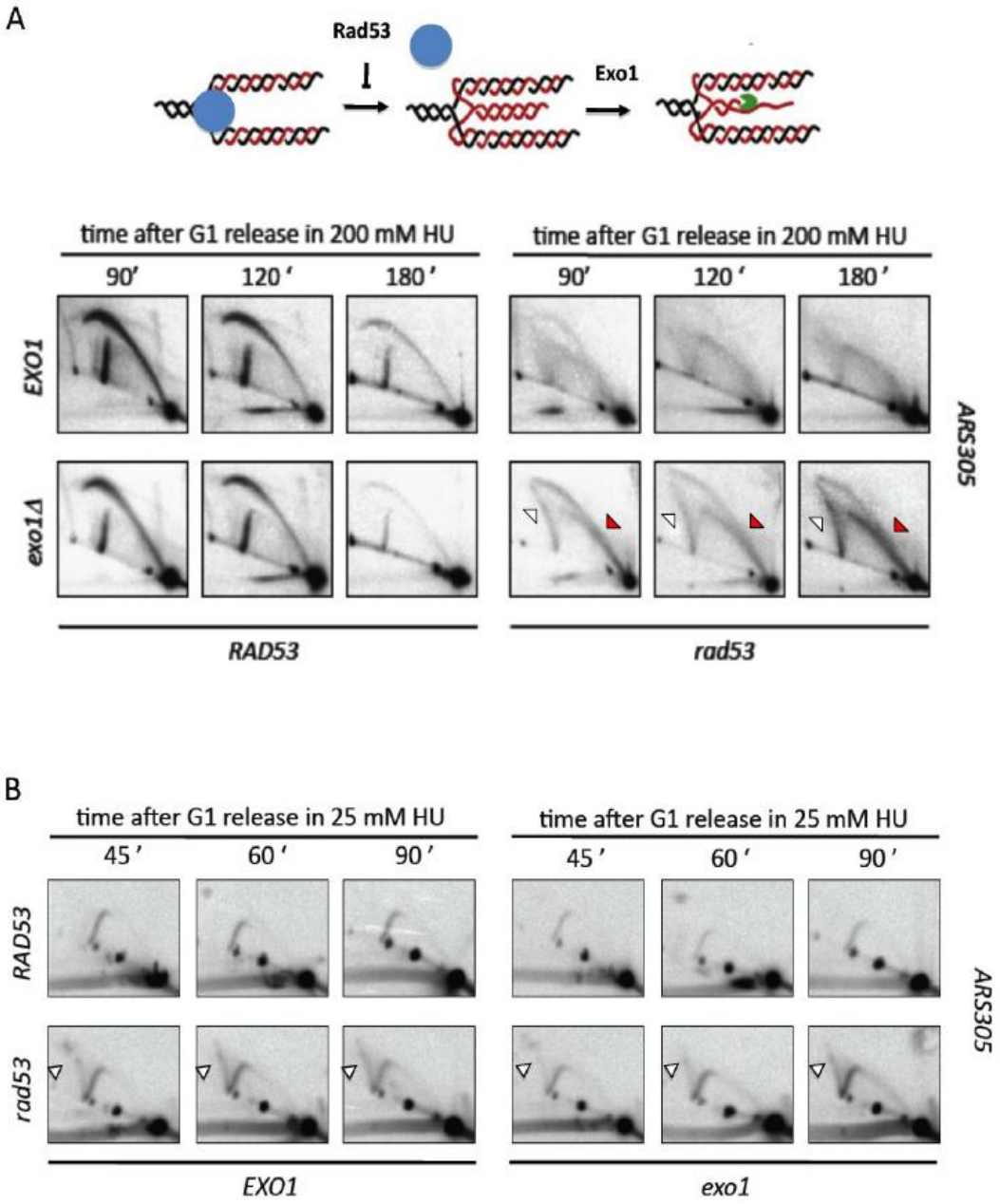

Figure 10. Replication forks reversal and resection in *rad53* and *rad53exo1Δ* cells following psoralen crosslink. (A) Fork collapse and resection following HU treatment: schematic representation of fork transitions (the blue circle represents the replisome) and 2D-gel analysis of replication intermediates accumulating in the *ARS305* region in WT, *exo1Δ*, *rad53* and *rad53exo1Δ* cells 90, 120 and 180 minutes after release from an α-factor induced G1 block into S-phase in the presence of 200 mM HU. Red arrowheads indicate the position of the fork branch-cleavage, while the white ones indicate X-shaped reversed forks. (B) 2D gel analysis of replication intermediates accumulating at the *ARS305* region in WT, *rad53*, *exo1Δ* and *rad53exo1Δ* cells at the indicated times (minutes) after release into S-phase in the presence of 25 mM HU. White arrowheads indicate the position of reversed forks.

I performed a 2D gel recovery experiment to evaluate reversed fork stability upon removal of HU from the culture medium. I treated *rad53* and *rad53exo1Δ* mutants with 200 mM HU for three hours, I washed the cells from the drug and released them in fresh YPDA medium for additional three hours, taking samples for 2D gel analysis at each hour (Figure 11). Bulk genomic DNA content analysis by FACS revealed that both mutants are unable to synthesize DNA during the recovery from the HU treatment and do not proceed further in the cell cycle (Figure 11B). Of notice, double mutants *rad53exo1Δ* accumulated reversed forks upon HU treatment, that persisted after the removal of the drug and the release in fresh medium along all the time points considered until the end of the experiment (Figure 11A). In contrast, *rad53* cells accumulated aberrant replication intermediates, as indicated by the presence of the cone and the small Y signals, that progressively disappeared within time after the washing from the drug, likely due to Exo1-dependent metabolism (Figure 11A).

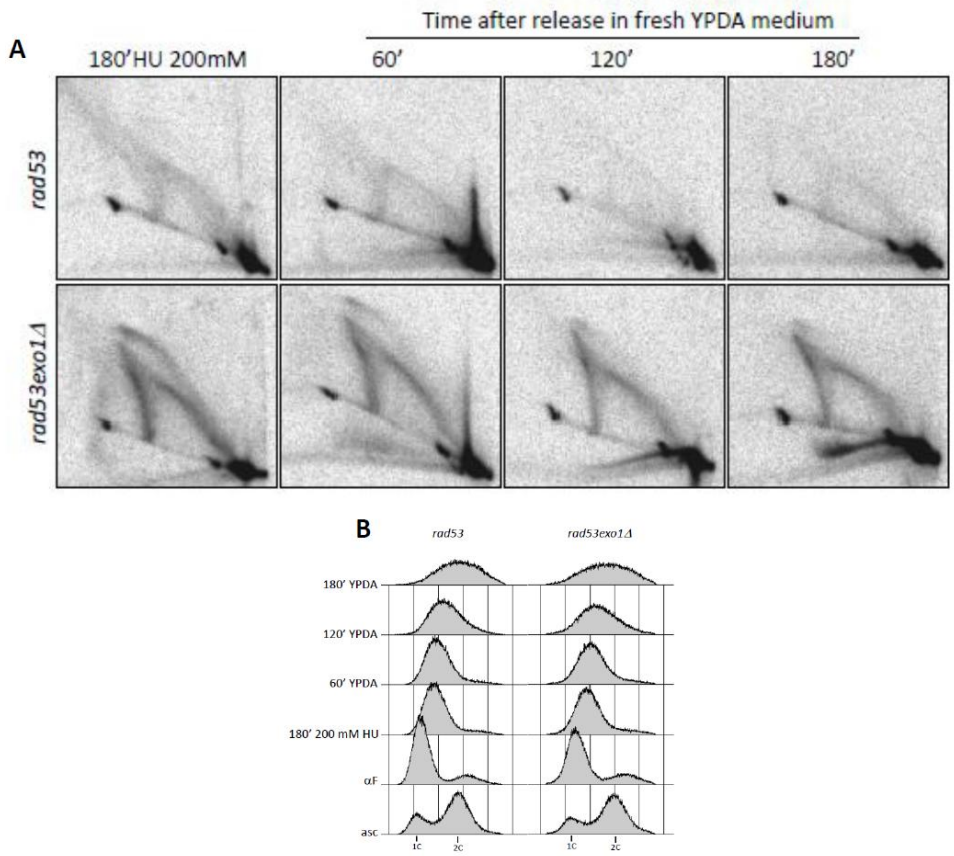

Figure 11. *EXO1* deletion results in a longer persistence of reversed forks during recovery to HU in checkpoint mutants. (A) 2D gel analysis of replication intermediates accumulating in *ARS305* in *rad53* and *rad53exo1Δ* mutant cells arrested in G1, treated with 200 mM HU for 3 hours and release in S-phase in fresh YPDA medium at 90, 120 and 180 minutes. (B) FACS analysis.

This experiment suggests that reversed forks formed in *rad53* mutants experiencing replication stress are progressively degraded in an Exo1-dependent fashion.

4.2 Analysis of the topological determinants modulating fork stability.

4.2.1 An experimental system for the analysis of the topological relaxation.

In vitro data show that reversed forks can form spontaneously at positively supercoiled plasmids upon replisome dissociation (Postow, Ullsperger et al., 2001). This observation implies that the accommodation of the energy accumulating as torsional stress (or positive supercoiling) in un-replicated DNA portions during template unwinding could drive the re-annealing of the parental strands and cause the formation of reversed forks (Postow, Ullsperger et al., 2001). In turn, the regression of the fork branching point could displace the nascent strands, favoring their base-pairing by homology (Postow, Crisona et al., 2001). These data made us reason that these transitions could occur also *in vivo* in checkpoint mutants in conditions of replicative stress, when the replisome is not stably attached to the replication fork (Lucca et al., 2004; Cobb et al., 2005). The hypothesis we considered was the following: if the stability of the replication forks in *rad53* mutants is susceptible to the topological stress accumulating during the replication of chromosomal topological domains, induction of a double stranded DNA break, relaxing DNA topology by creating a discontinuity in the helix that allows the rotation of the free ends, should counteract forks reversal (Figure 12).

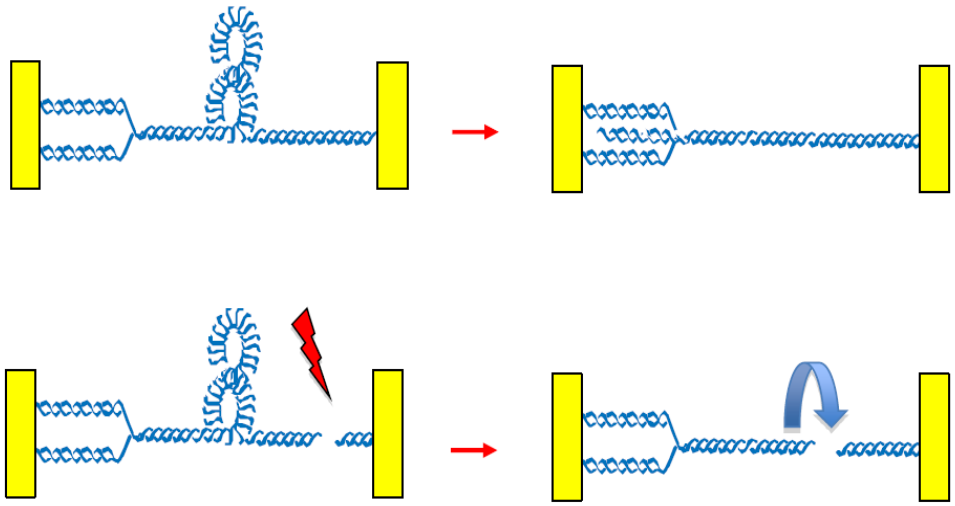

Figure 12. Schematic representation of the expected result on replication fork reversal of DNA topology relaxation by induction of a double strand break. Regions between yellow bars indicate a domain topologically isolated from the rest of the chromosome. We reasoned that if the stability of the replication fork does depend on the topological context, reliving this topology by introducing a DSB should suppress fork defects occurring in *rad53* mutants.

To further investigate and elucidate those cellular processes influencing replication fork stability by altering the topological state of replicating chromosomes, I took advantage of a genetic system that allows the relaxation of the topological tension accumulated within a region between replication forks and a highly transcribed gene. This experimental system comprises an ectopic consensus sequence for the HO endonuclease inserted between the early origin of replication *ARS305* (2 Kb distant) and the most proximal transcribed gene *PDI1*, on chromosome III (Doksani et al., 2009). In this system, the gene coding HO is placed under the galactose inducible *GAL1* promoter, so that the presence of this sugar in the medium causes HO endonuclease over-expression and the induction of a single un-reparable Double Strand Break (DSB) (Lee et al., 2000).

I combined strains carrying the HO site, referred to as "HO-cut" strains, with checkpoint deficient allele *rad53* and I generated, as controls, strains carrying a mutated version of the HO site that cannot be cut by HO, referred to as "HO-inc" strains. As a control of the specificity of potential effects on the topology of the *ARS305* region, I also analyzed the replication intermediates emanating from a second early replication origin, *ARS202*, which is topologically isolated from the *ARS305* domain since it is located on a different chromosome and therefore not affected by the induction of the break. I designed a restriction strategy that allowed visualizing both *ARS305* and *ARS202* forks using the same restriction enzymes digestion (Figure 13).

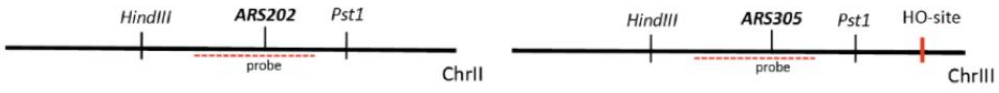

Figure 13. Schematic representation of the 2D gel strategy used to analyze the effect of DSB-induced topological simplification on fork reversal. The position of the HO-endonuclease and *HindIII* and *PstI* restriction enzymes on the regions on chromosome II and III analyzed is indicated.

To test the efficiency of DSB induction, I conducted a pilot experiment using wt-inc, wt-cut, *rad53*-inc and *rad53*-cut mutant strains. I arrested cells in G1 with α-factor, I waited until at least 80% of the culture was in G1 and I added galactose to the media for one hour to induce HO expression. I released the cells in S-phase in 25 mM of HU and I took samples 60 minutes after the release (Figure 14). In "cut" strains a DNA 4 kb fragment correspondent to the presence of the cut was observed in over a 90% of cells, while it was not present in the "inc" strains (Figure 14). This indicates that DSBs are efficiently induced during the G1 arrest prior to origin firing.

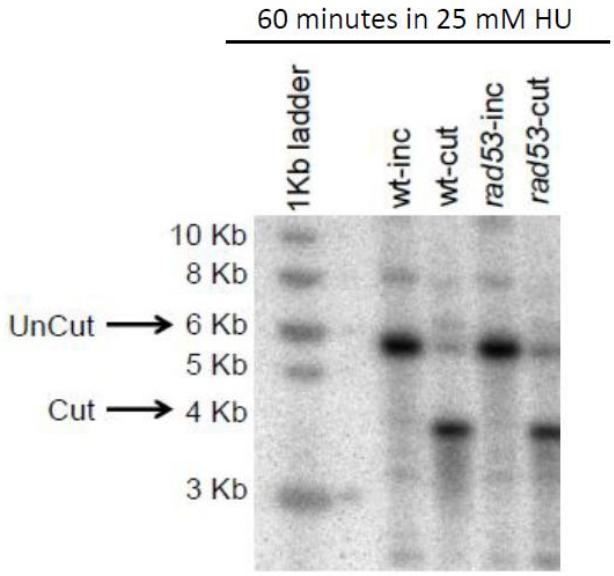

Figure 14. DSBs formation efficiency. Southern blot analysis to monitor DSBs formation efficiency in WT and *rad53* mutant strains, carrying a HO cut site (cut) or non - cuttable version (inc). HO cut was induced by addition of galactose to the culture medium when approximately 80% of the cells were arrested in G1. Genomic DNA was double digested with *HindIII* and *PstI* restriction enzymes and analyzed by southern blot with *ARS305* probe. In the *HO* strains, the presence of a 4 kb-fragment is detected as a consequence of the break.

4.2.2 Fork reversal is counteracted by double strand break-induced topological relaxation.

To test the *in vivo* contribution of topological relaxation on fork regression in checkpoint mutants, I compared by 2D gels replication fork collapse and progression in control strains (wt-inc and *rad53*-inc) and strains carrying the HO cut site (wt-cut and *rad53*-cut). I arrested the cells in G1 and I induced DSBs formation adding galactose to the medium for one hour, to give the cells the time to over-express the HO endonuclease. I released the cells into S-phase in the presence of 25 mM HU and I analyzed replication intermediates at early origin *ARS305* at 60, 90 and 120 minutes after release. I observed that in wild

type cells *ARS305* origin fires, regardless the presence or absence of the break, as indicated by the presence of big Y intermediates (Figure 15). In contrast, in HU-treated HO-inc *rad53* cells X-shaped intermediates corresponding to reversed replication fork accumulate (Figure 15). Of notice, DSB induction strongly reduced reversed-fork increase in HO-cut *rad53* mutants at each of the time points considered (Figure 15). This experiment suggests that resolving the topological constrains accumulated during replication counteracts reversed forks formation, implicating that positive supercoiling might be a driving force causing fork reversal *in vivo*.

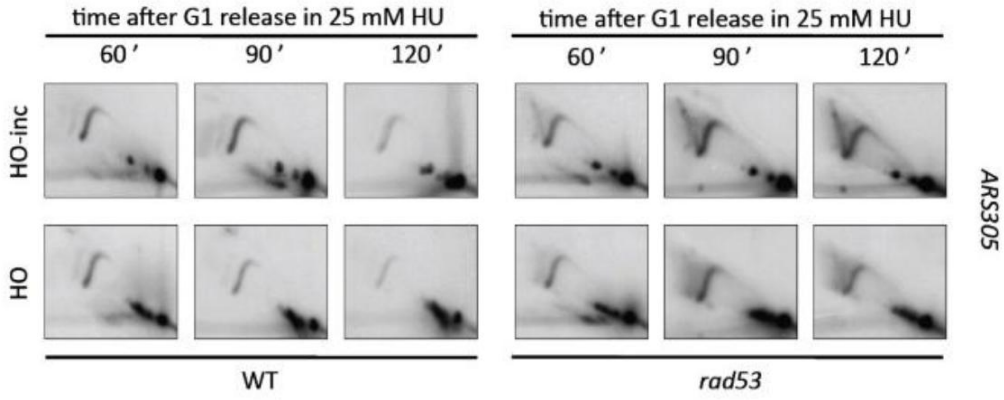

Figure 15. DSB induction counteracts fork reversal in *rad53* mutants. 2D gel analysis of replication intermediates in WT HO-inc, WT HO, *rad53* HO-inc and *rad53* HO cells following α-factor dependent arrest in G1, DSB induction by galactose addition, and release into S-phase in the presence of 25 mM HU.

To validate this result and control that the observed reduction in reversed forks accumulation was specific for the presence of the break, I hybridized the same membranes with a probe specific for *ARS202*, located on chromosome II. In both wild type strains (inc and HO) *ARS202* origin fired, as indicated by the presence of bubble-shaped replication intermediates (Figure 16). Similarly,

ARS202 fired in both HU-treated HO-inc *rad53* and HO-cut *rad53* cells, but in contrast to what observed for *ARS305*, the accumulation of X-shaped intermediates was equally detected in checkpoint mutant strains regardless the induction of a DSB in *ARS305* (Figure 16).

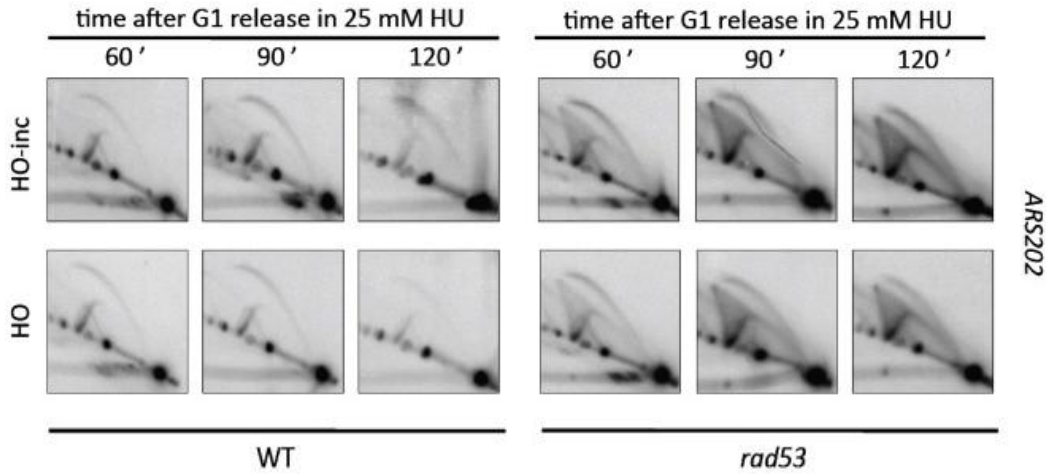

Figure 16. Forks reversal decrease is specific for the presence of the DSB. 2D gel analysis of replication intermediates in WT HO-inc, WT HO, *rad53* HO-inc and *rad53* HO cells following α-factor dependent arrest in G1, DSB induction by galactose addition and release into S-phase in the presence of 25 mM HU.

Quantification of reversed forks at *ARS305* and *ARS202* in *rad53* cells indicated an equal proportion (with a ratio of approximately 1) in HO-inc strains, while a dramatic decrease (ratios from 0.4 to 0.6) was observed in HO- strains (Figure 17). These data showed that the reduction in forks reversal accumulation detected in HO-cut *rad53* mutants is specific for the presence of the break, since *ARS202*, located in a different topological context, was not affected.

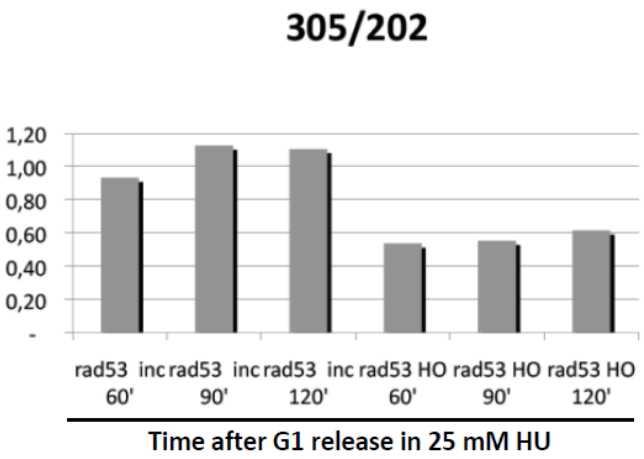

Figure 17. Spike signal ratio between *ARS305/ARS202* in *rad53* inc and HO strains. Histograms indicating the ratio (in arbitrary units) between reversed forks signal intensities at *ARS305* and *ARS202* detected in *rad53* mutants at the time points considered. The experiment was repeated twice.

Thus, this experiment suggests that local positive supercoil accumulation drives for reversal when replisome stability is challenged in checkpoint deficient cells.

4.2.3 Reduction in reversed fork accumulation upon DSB induction is not affected by ablation of *EXO1*.

I noticed that HO-cut *rad53* mutant strains accumulated a slight "cone-like shadow" close to the spike signal. I had previously shown that Exo1 does not have a significant contribution to reversed forks processing at 25 mM HU (Figure 10B), however Exo1 could play a role in the resection of the DSB generated in this kind of experiment. To exclude the possibility that the reduction in the reversed forks observed was somehow related to DSBs resection, I deleted *EXO1* in wt-inc, wt-cut, *rad53*-inc and *rad53*-cut strains to

visualize replication intermediates in these mutants upon HU treatment. I arrested in G1 the cells, added galactose to the media to induce the activation of HO endonuclease and I took samples at 45, 60 and 90 minutes after release. I observed the firing of *ARS305* in both *exo1Δ*-HO-inc and *exo1Δ*-cut strains, as indicated by the presence of the large Y-intermediates signal (Figure 18A). Accordingly with the data obtained in the previous experiment, comparing HU-treated mutants *exo1Δ*-HO-inc *rad53* and *exo1Δ*-cut *rad53,* I observed a strong reduction in the accumulation of X-shaped intermediates in the latter (Figure 18A), shown also by the quantification of the signals (Figure 18B). This experiment demonstrates that the decrease in reversed forks accumulation upon induction of a DSB is independent of Exo1-mediated resection. Therefore, this experiment further reinforces the idea that positive supercoiling can act as a driving force for replication fork reversion.

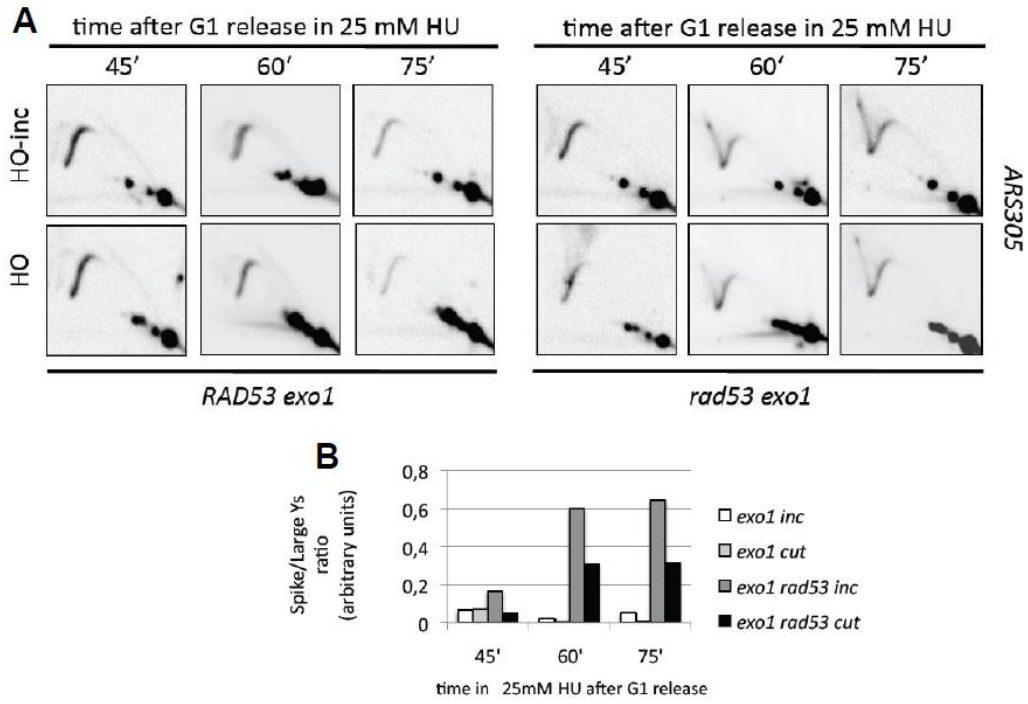

Figure 18. DSB-dependent reduction in reversed-fork accumulation is not affected by ablation of *EXO1*. (A) 2D gel analysis of replication intermediates in *EXO1* deleted strains *exo1Δ* HO-inc, *exo1Δ* HO, *rad53exo1Δ* HO-inc and *rad53exo1Δ* HO following an α-factor dependent arrest in G1, DSB induction by galactose addition, and release into S-phase in the presence of 25 mM HU. (B) Quantification of the spike signal intensities at *ARS305* in the different time points is shown. The experiment was repeated twice.

4.2.4 Cruciform structures accumulate in checkpoint-proficient cells following genetic inactivation of Top1 and Top2.

To further investigate the role of topology on replicating chromosomes stability, I performed complementary experiments to test the effect on replication forks of the concomitant inactivation of DNA topoisomerase I - Top1 - and DNA topoisomerase II - Top2, expected to entirely preclude topological constrains resolution. As previously described in the introduction section, these two enzymes are entirely responsible for the removal of positive

supercoiling arising during DNA replication, thus sustaining the elongation step of this process (Wang, 2002).

Since *TOP2* is an essential gene in the yeast *S. cerevisiae*, I took advantage of a conditional allele *top2-1*, in which the enzyme is inactivated at a temperature of 37 °C. I compared the replication intermediates in *top1Δtop2-1* and *top1Δtop2-1rad53* mutant strains by 2D gel. I released the cells previously arrested in G1 at the permissive temperature of 25°C for 30 minutes to allow replication to start and then I performed a second release by shifting at the non-permissive temperature of 37°C. I observed the accumulation of X-shaped molecules in *top1Δtop2-1* cells, both in checkpoint proficient and deficient backgrounds, upon Top2 inactivation (Figure 19A). Progressive X-shaped molecules accumulation was also shown by quantification of the 2D gel signals (Figure 19B). These data show that inactivation of both Top1 and Top2 leads to the accumulation of replication intermediates with a 2D gel migration pattern compatible with reversed forks (Bermejo et al., 2007) even in the absence of HU treatment and in checkpoint proficient cells. Thus, this experiment strongly sustains the idea that the topological context can affect the stability of replication forks further supporting the notion that accumulation of mechanical strains is the main cause of forks reversal *in vivo*.

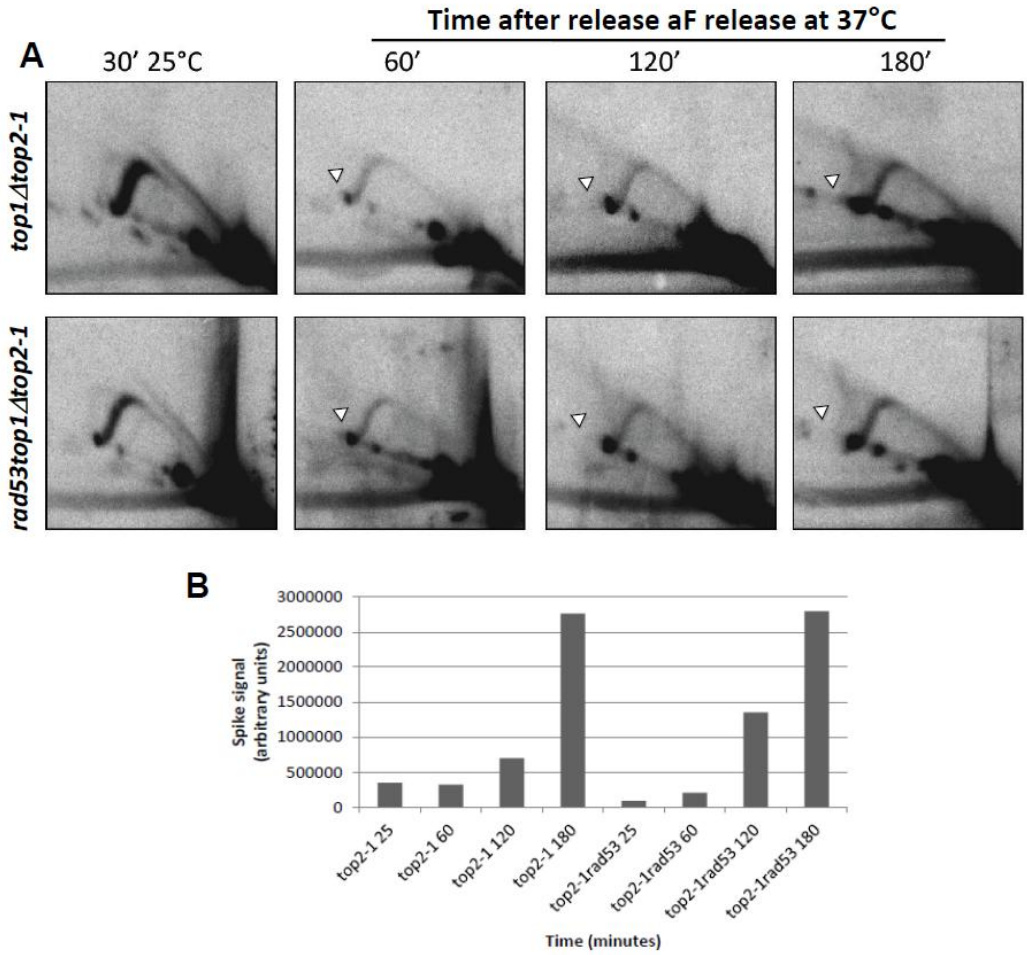

Figure 19. X-shaped molecules resembling reversed forks accumulate upon contemporary inactivation of Top1 and Top2 activities. (A) 2D gel analysis of replication intermediates at *ARS305* region in *top1Δtop2-1* and *top1Δtop2-1rad53* cells released from an α-factor induced G1 block into S-phase at 25 ºC (permissive temperature for the *top2-1* allele). After 30 minutes cells were transferred to fresh medium pre-warmed to 37 ºC, in order to inactivate Top2, and samples were collected at the indicated time points and psoralen cross-linked. White arrowheads indicate the position of cruciform molecules migrating as spike signals. (B) Quantification of the spike signal intensities at the different time points (minutes) is shown. The experiment was repeated twice.

4.2.5 Over-expression of Top2 reduces reversed-fork accumulation.

I proceeded analysing the effects of over-expressing Top2 on replication intermediates in checkpoint mutants experiencing replication stress. An increase of Top2 levels is expected to reduce the steady-state levels of positive supercoiling leading to an overall relaxation of the DNA within replicated topological domains. I arrested in G1 strains wt and *rad53* carrying an empty vector *PYESGAL1* (e/v) or a vector over-expressing DNA topoisomerase II under the control of the galactose promoter *GAL1* (Figure 20A). I added galactose to the media to induce Top2 over-expression (Bermejo et al., 2007) and I released the cells in 25 mM HU. Comparing the replication intermediate profiles, I observed a reduction in reversed-fork accumulation in checkpoint-defective cells over-expressing Top2 (Figure 20B). Thus, reducing the topological stress *in vivo* counteracts replication fork reversal, further supporting the hypothesis that topology is a key player in mediating this process.

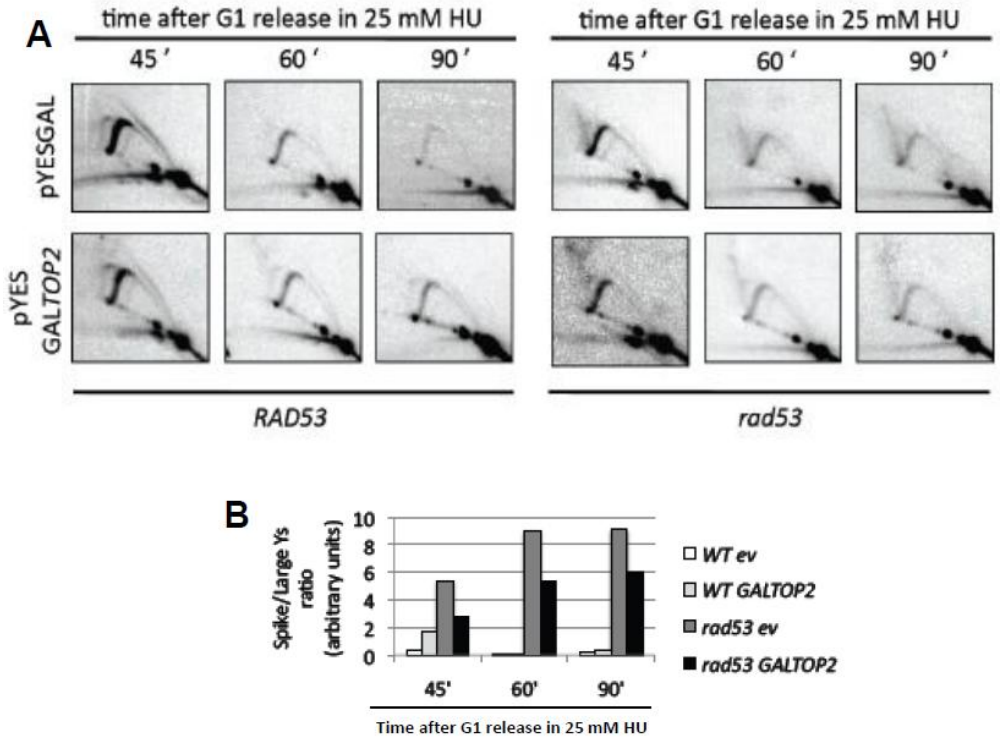

Figure 20. *TOP2* over-expression counteracts reversed-fork accumulation. (A) 2D gel analysis of replication intermediates in WT *empty vector (pYESGAL)*, WT *GALTOP2*, *rad53 empty vector (pYESGAL*) and *rad53 GALTOP2* strains released from an α-factor induced G1 block into S-phase in the presence 25 mM HU. (B) Quantification of the spike signal intensities detected at *ARS305* in the corresponding time points analysed is shown. The experiment was repeated twice.

Noteworthy, *TOP1* over-expression also partially decreased reversed forks accumulation (Figure 21A and B), although the effect is less evident than the one observed upon over-expression of *TOP2*.

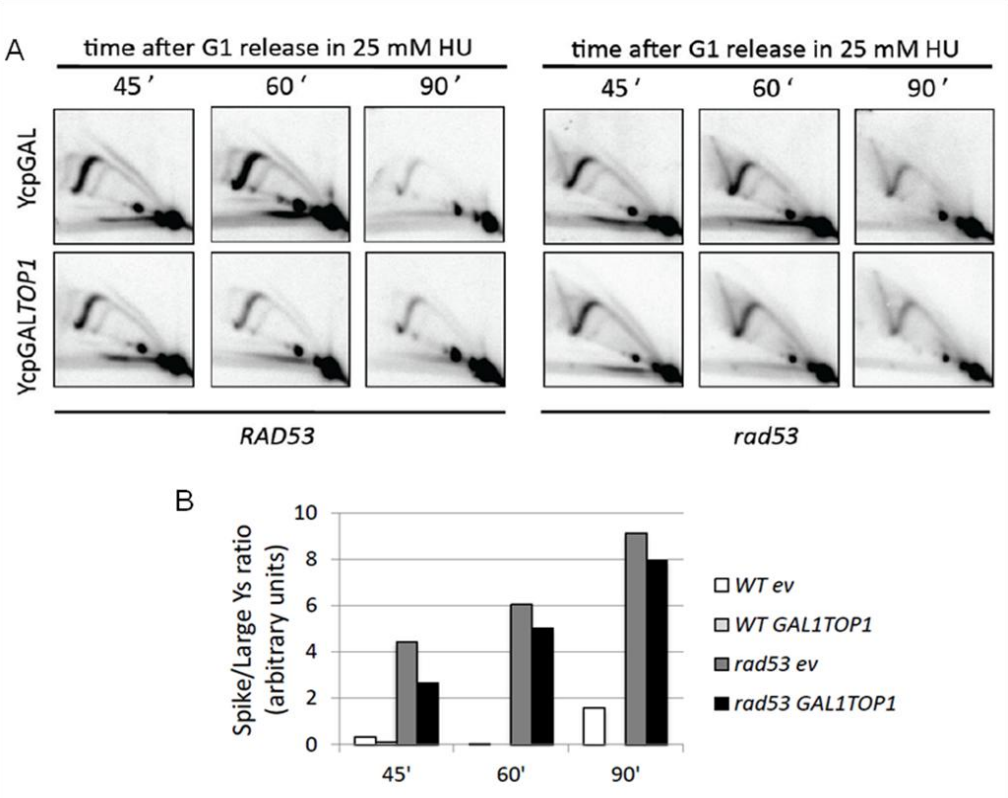

Figure 21. *TOP1* over-expression marginally counteracts reversed-fork accumulation.

(A) 2D gel analysis showing replication intermediates at *ARS305* of WT *empty vector (WT-GAL1),* WT *GALTOP1*, *rad53 empty vector (rad53GAL1*) and *rad53 GAL1TOP1* strains released from an α-factor induced G1 block into S-phase in the presence 25 mM HU. (B) Quantification of the spike signal (arbitrary units) intensities detected at *ARS305* in the corresponding time points analysed is shown. The experiment was repeated twice.

In both the experiments, and more noticeable upon Top1 over-expression, we detected the residual presence of reversed forks, suggesting a partial persistence of topological constrains not fully eliminated by topoisomerases over-production in these strains.

Altogether these data constitute the first *in vivo* demonstration indicating that the torsional strain accumulated during replication is a determinant driving the collapse and reversion of replication forks.

4.3 Identification of nucleases acting on collapsed replication forks.

4.3.1 An "educated guess 2D screen".

In checkpoint mutants, stalled replication forks undergo pathological events due to the formation of aberrant replication intermediates that become exposed to unscheduled nucleolytic processing (Cotta-Ramusino et al., 2005; Sogo et al., 2002). These events likely contribute to abrogate replication fork re-start and viability in checkpoint mutants after exposure to HU (Lopes et al., 2001; Sogo et al. 2002; Segurado and Diffley, 2008). As mentioned previously, the *S. cerevisiae* endonuclease Exo1 is a well characterized example of this as it processes reversed forks into gapped and hemireplicated structures (Cotta-Ramusino et al., 2005; Sogo et al., 2002) leading to the formation of DNA double strand breaks and extended single stranded DNA patches, that might provide templates for unscheduled recombination events at replication forks (Cobb et al., 2005).

As described previously (see section 4.1), two prominent phenotypes are observed when comparing replication intermediates of *rad53exo1Δ* and *rad53* cells treated with 200 mM HU. First, a transition from a cone signal, correspondent to resected forks, to a spike signal, correspondent to unprocessed reversed forks. Second, the accumulation of a prominent small Y's signal during time, compatible with a branch cleavage at the fork junction by an unknown factor "X" (Figure 22).

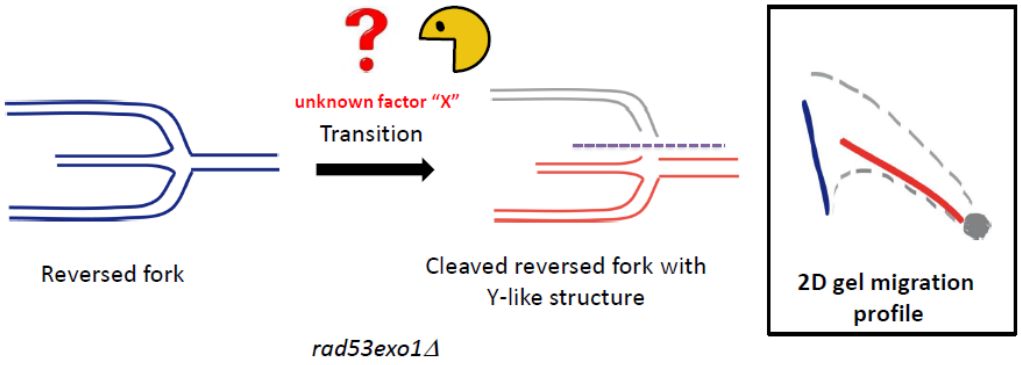

Figure 22. Interpretation of the 2D gel pattern observed in HU treated *rad53exo1Δ* mutants. Un-resected cruciform reversed forks (in blue) generate a spike signal, while cleavage of a branch of regressed forks by unknown factors would give rise to Y-like structure intermediates characterized by lower mass (in red), that migrate along the small Y's arc.

Nevertheless, a faint cone signal evidencing residual nucleolytic resection events is detected in *rad53exo1Δ* mutants (Figure 10A), strongly suggesting the involvement of additional factors in collapsed forks processing. Consistently, ablating *EXO1* is not sufficient to suppress checkpoint mutants' sensitivity to HU (Segurado and Diffley, 2008). The identity of additional nucleases acting at collapsed forks remains elusive.

The second part of this work was aimed at unmasking novel players involved in collapsed fork metabolism and loss of functionality. More precisely, I aimed at identifying an endonuclease "X" able to mediate the branch-cleavage transition observed at forks in *rad53exo1Δ* mutants. To reach this purpose, I designed an "educated guess" 2D gel screen, analysing by 2D gel electrophoresis, the effects on the structure of replication intermediates of the ablation of candidate nucleases in *rad53* or *rad53exo1Δ* genetic backgrounds.

The identification of the factors that contribute to replication forks loss of functionality under replication stress conditions is an extremely relevant matter as it might shed light on the mechanisms that generate pathological chromosomal rearrangements and the consequent loss of genome integrity observed in checkpoint mutants.

4.3.2 2D-gel screen: experimental conditions and first candidates.

All the experiments carried on in this part of the project focused on the early origin *ARS305* and I adopted the following experimental conditions: cells arrest in G1 by α-factor treatment, release in S-phase in the presence of 200 mM HU, sampling at late time points (90, 120,180 minutes) and *in vivo* psoralen crosslink.

The first candidates I decided to test were members of the Structure Specific Endonucleases (SSEs) family, Mus81, Yen1, Slx1 and Rad1. These enzymes are the sole Holliday Junctions resolvases currently known in *S. cerevisiae*, and act specifically on different kinds of DNA four way junction structures (Swartz et al., 2011). Cells have developed a wide range of conserved structure specific nucleases characterized by different substrate specificities in order to resolve DNA joint molecules, such as Holliday junctions (HJs), as well as flaps or various structures arising at both damaged replication forks or during unperturbed replication (Schwartz et al., 2011). Reversed forks are four-way junctions molecules that resemble HJs and can acquire conformations resembling other structurally analogue intermediates arising during physiological cellular processes, such as repair and replication, thus favoring

unscheduled chromosome rearrangements and genome instability (Branzei and Foiani, 2010). Furthermore, in cells lacking a functional checkpoint, structure specific endonucleases generate aberrant replication intermediates by endonucleolytic cleavage upon anticipation of mitotic entry due to premature CDK1 inactivation (Neelsen et al., 2013).

Thus, I reasoned that these enzymes, able to recognize and resolve four way-junction structures, were likely candidates to mediate the collapsed fork branch cleavage observed in *rad53exo1Δ* mutants, since they biochemically target these kind of DNA joint molecules (Figure 23).

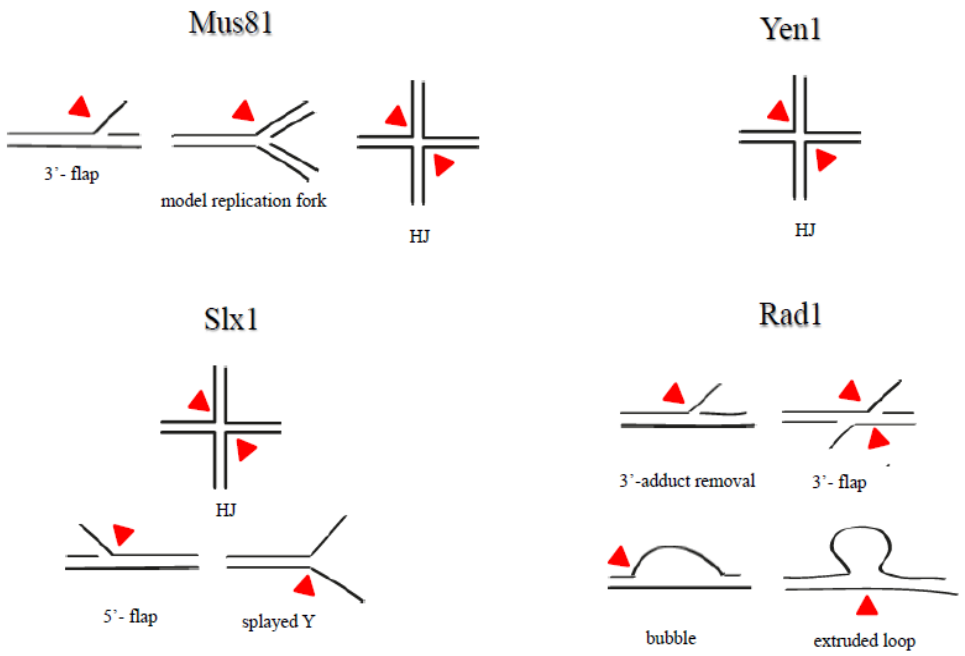

Figure 23. Schematic representation of the preferred substrates of structure specific endonucleases. Mus81, Yen1, Slx1 and Rad1 incision sites are indicated by red triangles.

4.3.3 The structure specific endonucleases Mus81, Yen1, Slx1 and Rad1 are dispensable for collapsed forks branch cleavage.

4.3.3.1 Analysis of Mus81 role in collapsed fork processing.

The *Saccharomyces cerevisiae* Mus81 nuclease is able to *in vitro* cleave DNA branched structures that resemble replication forks (Whitby et al., 2002) and its depletion makes the cells sensitive to chemicals that interfere with fork progression, such as HU (Blanco et al., 2010).

Intriguingly, *Schizosaccharomyces pombe* Mus81 is regulated by the Rad53 homolog Cds1 during replication stress (Kai et al., 2005) and process stalled replication forks in the absence of a functional DNA replication checkpoint (Froget et al., 2008; Doe et al., 2002). Recent data show that *MUS81* ablation increases fork reversal accumulation upon oncogene over-expression in human cells (Neelsen et al., 2013).

To analyze the contribution of Mus81 to collapsed fork processing, I performed 2D gel analyses in *rad53, rad53mus81Δ, rad53exo1Δmus81Δ* and *rad53exo1Δmus81Δ* mutants. Although the signals detected were very low, I failed to observe differences between replication intermediate patterns of *rad53* and *rad53mus81Δ* cells (Figure 24), which accumulate resected replication forks with time. Deletion of *MUS81* did not change the replication intermediates profile of *EXO1*-ablated checkpoint mutants as both the strains accumulated spike and prominent small Y signals with equivalent intensity and

kinetics (Figure 24). These observations suggest that *MUS81* is dispensable for the branch cleavage of collapsed forks.

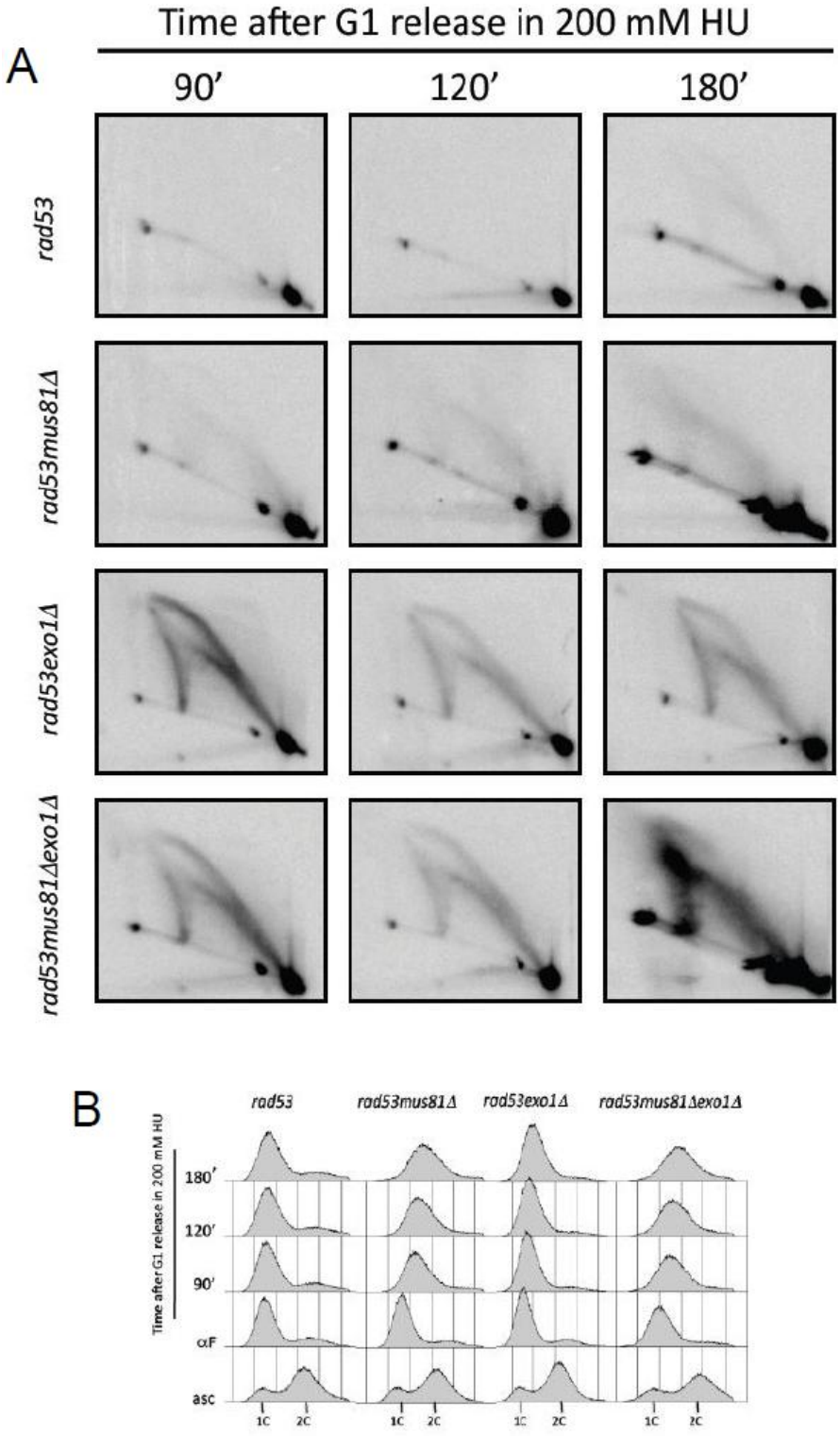

Figure 24. Replication intermediates in *MUS81*- and *EXO1*- ablated checkpoint-deficient cells*:* (A) 2D gel analysis of replication intermediates accumulating in *rad53, rad53mus81Δ, rad53exo1Δ* and *rad53mus81Δexo1 Δ* cells 90, 120 and 180

minutes after release from an α-factor induced G1 block into S-phase in the presence of 200 mM HU. (B) FACS analysis.

Accordingly, *MUS81* depletion does not contribute to the viability of checkpoint mutants in the presence of HU, either in *rad53* or *rad53exo1Δ* backgrounds (Figure 25). However, intriguingly, *MUS81* ablated mutants proceed further into S-phase as judged by the FACS analysis (Figure 24 B), suggesting that Mus81 could counteract bulk chromosome replication under these conditions.

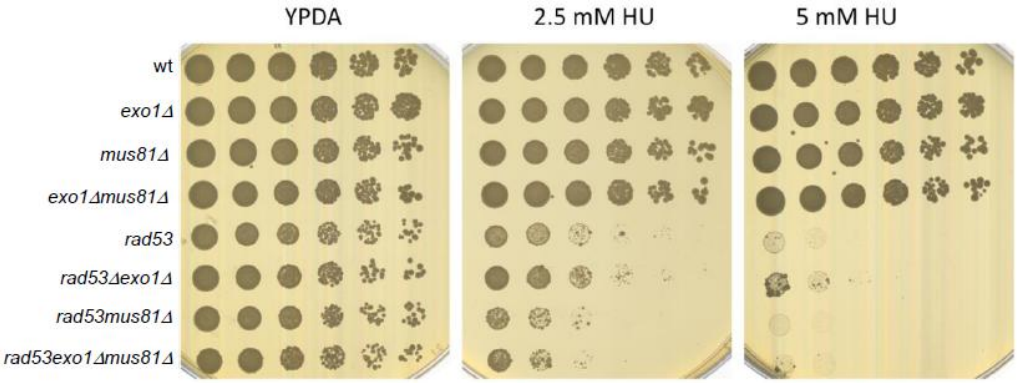

Figure 25. Effect of *MUS81* ablation on checkpoint mutants HU sensitivity. Serial dilutions of wt, *exo1Δ, mus81Δ, exo1Δmus81Δ, rad53, rad53exo1Δ, rad53mus81Δ* and *rad53exo1Δmus81Δ* cells plated in the absence or presence of 2.5 and 5 mM HU.

Altogether, these data suggest that Mus81 does not mediate branch cleavage transitions at collapsed replication forks in checkpoint mutants.

4.3.3.2 Analysis of Yen1 role in collapsed fork processing.

Yen1 was recently reported as a novel HJ resolvase in *S. cerevisiae* (Ip et al., 2008). Interestingly, Yen1 target-specificity is directed preferentially towards HJs structures and less for flaps or replication fork structures (Ip et al., 2008). To analyze the possible contribution of Yen1 to collapsed fork processing, I performed 2D gel experiments on *YEN1* ablated strains combined with *rad53* and *rad53exo1Δ* mutants. The replication intermediates profile did not show evident differences neither between *rad53* and *rad53yen1Δ*, nor between *rad53exo1Δyen1Δ* and *rad53exo1Δyen1Δ* mutant cells (Figure 26).

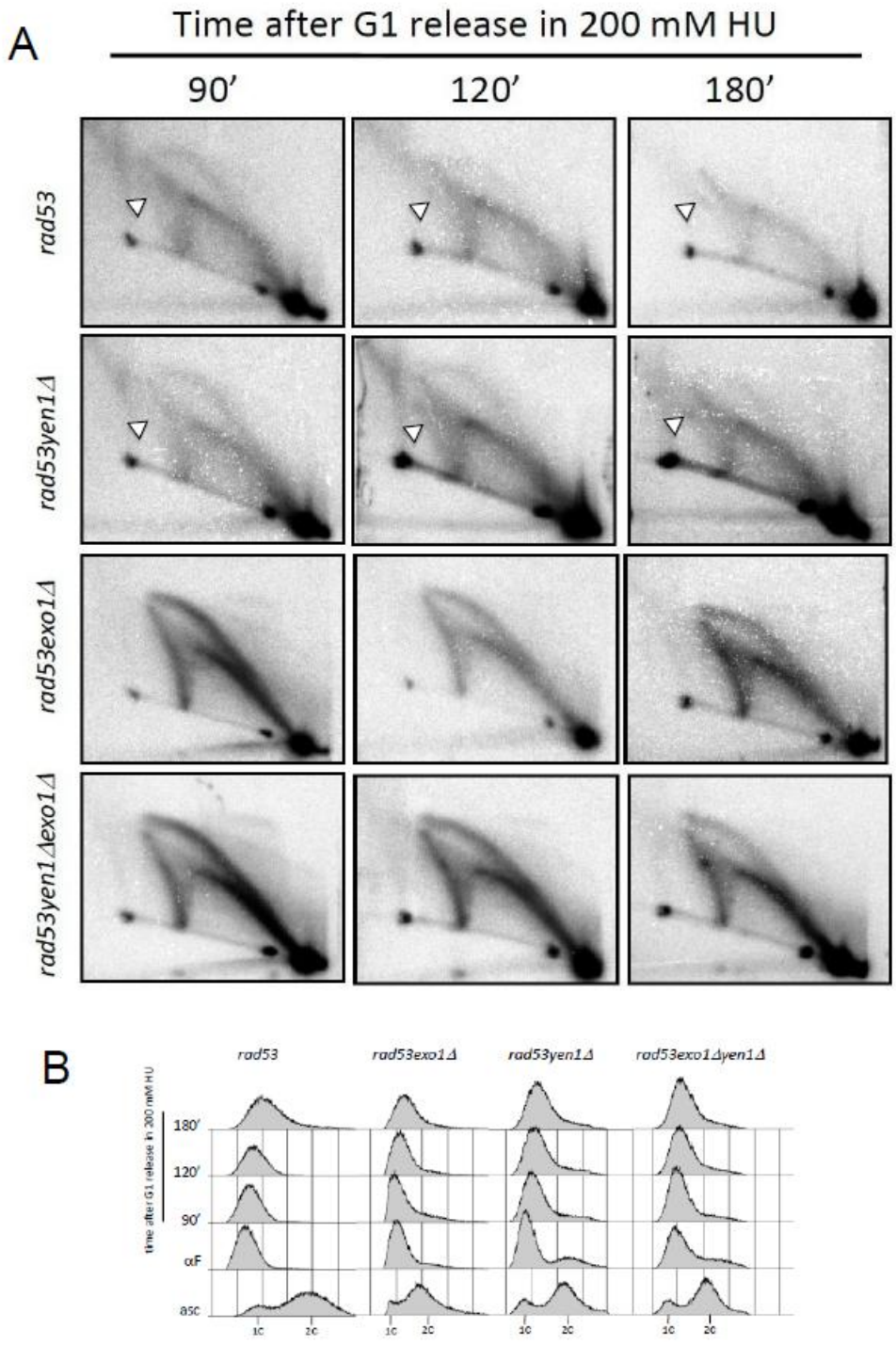

Figure 26. Replication intermediates in the absence of *YEN1* and *EXO1* in checkpoint deficient cells. (A) 2D-gel analysis of replication intermediates accumulating in *rad53*, *rad53yen1Δ*, *rad53exo1Δ* and *rad53yen1Δexo1Δ* cells 90, 120 and 180 minutes after release from an a-factor induced G1 block into S-phase in the presence of 200 mM HU. White arrowheads indicate the "double spike signal" (see text for details). (B) FACS analysis.

Furthermore, *YEN1* ablation did not affect the sensitivity to HU of *rad53* and *rad53exo1Δ* mutants (Figure 27).

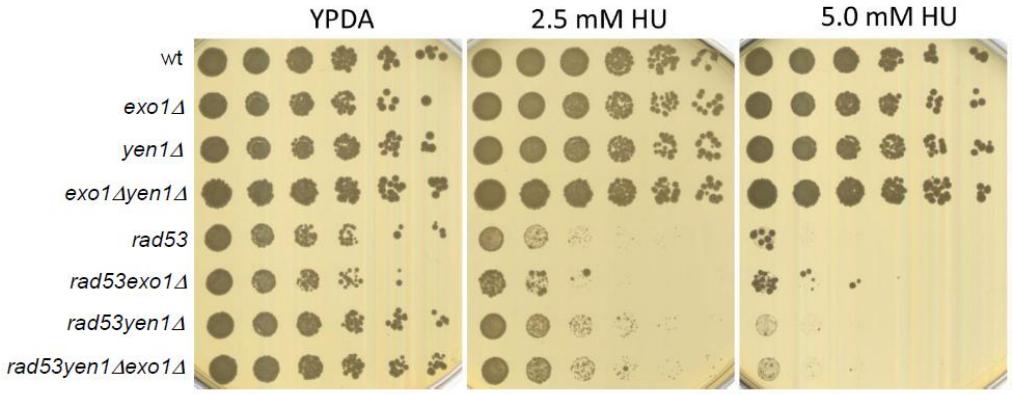

Figure 27. *yen1Δ* cells HU sensitivity. Serial dilutions of wt, *exo1Δ, yen1Δ, exo1Δyen1Δ, rad53, rad53exo1Δ, rad53yen1Δ* and *rad53exo1Δ yen1Δ* cells plated in the absence or presence of 2.5 and 5.0 mM HU.

These data suggest that Yen1 endonucleolytic activity is dispensable for the branch fork cleavage. Intriguingly, we noticed in this experiment the presence of a "second spike signal" accumulating in both psoralen - treated *rad53* and *rad53yen1Δ* mutants, that was more prominent in the latter (Figure 26). Even if the nature of the intermediates migrating in this second X-spike is yet to be determined, the observed difference upon *YEN1* deletion might hint at the involvement of Yen1 in collapsed fork processing. Yen1 substrates, however, would be different than the one initially considered.

4.3.3.3 Analysis of possible Mus81 and Yen1 redundancy of function in collapsed fork metabolism.

Since Mus81 and Yen1 functionally overlap in DNA repair in yeast and in the resolution of HJs *in vivo* also in mammals (Tay et al., 2010; Wechster et al., 2011), I reasoned that the presence of either functional Yen1 or Mus81 could have masked a phenotype in *rad53mus81Δ* and *rad53yen1Δ* mutants, respectively. Of notice, deletion of *YEN1* in a *mus81Δ* background increases the cells sensitivity to drugs that impede replication fork progression, such as HU (Blanco et al., 2010), reinforcing the idea that they might share common functions.

Therefore, to exclude this possibility, I analyzed replication intermediates in *rad53* and *rad53exo1Δ* mutants combined with the ablation of both the HJs resolvase proteins Mus81 and Yen1. I compared by 2D gel analysis replication intermediates accumulated in wt, triple mutant *mus81Δexo1Δyen1Δ* and *rad53exo1Δmus81Δyen1Δ* and *rad53exo1Δ* mutants. Wt cells fired replication origins and replication forks proceeded out of the fragment, as indicated by the presence of bubble and big-Y arcs (Figure 28A). The same pattern occurs in triple nuclease mutant *mus81Δexo1Δyen1Δ*, although the detection of replication intermediates is reduced perhaps due to a faster replication fork progression, as suggested also by the FACS analysis (Figure 28A and B), and similarly to what previously noticed upon *MUS81* deletion. I failed to observe differences between the replication intermediate profiles of *rad53exo1Δ* double mutants and *rad53exo1Δmus81Δyen1Δ* quadruple mutants, which

accumulate a prominent small Y's signals of comparable as intensity along the time course (Figure 28A).

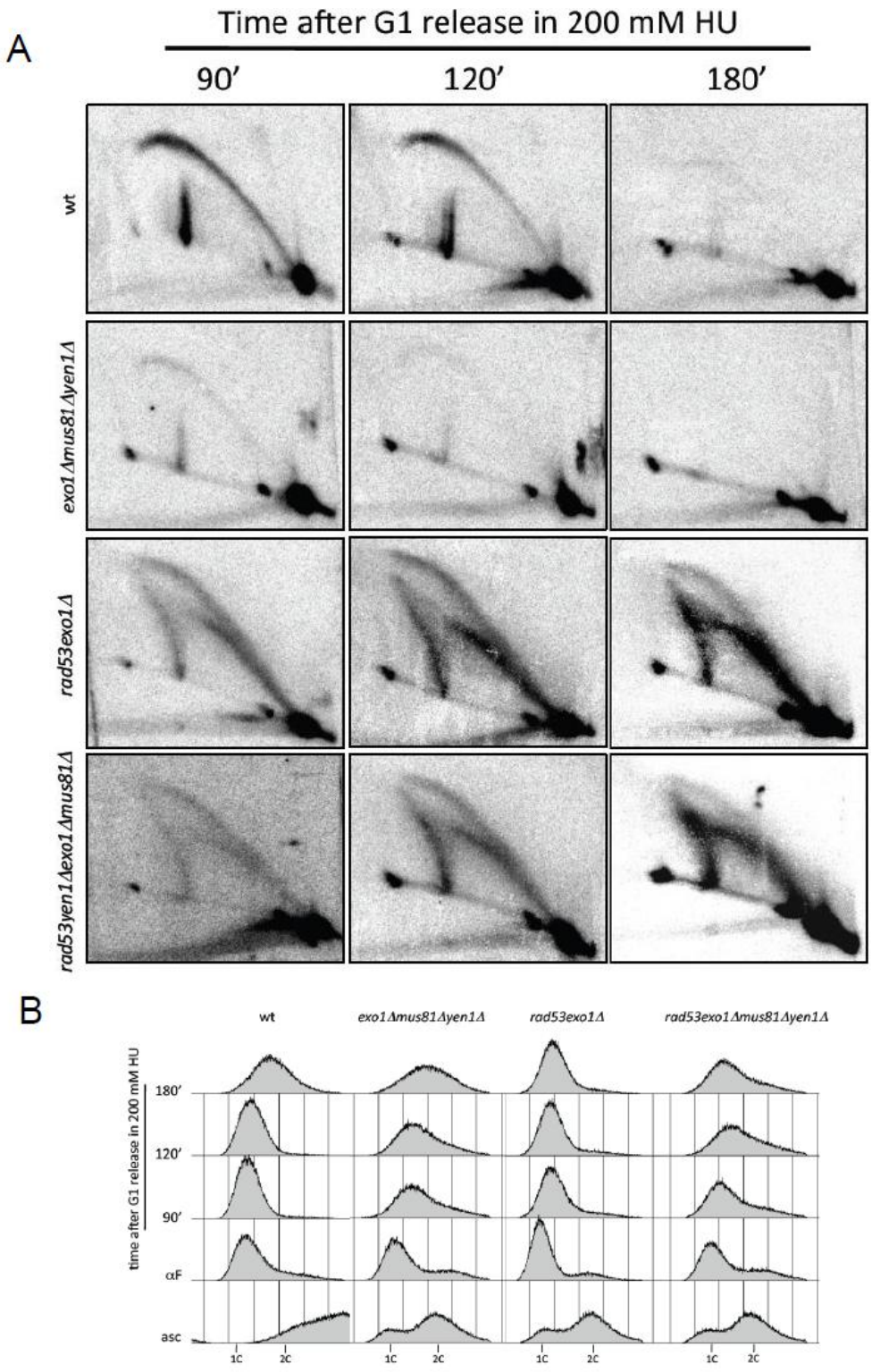

Figure 28. Replication intermediates in strains ablated for *YEN1* and/or *MUS81:* (A) 2D gel analysis of replication intermediates accumulating in wt,

exo1Δmus81Δyen1Δ, rad53exo1Δ and *rad53exo1Δmus81Δyen1Δ* cells 90, 120 and 180 minutes after release from an α-factor induced G1 block into S-phase in the presence of 200 mM HU. (B) FACS analysis.

Furthermore, differences were not observed in the HU sensitivity of *rad53exo1Δ* mutants upon contemporary ablation of *MUS81* and *YEN1* (Figure 29).

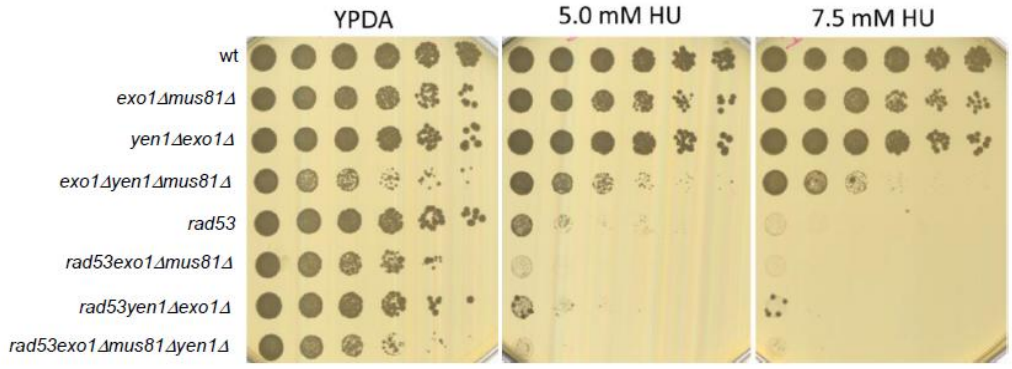

Figure 29. *mus81Δ* combined with *yen1Δ* cells HU sensitivity. Serial dilutions of wt, *exo1Δmus81Δ, exo1Δyen1Δ, exo1Δmus81Δ yen1Δ, rad53, rad53exo1Δmus81Δ, rad53exo1Δyen1Δ* and *rad53exo1Δyen1Δmus81Δ* cells plated in the absence or presence of 5 and 7.5 mM HU.

These data allowed us to exclude a redundancy in activity of *MUS81* and *YEN1* in the collapsed fork branch cleavage.

Intriguingly, I observed that *exo1Δ yen1Δ mus81Δ* triple mutants exhibited a synthetic sensitivity to low concentrations of HU when compared with *exo1Δ yen1Δ* or *exo1Δmus81Δ* cells (Figure 21). This evidence suggests that upon HU treatment structures might form requiring nucleolytic processing by either of these enzymes to promote survival in cells having a functional

checkpoint response. In line with this reasoning, the slow growth phenotype observed in the triple mutant could be related to such structures, perhaps forming during the repair of spontaneous damages generated during replication. In addition, further sustaining this idea, we observed that checkpoint proficient cells lacking contemporary Mus81 and Yen1 activity are extremely sensitive to high concentration of HU (Figure 30), suggesting that the two enzymes might act redundantly in the processing of aberrant intermediates of replication in cells experiencing replication stress.

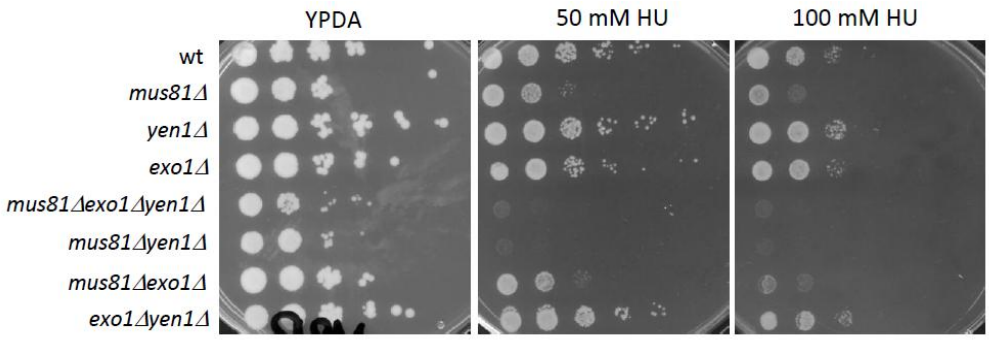

Figure 30. *mus81Δ, yen1Δ* and *exo1Δ* cells combined HU sensitivity. Serial dilutions of wt, *mus81Δ*, *yen1Δ*, *exo1Δ*, *exo1Δyen1Δmus81Δ*, *yen1Δmus81Δ*, *exo1Δmus81Δ* and *exo1Δyen1Δ* cells plated in the absence or presence of 50 and 100 mM HU.

4.3.3.4 Analysis of possible Mus81, Yen1 and Slx1 redundancy of function in collapsed fork metabolism.

It is possible that additional endonucleases could act redundantly at the level of collapsed forks. Another good candidate is the structure specific complex composed by the heterodimer Slx1/Slx4 that shows branched DNA structure specificity *in vitro* (Fricke and Brill, 2003), with strong preference for structures such as Y-forks, 3'-5' flaps, replication forks and also HJs. Furthermore, Slx4 is a checkpoint target during DNA damage repair after exposure to campotechin (CPT) and HU in *S. cerevisiae* (Flott and Rouse, 2005) and this gene is required for correct chromosome segregation in mammals, together with MUS81 and GEN1 (Wechster et al., 2011).

To analyze possible redundant roles in the observed branch cleavage transition with the previously analyzed proteins, I deleted *SLX1* in cells bearing *rad53exo1Δ* alleles alone or combined with *mus81Δyen1Δ* mutations and I scored for replication intermediates by 2D gels (Figure 31). All the *rad53exo1Δ* mutant strains bearing *slx1Δ, slx1Δyen1Δ, slx1Δmus81Δ* or *slx1Δyen1Δmus81Δ* mutations showed a prominent small Y signal, comparable as intensity with the one observed in *rad53exo1Δ* mutants (Figure 31). Furthermore, in the same strains reversed forks accumulation followed the same kinetics (Figure 31).

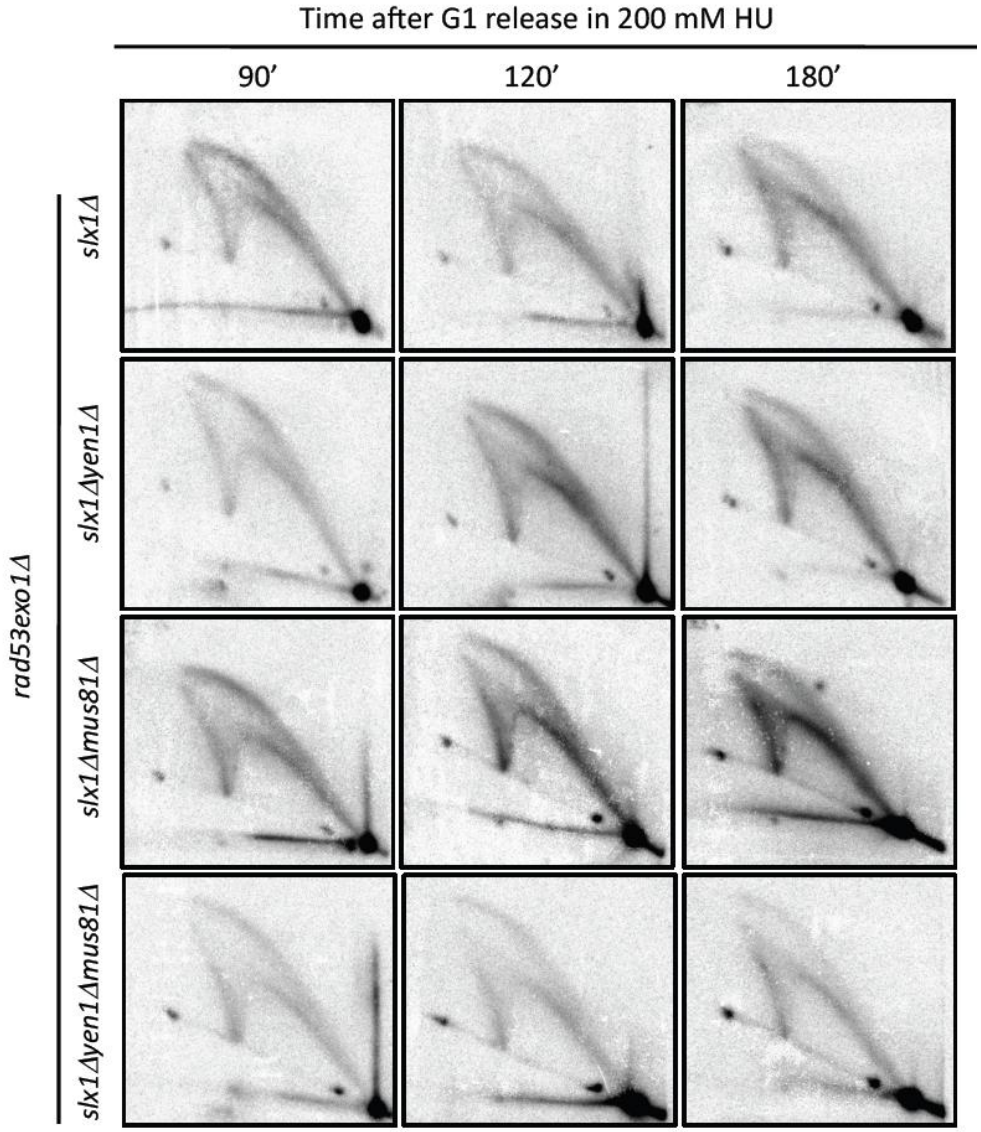

Figure 31. Replication intermediates in the combined absence of *YEN1, SLX1* and *MUS81* in *exo1Δrad53* mutant cells*:* 2D gel analysis of replication intermediates accumulating in *rad53exo1Δslx1Δ, rad53exo1Δslx1Δyen1Δ, rad53exo1Δslx1Δmus81Δ* and *rad53slx1Δexo1Δmus81Δyen1Δ* cells 90, 120 and 180 minutes after release from an α-factor induced G1 block into S-phase in the presence of 200 mM HU.

This result suggests that Slx1 is dispensable for collapsed fork processing and does not share a role with Mus81 and Yen1 in this process.

4.3.3.5 Analysis of Rad1 contribution to collapsed fork processing.

A last protein described to have Holliday junction resolvase activity in *S.cerevisiae* is Rad1. This protein is a structure specific endonuclease (Bardwell et al., 1994) that recognizes bubble, flapped substrates and HJ structures *in vitro* (Habraken et al., 1994). As Mus81, it belongs to the XPF superfamily of endonucleases and participates to DSBs repair in *S. cerevisiae* (Moore et al., 2009). To investigate a putative role for Rad1 in collapsed fork processing, I analyzed replication fork intermediates in *rad53*, *rad53rad1Δ*, *rad53exo1Δ* and *rad53exo1Δrad1Δ* mutant strains. I did not detect differences in the replication intermediate profiles in strains deleted for *RAD1*, nor in a *rad53* or *rad53exo1Δ* backgrounds, suggesting that Rad1 is dispensable for collapsed forks processing (Figure 32).

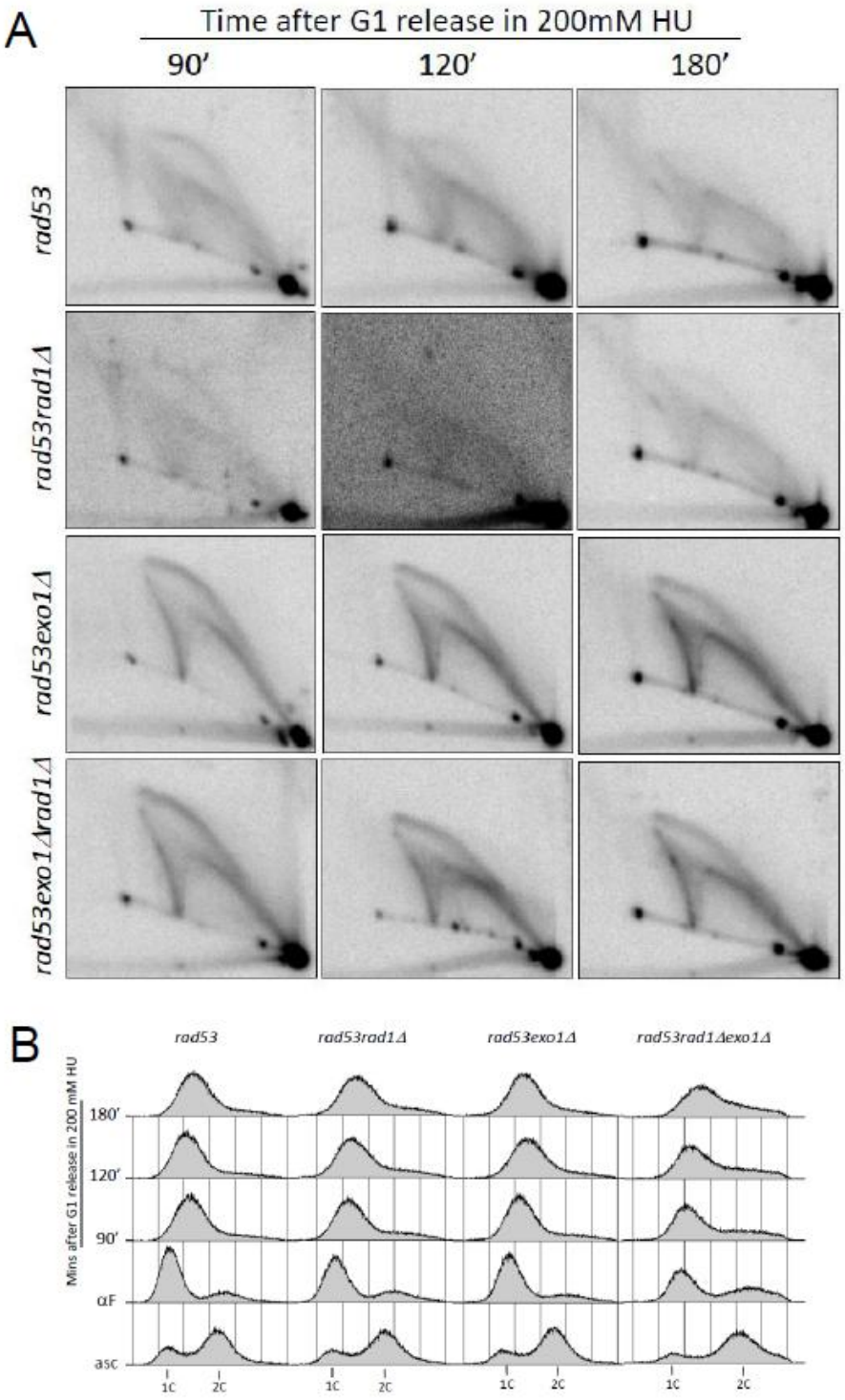

Figure 32. Replication intermediates accumulating in checkpoint deficient cells in the absence of *RAD1* and *EXO1*. (A) 2D gel analysis of replication intermediates accumulating in *rad53, rad53rad1Δ, rad53exo1Δ* and *rad53rad1Δexo1Δ* cells 90, 120 and 180 minutes after release from an α-factor induced G1 block into S-phase in the presence of 200 mM HU. (B) FACS analysis.

Overall the data obtained allow me to propose that the structure specific endonucleases Mus81, Yen1, Slx1 and Rad1 are not involved in collapsed forks metabolism in checkpoint mutants exposed to replicative stress and, specifically, do not mediate the branch cleavage observed in *rad53exo1Δ* mutants. Alternatively, these enzymes might share redundant roles with other enzymes yet to be characterized.

4.3.4 Sae2 processes stalled replication forks in checkpoint-defective cells, independently from Mre11.

Sae2 and Mre11 work as a complex at the initial steps of DSB repair pathways (Klein et al, 2008; Clerici et al., 2005; D. D'Amours et al., 2001) and were previously proposed as candidates for processing collapsed forks (Branzei and Foiani, 2009). Of notice, a recent paper reported the accumulation of a prominent small Y-signal at forks that approach double strand breaks in *mre11Δ* and *sae2Δ* mutants (Doksani et al., 2009). The migration of these Y-signal intermediates highly resembled the one observed in *rad53exo1Δ* mutants. Furthermore, Sae2 possesses an endonuclease activity that enables it to cleave DNA branched structures *in vitro* also in the absence of Mre11 (Lengsfeld et al., 2007). In higher eucaryotes, Mre11 is involved in processing replication forks to generate ssDNA stretches thought to promote the restart of collapsed forks (Hashimoto et al., 2010; Trenz et al., 2006).

To test Sae2 contribution in collapsed fork metabolism, I deleted *SAE2* in *rad53* and *rad53exo1*Δ mutant backgrounds and scored for replication intermediates by 2D gels.

I observed a transition from the cone signal detected in the *rad53* single mutants to a spike signal in *sae2Δ* cells (Figure 33), resembling the pattern described for *EXO1* ablation. This transition was evidenced by quantification of the replication intermediate signals (Figure 33B).

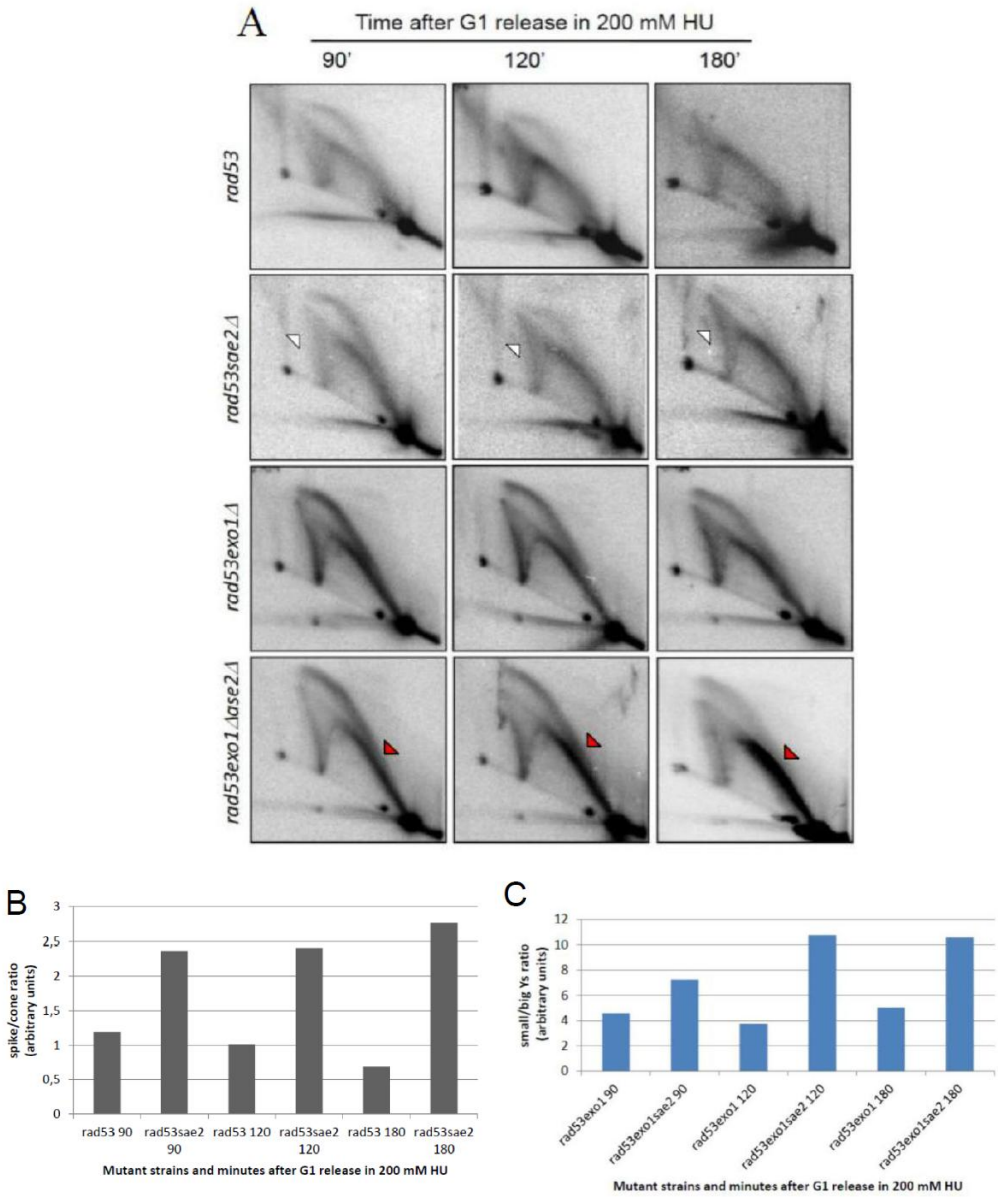

Figure 33. Sae2-dependent reversed forks processing in *rad53* HU treated cells. (A) 2D gel analysis of replication intermediates accumulating in *rad53*, *rad5sae2Δ*, *rad53exo1Δ and rad53exo1Δ sae2Δ* cells 90, 120 and 180 minutes after release from an α-factor induced G1 block into S-phase in the presence of 200 mM HU. Spike signal is indicated by white arrowheads, while in red the small Y's signal.

Quantification of the spike/cone ratio signal (B) and of small /big Y's (C) is shown. The experiment was repeated twice.

This result suggests that Sae2 processes collapsed replication forks in *rad53* cells experiencing replication stress; the residual cone signal observed in *rad53sae2Δ* cells could be due to Exo1-dependent resection. Noteworthy, *rad53exo1Δsae2Δ* cells showed a marked increase accumulation of small Y-shaped intermediates if compared to *rad53exo1Δ* mutants (Figure 33C). This suggests that Sae2 and Exo1 have overlapping roles in reversed fork processing and that this activity counteracts fork branch cleavage reactions. Small Y arc intermediates accumulation in *rad53sae2Δ* mutants is somewhat delayed if compared to *rad53exo1Δ* cells. This raises the possibility that Exo1 might be more efficient in promoting the resection events preventing branch cleavage and that Sae2 might take over when Exo1 is absent. These data suggest the existence of a *SAE2* and *EXO1*- dependent pathway that processes collapsed replication forks. In support of this idea, the combined depletion of *SAE2* and *EXO1* results in synthetic sensitivity to response to HU in a checkpoint proficient context (Figure 34).

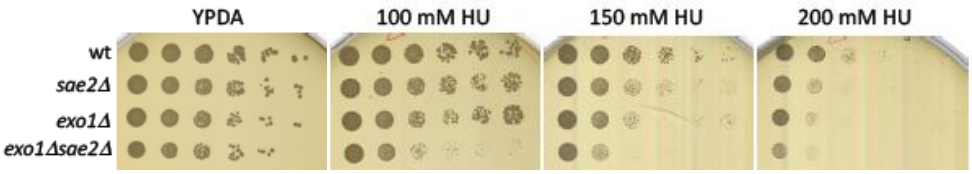

Figure 34. **Synthetic sensitivity to HU of *sae2Δ* and *exo1Δ* alleles**. Serial dilutions of wt, *sae2Δ, exo1Δ* and *exo1Δsae2Δ* cells plated in the absence or presence of 100, 150 and 200 mM HU.

Searching for additional players that might contribute to this pathway, Mre11 seemed a good candidate, since it works in a complex with Sae2 in the DSBs repair pathway, mediating very early resection steps prior to Exo1 contribution (Klein et al, 2008).

Therefore, I analyzed replication intermediates by 2D gel in strains carrying *MRE11* deletion combined with *rad53* and *rad53exo1Δ* mutations (Figure 35). Double *rad53mre11Δ* mutants showed a faint small-Y signal resulting from the proposed reversed fork branch cleavage, as compared to *rad53* cells (Figure 35). This observation suggests a contribution of Mre11 in reversed fork processing, less important however than the one of Exo1 or Sae2. In support to this idea, the contemporary depletion of Mre11 and Exo1 does not significantly alter the cells viability in hydroxyurea (Figure 36). However, double deletion of *MRE11* and *EXO1* in checkpoints mutants did not affect the branch cleavage transition and small Y signal accumulated with comparable intensities (Figure 35).

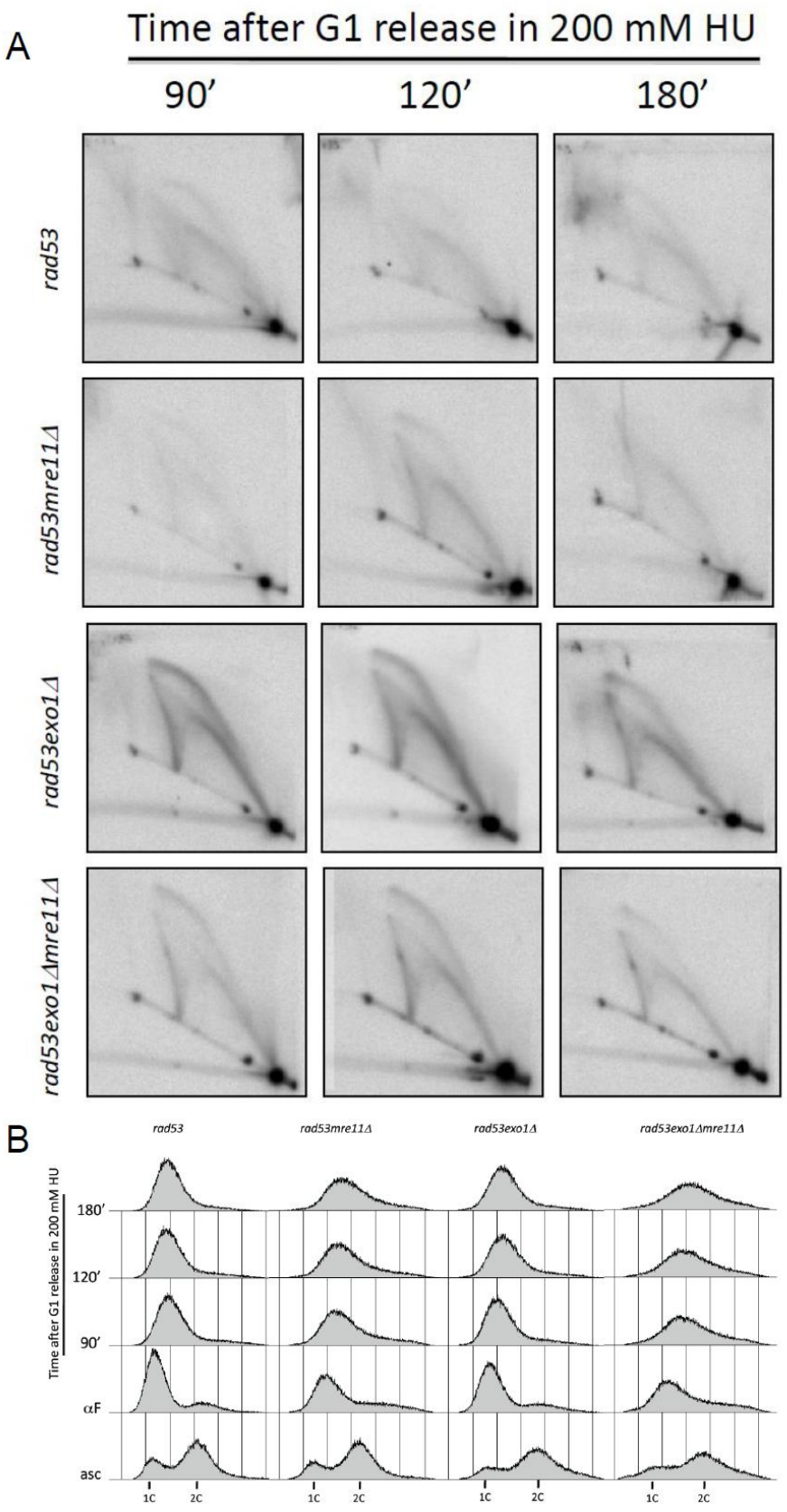

Figure 35. Mre11 marginally contributes to reversed forks processing*:* (A) 2D gel analysis of replication intermediates accumulating in *rad53*, *rad53mre11Δ*, *rad53exo1Δ* and *rad53mre11Δ exo1Δ* cells 90, 120 and 180 minutes after release from an α-factor induced G1 block into S-phase in the presence of 200 mM HU. (B) FACS analysis.

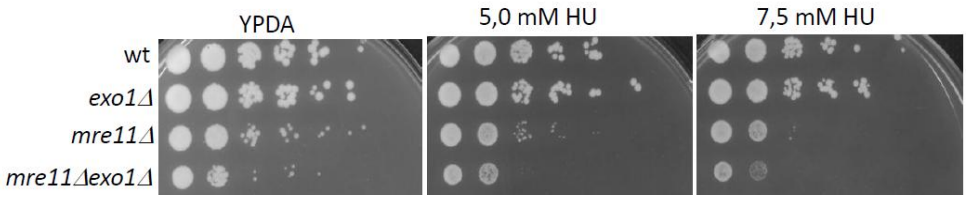

Figure 36. HU sensitivity of cells bearing *exo1Δ* and *mre11Δ*. Serial dilutions of wt, *exo1Δ*, *mre11Δ* and *exo1Δ mre11Δ* cells plated in the absence or presence of 5 and 7.5 mM HU.

Overall, these data indicate that Mre11 does not play a prominent role in protecting replication fork integrity. More work will be required to address whether Sae2 functions independently from Mre11 in this process.

4.3.5 Dna2 counteracts reversed forks in checkpoint-defective mutants.

Dna2 is a very well conserved endonuclease/helicase involved in DNA replication (Braguglia et al., 1998) and Okazaky fragments processing (Bae and Seo, 2000). The biochemical role of Dna2 is to cut long flaps generated by excessive strand displacement during replication. Therefore, it is reasonable to think that in the absence of Dna2 processing activity, long flaps could bind together forming more complex structures, such as reversed forks, in the absence of checkpoint control. Moreover, *S. pombe* Dna2 was proposed to be targeted by the checkpoint kinase Cds1 to counteract forks reversal through its

nuclease activity (Hu et al., 2012) and the mechanism suggested is that Dna2 resects the nascent strands, preventing their annealing (Hu et al., 2012).

Since *DNA2* is an essential gene, I used a thermo-sensitive allele *dna2-1*, defective in both helicase and endonuclease functions (Budd et al., 1995). The *dna2-1* allele is inactivated at the non-permissive temperature of 33°C and in these conditions replication can start but cannot proceed (data not shown). Of notice, I observed that *dna2-1* mutant cells are sensitive to the replication inhibitor hydroxyurea (see below), indicating that Dna2 is required for the cellular response to agents that stall the replication forks also in *S. cerevisiae*.

In *S. pombe*, Dna2 inactivation is sufficient to drive fork reversion even in the presence of a functional checkpoint response (Hu et al., 2012). Interestingly, Exo1 and Dna2 are involved in Okazaky fragment processing maturation and are thought to cooperate to this process (Bae et al., 2000). Therefore, to better elucidate the role of Dna2 in response to replicative stress, I analyzed by 2D gels the replication intermediates accumulating in wt, *dna2-1*, *exo1Δ* and *dna2-1exo1Δ* mutants after treatment with HU (Figure 37). In wt cells, origins fired and replication forks progressively moved out of the analyzed fragment, as shown by the presence of the bubbles and big Y's arcs, which became very faint at 180 minutes after release. A similar pattern occurred in *dna2-1* mutant cells, although the signals correspondent to the replication intermediates were fainter and started to disappear earlier, at 120 minutes, suggesting that in this mutants the forks are proceeded faster at least at initial steps (Figure 37A), as suggested also by the FACS analysis (Figure 37B). I did not observe aberrant replication intermediates, suggesting that in the presence of replicative stress *S. cerevisiae* Dna2 is dispensable to prevent forks reversal in a checkpoint proficient context. *EXO1*-ablated cells showed a replication intermediate

pattern similar to the one observed in wt cells, while double mutant *exo1Δdna2-1* resembled *dna2-1* single mutants (Figure 37A). Aberrant replication intermediates were not detected in double mutant strains, suggesting that the contemporary inactivation of *EXO1* and *DNA2* is not sufficient to induce forks reversal in this context.

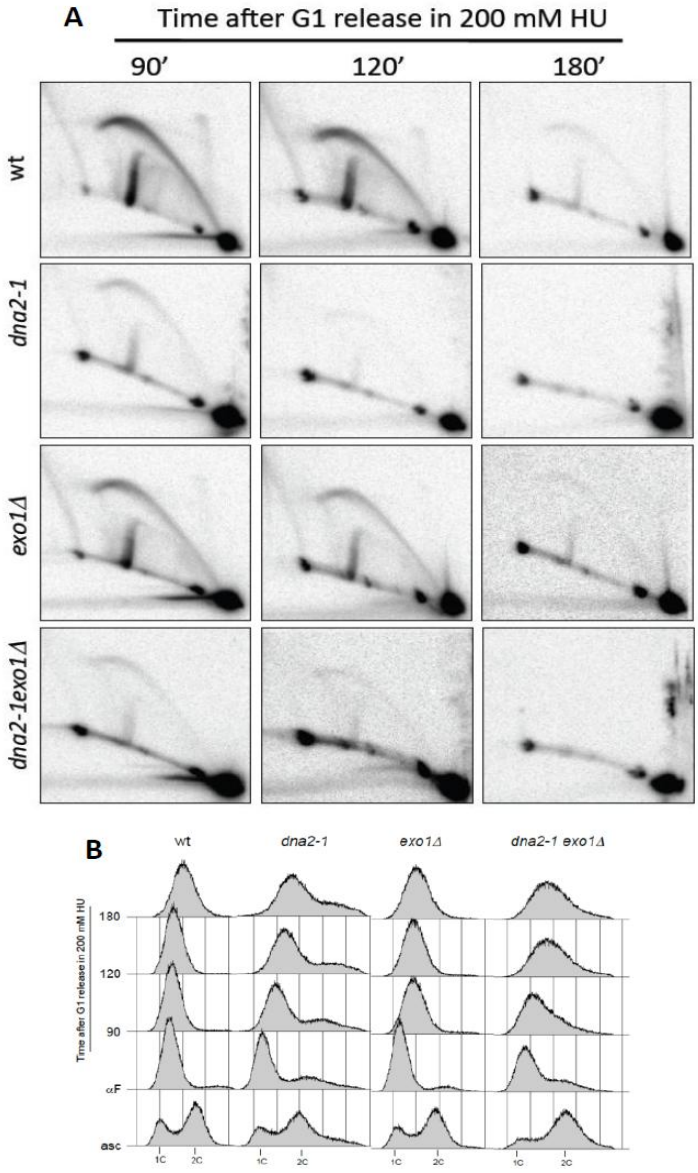

Figure 37. Dna2 inactivation does not result in forks reversal in checkpoint proficient cells. (A) 2D gel images of replication intermediates accumulating in wt, *dna2-1*, *exo1Δ* and *dna2-1exo1Δ* cells 90, 120 and 180 minutes after release from an α-factor induced G1 block into S-phase at 33°C in the presence of 200 mM HU. (B) FACS analysis.

These data suggest that *DNA2* inactivation in a checkpoint proficient background does not cause fork reversion, as occurs in *S. pombe* (Hu et al., 2012), not even in combination with Exo1 ablation. Accordingly, *EXO1* deletion does not affect the HU sensitivity of *dna2-1* mutants (Figure 38), considering the severe slow growth phenotype of *dna2-1exo1Δ* double mutants.

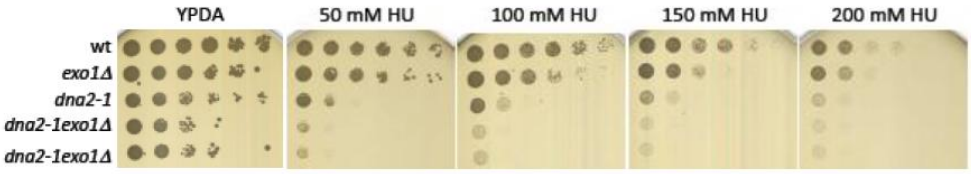

Figure 38. *dna2-1* HU sensitivity is not affected by *EXO1* deletion. Serial dilutions of wt, *exo1Δ, dna2-1* and *dna2-1exo1Δ* cells plated in the absence or presence of 50, 100, 150 and 200 mM HU at 23 °C.

I proceeded analyzing the effect of *DNA2* inactivation in the absence of a functional checkpoint. I performed 2D gel experiments comparing replication intermediates profiles of *rad53* and *dna2-1rad53* mutants, also in combination with *EXO1* deletion (Figure 39). Upon the conditional inactivation of Dna2 by temperature shift, I observed a prominent presence of intermediates migrating in the X-shaped spike likely corresponding to unprocessed reversed forks in *dna2-1rad53* cells if compared to single *rad53* mutants (Figure 39), in which a marked cone signal is detectable.

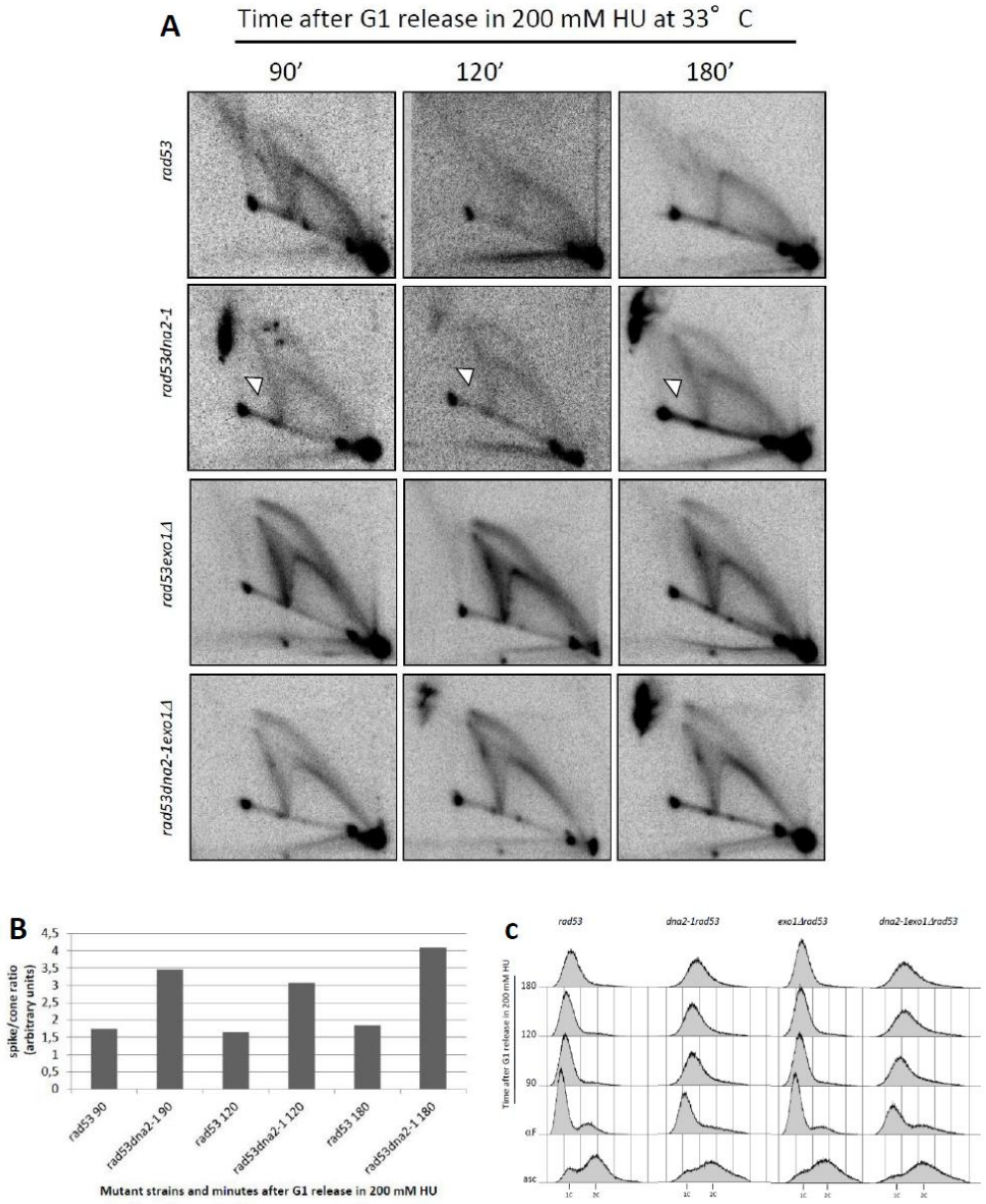

Figure 39. Dna2-dependent reversed forks processing in *rad53* HU treated cells. (A) 2D gel images of replication intermediates accumulating in *rad53*, *rad53dna2-1*, *rad53exo1Δ* and *rad53exo1Δ dna2-1* cells 90, 120 and 180 minutes after release from an α-factor induced G1 block into S-phase at 33°C in the presence of 200 mM HU. White arrows indicate reversed forks accumulation. (B) Quantification of the spike/cone ratio signal (arbitrary units) as intensities detected in correspondence of the time points analyzed is shown. The experiment was repeated twice. (C) FACS analysis.

This observation suggests that Dna2 contributes to reversed forks processing. In *dna2-1rad53* double mutants, residual nucleolytic processing is still observed, likely due to Exo1- or/and Sae2- dependent activities. Furthermore, triple mutant *dna2-1exo1Δrad53* showed a slight reduction in replication intermediates intensity, perhaps due to the fragility of the replication forks in those cells, that are very sick and slow growing, since they are contemporarily deprived of two crucial factors in Okazaky fragments processing. However, both *dna2-1exo1Δrad53* mutants, as *exo1Δrad53* cells, accumulated small Y's to comparable levels, suggesting that Dna2 is not involved in the branch fork cleavage of collapsed forks. In accordance, *DNA2* and *EXO1* ablation did not confer synthetic sensitivity to HU (Figure 40).

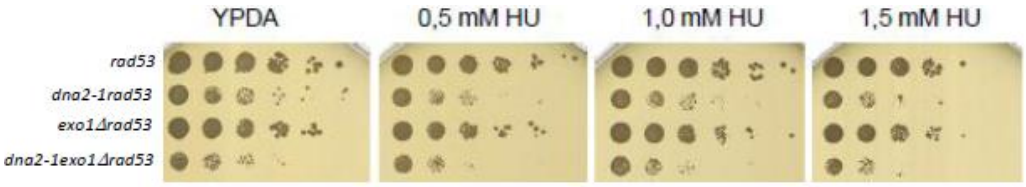

Figure 40. *rad53dna2-1* HU sensitivity is not affected by *EXO1* ablation. Serial dilutions of *rad53, dna2-1rad53, rad53exo1Δ, rad53exo1Δdna2-1* cells plated in the absence or presence of 0.5, 1.0 and 1.5 mM HU and grown at 23°C.

In summary, these data indicate that in the absence of a functional checkpoint and in conditions of replicative stress, Dna2 might counteract forks reversal, but is dispensable for branch cleavage transitions. It is reasonable to think that upon *DNA2* inactivation cells accumulate structures - likely flaps - that could be relevant for driving reversed forks formation and in this scenario the activity of Dna2 in removing those flaps is crucial to avoid the homology base pairing of the nascent strands. Furthermore, branch cleavage transitions are still

observed in HU-treated *rad53exo1Δ* cells upon *DNA2* inactivation, suggesting that Dna2 is not involved in this cleavage.

4.4 Homologous recombination factors involvement in replication fork stability.

In prokaryotic cells, fork re-start by replisome reassembly after replication arrest by DNA damages depends on homologous recombination mechanisms, in a process called recombination-dependent replication (RDR) (Kogoma, 1997). An alternative pathway mediates a direct restart of replication after fork processing into a HJ intermediate (Michel et al., 2004; McGlynn et al., 2002). Intriguingly, *S. cerevisiae* yeast cells lacking Rad51 and Rad52, the factors initiating HR repair pathways, are sensitive to HU, although the underlying mechanisms are poorly understood (Lambert et al., 2007).

In this part of the project, I asked whether homologous recombination plays a role in the stability of stalled forks challenged by HU treatment and whether such role might interplay with the DNA damage checkpoint response.

4.4.1 Homologous recombination is dispensable for forks reversal.

To analyse the involvement of homologous recombination on reversed forks formation, I constructed strains combining *rad52Δ* and *rad53* mutations and scored for intermediates of replication in the presence of 25 mM HU (Figure 41). I could not observe significant differences on the replication intermediates

pattern of *rad52Δ* and *rad53* mutants, if compared to those of wt and *rad53rad52Δ* cells, respectively (Figure 41). However, I observed a lower replication intermediate signal in both *RAD52* deletion strains, probably due to the intrinsic fragility of the replication forks in the absence of the protein. Noteworthy, double mutant *rad53rad52Δ* and *rad53* cells accumulate reversed forks in similar proportions when compared to other replication intermediates (Figure 41). These data indicate that, as proposed previously (Lopes et al., 2003), Rad52 is not required for the reversion of replication forks challenged by HU treatment observed upon fork collapse in checkpoint mutants.

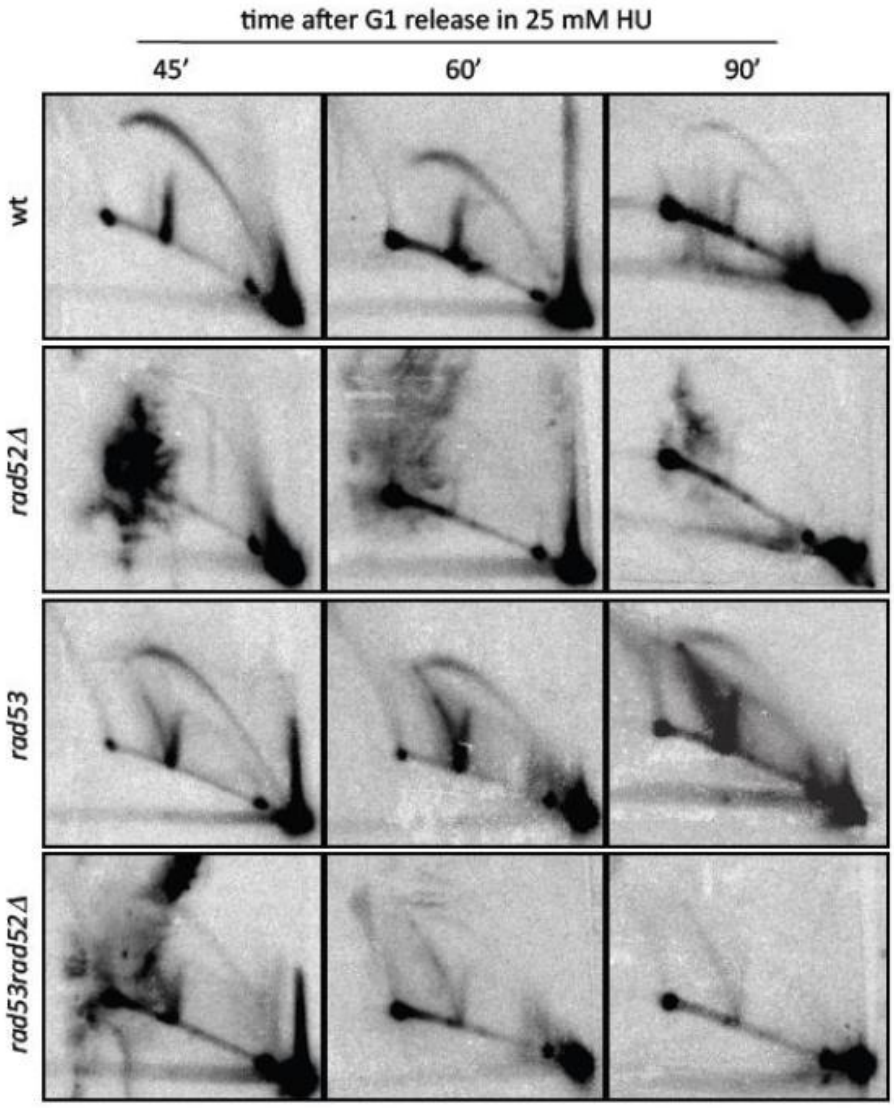

Figure 41. Homologous recombination is not required for reversed forks formation. 2D gel analysis of replication intermediates at *ARS305* region accumulating in wt, *rad52Δ, rad53* and *rad53rad52Δ* cells 90, 120 and 180 minutes after release from an α-factor induced G1 block into S-phase in the presence of 25 mM HU.

4.4.2 *RAD51* and *RAD52* mutants are differentially sensitive to HU.

Interestingly, I noticed that in checkpoint proficient cells single deletion *rad52Δ* mutants were very sensitive to low doses of HU (Figure 42), such as 5.0 or 7.5 mM, while *rad51Δ* mutants show HU sensitivity only at high doses, such as 50 mM (Figure 43). These data suggest that Rad52 and Rad51 might play different roles in the cellular response to HU-induced replication stress. At low concentrations of the drug, survival after HU treatment seems dependent on Rad52 and not on Rad51. There are repair pathways that depend on Rad52 but not on Rad51, such as SSA or BIR, that could mediate cells viability in the presence of low concentrations of HU. At higher concentrations of the drug, instead, both Rad51 and Rad52 are required for cells viability, suggesting that when replication is further challenged by a more pronounced dNTPs depletion additional Rad51-dependent HR pathways are required for survival.

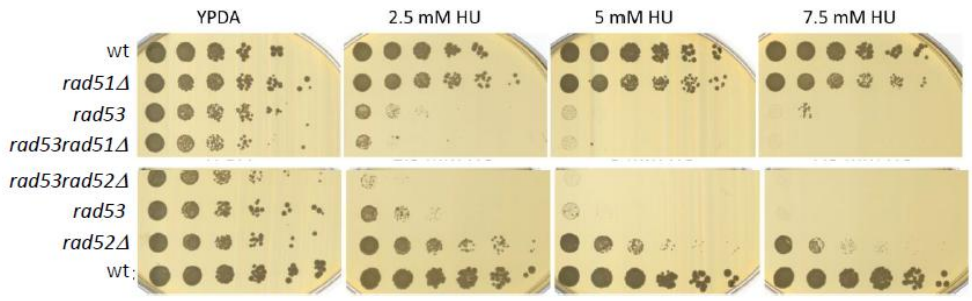

Figure 42. *rad52Δ* and *rad51Δ* alleles sensitivity to low doses of HU in checkpoint proficient and deficient backgrounds. Serial dilutions of wt, *rad51Δ, rad52Δ,*

rad53, *rad53rad51Δ* and *rad53rad52Δ* cells plated in the absence or presence of 2.5, 5 or 7.5 mM HU.

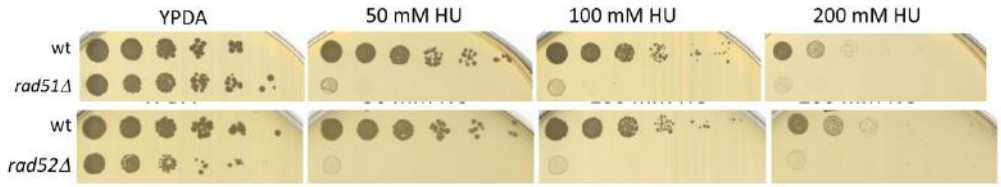

Figure 43. *rad52Δ* and *rad51Δ* cells sensitivity to high doses of HU. Serial dilutions of wt, *rad51Δ* and r*ad52Δ* cells plated in the absence or presence of 50, 100 or 200 mM HU.

Noteworthy, I observed that double *rad53rad52Δ* mutants are more sensitive to very low doses of HU (1.5 mM) than *rad53* cells (Figure 44). This non-epistatic interaction suggests the existence of two alternative pathways for cells viability in the presence of replication stress HU-induced, one Rad52-dependent and the other Rad53-dependent, and therefore Rad52-dependent mechanism might protect fork stability through mechanisms independent of the DNA damage checkpoint pathway.

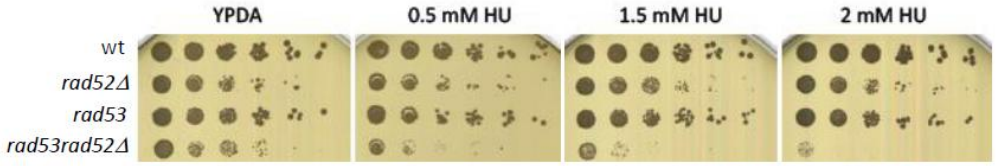

Figure 44. *rad52Δ* and *rad53* alleles HU sensitivity is not epistatic. Serial dilutions of wt, *rad52Δ*, *rad53* and *rad53rad52Δ* cells plated in the absence or presence of 0.5, 1.5 or 2 mM HU.

4.4.3 *RAD51* and *RAD52* are required for S-phase progression in the presence of replication stress.

To further characterize the role of Rad52 and Rad51 in replication fork stability, I analysed the impact of the absence of these HR factors on S-phase progression in the presence of replicative stress. Thus, I performed an experiment in which I released wt, *rad51Δ* and *rad52Δ* cells from a G1 block in the presence of 50 mM HU for four hours and I analysed the DNA content by FACS (Figure 45). Wild type cells were able to replicate their genomic DNA in the presence of the drug reaching a 2C DNA content by 180 minutes and by 210 minutes cells divided and engaged a second round of replication. I observed, however, that both *rad52Δ* and *rad51Δ* mutants exhibited a delayed progression through S-phase of the cell cycle with cells not having reached a 2C DNA content by 240 minutes (Figure 45). These data suggest that *RAD51* and *RAD52* are required to support bulky genomic replication and normal progression through S-phase in conditions of replication stress.

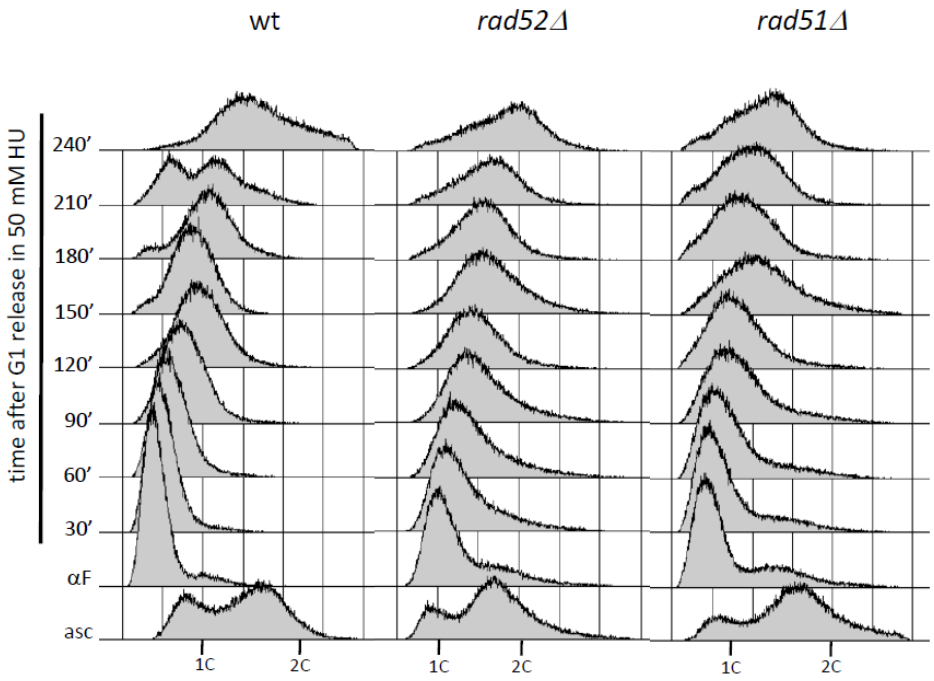

Figure 45. Rad51 and Rad52 are required for DNA replication in the presence of HU. wt, *rad52Δ* and *rad51Δ* cells were arrested in G1 and released into 50 mM HU. Samples were collected at the indicated time points for FACS analysis.

4.4.4. *RAD51* and *RAD52* mutants are required for replication resumption after replication stress.

I conducted an experiment, aimed at understanding if homologous recombination factors are required to stabilize replication forks in the presence of HU, in which I analysed the cell cycle progression during the recovery from replication stress. I treated wt, *rad51Δ* and *rad52Δ* cells, pre-synchronized in G1, with 200 mM HU for one hour and, after washing of the drug, released the cultures in fresh YPDA medium. I took samples for FACS analysis for up to two hours (Figure 46). In these conditions, wt cells recover from the drug

treatment and complete bulk DNA synthesis by 60 minutes and by 90 minutes cells divided and engaged a new round of replication. *rad52Δ* and *rad51Δ* mutants resumed DNA replication and reached a 2C DNA content with timings similar to those of wild type cells. However these mutants arrested with a 2C DNA content failing to undergo mitotic division and start a new round of replication (Figure 46).

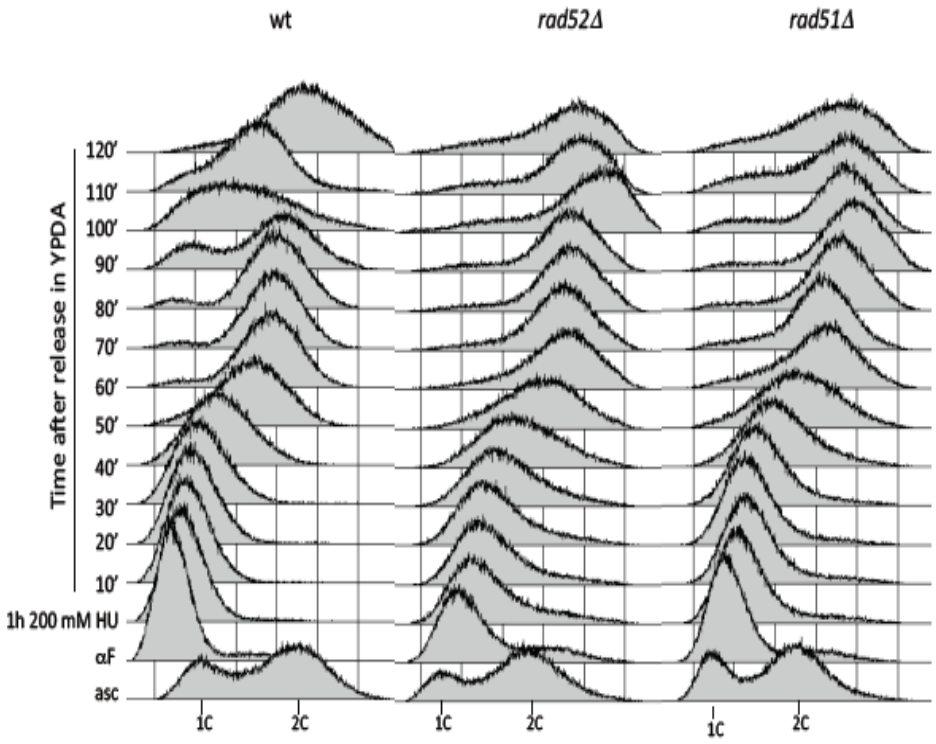

Figure 46. Rad51 and Rad52 are required for recovery from HU treatment. Wt, *rad52Δ* and r*ad51Δ* cells were arrested in G1, released into 200 mM HU for one hour, washed, and then transfer to fresh YPDA medium for 2 hours. Samples were collected for FACS analysis.

This observation suggests that even if the bulk of genome replication is completed upon HU treatment in the absence of either Rad51 or Rad52, problems might arise leading to the persistence of structures precluding chromosomes segregation and proper cell cycle progression.

These data, taken together, suggest that *RAD52* and *RAD51* are important to preserve the integrity of replication forks in the presence of HU-induced replication stress. Further work will be required to characterize the role of these HR factors in fork protection. However, the results here presented suggest that HR might act independently of the DNA damage checkpoint and that Rad52-mediated pathways might play a prominent role in fork stabilization, as Rad52 ablation renders cells sensitive to very low HU doses, while Rad51 ablation does not.

5. DISCUSSION

The mechanisms driving replication fork collapse and reversal are still poorly understood and matter of intense study. Two alternative hypotheses were proposed that picture forks reversal as the result of topological transitions: one as the consequence of positive supercoiling accumulation (Postow et al., 2001, Bermejo et al. 2011), while the second as the result of hemicatenanes junctions run-off at stalled forks (Lopes et al., 2003; Cotta-Ramusino et al.; Bermejo et al., 2007). It has also been predicted, based on *in vitro* data, that specialized enzymes could mediate forks reversal. The budding yeast Rad5 helicase, as well as its mammalian ortholog HLTF, presents such activity *in vitro* (Blastyak et al., 2007, Achar et al., 2011). Moreover, in checkpoint defective mutants collapsed forks are engaged in pathological resection events mediated by nucleolytic activities, (Sogo et al., 2002; Cotta-Ramusino et al., 2005), although the precise identity of the enzymes carrying out those transitions are still unknown. In this work, I attempted to shed light on the events mediating replication fork collapse, as well as on the pathological transitions that take place at collapse forks and prime chromosomal rearrangements in checkpoint mutants.

5.1 DNA topology: the engine of fork reversal.

In the first part of this work, I showed that the cellular machinery modulating the topology of replicating chromosomes plays a crucial role on replication fork stability and therefore genome integrity. In particular, the observation that simplifying DNA topology *in vivo* counteracts reversed fork accumulation in checkpoint mutants supports the hypothesis that the mechanical strain accumulated as positive supercoiling during replication represents the main cause of forks reversion.

In vitro positive supercoil accumulating in partially replicated circular plasmids can determine reversed forks formation (Postow et al., 2001). Here, I support this notion by providing three lines of evidence arguing that positive supercoil is *per se* a crucial determinant of fork reversal in checkpoint mutants experiencing HU-induced replication stress. First, I showed that induction of a DSB between an origin of replication and a transcribed gene, thus relaxing a chromosomal topological domain, is sufficient to counteract forks reversal. Second, I showed that reversed fork accumulation is reduced upon over-expression of Top2 and, to a lesser extent, by over-expression of Top1. Increasing Top2 or Top1 steady state levels should shift supercoiled DNA segments towards a topologically relaxed state. Lastly, I observed that precluding topological constrains resolution, by contemporary inactivation of Top1 and Top2 (Bermejo et al., 2007), induces the accumulation of abnormal X-shaped replication intermediates, likely representing reversed forks in unperturbed cells, even in a checkpoint proficient context. Taken together, these experiments support the idea that a tight regulation of DNA topology

simplification is essential to promote the stability of replication forks. This applies to forks challenged by dNTP pools reduction and checkpoint defects and might be also valid for cells replicating their DNA in the absence of exogenous agents and with an integrate checkpoint response. In agreement with our data, positive supercoiling accumulation, rather than replisome run-off at topoisomerase-mediated nicks, has recently been shown to be the cause of replication fork arrest and loss of cellular viability in cells treated with the Top1-poison camptothechin (CPT) (Koster et al., 2007). Furthermore, electron microscopy experiments showed that Top1-poisoning induces forks reversal formation in yeast cells, as well as in mammalian and *Xenopus* cells (Ray-Chaudhuri et al., 2012), suggesting that efficiently and timely resolution of topological stress is a requirement for the stabilization of replication fork along the evolution.

Moreover, a mechanism has been proposed by which cells can simplify chromosomal topology to promote replication fork progression and stability. *In vivo* topological domain barriers are likely to establish when transcribed chromosomal regions physically associate with Nuclear Pore Complexes (NPCs). Transcribed chromatin engagement at NPCs, known as “gene gating” limits the diffusion of topological changes by preventing the rotations of the DNA double helix around each other (Bermejo et al., 2012). The topological tension generated when replication forks approach NPC-associated chromosomal regions was proposed to be resolved by the Mec1/ATR checkpoint, that targets the Mlp1 nucleoporin to detach transcribed genes from the NPCs (Bermejo et al., 2011), thus dismantling the topological domain so generated. In agreement, formation of reversed forks was also recently observed in checkpoint deficient human cells experiencing replication stress

due to oncogene over-expression (Neelsen et al., 2013), which has been proposed to be caused by an increase in unscheduled encounters between replication and transcription machineries (Bermejo et al. 2012).

All this evidence, together with the data presented in this thesis, indicate that fork reversal is tightly connected to the regulation of the topological constrains arising at replicating chromosomes. In agreement with this view, I showed, in addition, that Rad52 and Rad51 homologous recombination is dispensable for the accumulation of reversed forks, indicating that fork reversal is mechanistically independent of recombinational repair pathways, as previously suggested (Lopes et al. 2003).

These data imply that the transitions driving the annealing of nascent strands at stalled replication forks would not depend on enzymatic activities, as occurs for instance in the formation of HJs by strand invasion, but rather depend on mechanical forces exerted by the torsional stress accumulated as positive supercoiling ahead of replication forks. Of notice, homologous recombination factors seem dispensable for fork reversal also in higher eukaryotes, such as *Xenopus* eggs and human cells (Ray-Chaudhuri et al., 2012; Neelsen et al., 2013).

5.2 Rad51 and Rad52: guardians of replication fork stability?

While not playing a role in mediating fork reversal, the results in this work provide evidence that budding yeast homologous recombination factors are crucial for the cellular response to replication stress. I observed that both Rad52 and Rad51 are required for cell viability in the presence of HU, although at low concentrations of the drug survival is solely dependent on Rad52, suggesting that Rad52 - dependent pathways can deal with low levels of replications stress, but upon major fork stalling Rad51 is also engaged to sustain viability. In *S. cerevisiae* two main Rad52 - dependent homologous recombination repair pathways that do not require Rad51 have been described: single strand annealing (SSA) and break induce replication (BIR). SSA takes place in the absence of homologous donor sequences and it is restricted to DSBs that arise between directed repeats (Ataian and Krebs, 2006). BIR is involved in fork restart and engages broken chromosomes that present only one end, intermediates that could prominently form upon fork collapse (Kraus et al., 2001). It is reasonable to think that at low HU concentrations BIR-related mechanisms might act to sustain stalled forks functionality. Interestingly, Rad51-mediated mechanisms of replication fork restart upon replication stress that do not depend on the HR pathway have also been described in higher eukaryotes (Petermann et al., 2010). Of notice, *rad52Δ* is not epistatic with *rad53* for sensitivity to low concentrations of HU, suggesting that these factors might act as part of two independent pathways contributing to fork stability.

As mentioned, I speculate that at higher HU concentrations severe genome wide fork stalling requires the activity of additional homologous recombination pathways mediated by Rad51 and Rad52. Accordingly, both *rad52Δ* and *rad51Δ* cells treated with high HU concentrations do not proceed normally through S-phase, probably due to defects in stabilizing replication forks. These mutants, however, can complete the bulk of genome replication following arrest in HU and removal of the drug. In these conditions *rad52Δ* and *rad51Δ* cells do not proceed into mitosis nor initiate a new round of replication. This suggest that in the absence of Rad51 or Rad52 abnormal structures might accumulate at replication forks precluding the completion of chromosome duplication and further advancement in the cell cycle. Resumption of DNA synthesis in these mutants upon removal of the drug could reflect a necessity for HR factors to stabilize replication forks in the presence of the drug only. Alternatively, the bulk of genomic DNA replication could be accomplished by firing of late replication origins, which would establish forks that could then proceed unchallenged in the absence of the drug (Santocanale et al., 1999).

The role of HR factors in sustaining replication fork stability remains intriguing. These factors could directly protect replication forks by stabilizing ssDNA tracks accumulating as a result of helicase and polymerases uncoupling, thus counteracting the formation of DNA breaks. Such role in preventing fork collapse, independently of DSBs repair events, has recently been proposed in higher eukaryotes (Hashimoto et al., 2010; Schlacher et al., 2011). In agreement with this possibility, electron microscopy data reported the accumulation of extensive ssDNA gaps at replication forks fork in budding yeast cells ablated of Rad52 or Rad51. These gaps were proposed to provide

harmful substrates for uncontrolled endonucleolytic resection (Hashimoto et al., 2010).

Altogether, the evidence provided in this work support recent data in higher eukaryotes proposing a direct role for recombination factors Rad51 and Rad52 in the protection of replication fork integrity. The precise mechanisms by which recombination factors fulfill this task remain to be elucidated.

5.3 Reversed forks: protective or terminal structures?

Our data and recent studies, evidence that reversed forks readily form upon accumulation of positive supercoiling in eukaryotes perhaps reflecting the conservation of topology-modulating and replication machineries along eukaryotic cells (Wang et al., 2002; Bermejo et al., 2007; Ray-Chaudhuri et al., 2012; Neelsen et al., 2013). Whether reversed fork structures are pathological or physiological intermediates is still a matter of debate.

In bacteria four branched molecules forming at reversed forks have been described mainly as intermediate structures in the restart of replication forks stalled by DNA damages. In this view, fork reversal represents a physiological intermediate of forks rescue, rather than a pathological intermediates of replication accumulating when mechanisms preventing fork collapse fail. An important consideration to take into account is that in bacteria replication is completed from a single origin. Therefore, mechanisms ensuring fork restart might be crucial as replication cannot be completed by forks emanating from other origins as in the case in eucaryotes (Michel et al., 2004). In human cells, forks reversal have been observed during unperturbed replication, although

very rarely, and were interpreted as transient events (Neelsen et al., 2013). It was proposed that reversed forks in higher eucaryotes could be relatively common replication intermediates, but they could represent potentially dangerous structures and be thus quickly dismantled (Neelsen et al., 2013).

Reversed forks are common intermediates in cells experiencing replication stress and in the absence of a functional checkpoint response. Reversed forks form upon treatment with sub-lethal doses of camptotechin and DNA breaks together with checkpoint activation when their formation is suppressed by inhibition of the Poly ADP-ribose polymerase (PARP) pathway (Ray-Chaudhuri et al., 2012). This observation led to the suggestion that upon Top1 poisoning transient reversal might be part of a PARP-mediated fork protection mechanism bypassing checkpoint activation. However, higher CPT doses are lethal for the cells (Ray-Chaudhuri et al., 2012), raising the possibility that reversed forks can only be tolerated as fork-restart intermediates at low levels of torsional stress. In this line, it was recently shown that human cells accumulate reversed forks upon oncogene over-expression in the absence of detectable DNA breaks and without fully activating the DNA damage response. In this context, reversed forks are tolerated for a limited number of cell cycles, before the induction of a delay in cell proliferation (Neelsen et al., 2013).

In the absence of a functional DNA checkpoint, reversed forks might represent terminal structures counteracting forks restart and prone to generate further aberrant intermediates (Sogo et al., 2002), consequently contributing to cells lethality following replication stress. In accordance with this view, checkpoint deficient human cells do not proceed in the cell cycle and accumulate reversed forks, together with chromosomal breaks, upon oncogene over-expression

(Neelsen et al., 2013). Mechanisms of fork restart in the absence of a functional checkpoint have not been described so far and mutations able to suppress fork reversal positively affect checkpoint deficient cells survival to replication stress inducing drugs (Bermejo et al., 2011). Therefore, reversed forks likely represent pathological structures whose formation at stalled forks, if not prevented through modulation of DNA topology, can cause cells death.

However, a critical issue for cell viability upon fork collapse in checkpoint mutants might be the processing of reversed forks by unscheduled nucleolytic activities (Sogo et al., 2002; Cotta-Ramusino et al., 2005; Neelsen et al, 2013). Recently, Mus81 has been shown to be the main cause of cell lethality due to reversed forks cleavage upon premature mitotic entry, in checkpoint defective human cells (Neelsen et al, 2013). In budding yeast, Exo1 resects reversed forks (Cotta-Ramusino et al., 2005). I observed the formation of reversed forks also in the presence of lower concentrations of HU and in these conditions intermediates resulting from Exo1 processing were not observed. This observation might imply the nucleolytic processing is primed by prolonged fork stalling and is concomitant with replication forks collapse.

5.4 Exo1: the *Maestro* of fork resection.

Collapsed forks are characterized by the appearance of aberrant replication intermediates, such as gapped or hemireplicated structures, thought to underlie loss of cell viability and genome instability in checkpoint mutants (Cotta-Ramusino et al., 2005; Sogo et al., 2002). The *S. cerevisiae* Exo1 exonuclease actively metabolizes collapsed forks, and is thought to generate extended ssDNA patches (Cotta-Ramusino et al., 2005), that could interfere with fork restart and the completion of chromosomes duplication (Pellicioli and Foiani, 2005). Exo1 is a phosphorylation target of Rad53 (Smolka et al., 2007) and it was proposed that checkpoint activation induced by telomere erosion down-regulates its nuclease activity (Morin et al., 2008). It is therefore assumed that, in cells experiencing replication stress, checkpoint activation inhibits Exo1 to prevent deleterious processing of stalled forks. In this view, Exo1-mediated resection events, observed in *rad53* mutants, leading to the accumulation of extended ssDNA tracks, could provide substrates for unscheduled recombination events. A similar role for Exo1 was proposed in the metabolism of replication forks collapsing upon topological stress accumulation by inactivation of Top1 and Top2 (Bermejo et al., 2007). Exo1 binds replication forks in the presence of replication stress both in wild type cells and *rad53* mutants (Cotta-Ramusino et al., 2005), suggesting that also in a checkpoint proficient context Exo1 activity might be finely modulated to preserve fork integrity. A possibility is that Exo1 prevents abnormal transitions at replication forks during unperturbed replication. Noteworthy, Exo1 plays a role in Okazaky fragments processing (Sun et al., 2003).

My analysis of replication intermediates accumulating at collapsed forks after *in vivo* stabilization by psoralen crosslink revealed that additional activities can engage stalled forks. However, Exo1 seem to have a prominent role in fork processing: first, upon fork collapse aberrant intermediates progressively disappear in *rad53* cells. This effect might be mainly due to Exo1-mediated resection as intermediates seem more stable in *rad53exo1Δ* mutants. Second, additional aberrant replication intermediates accumulate in checkpoint defective cells upon *EXO1* ablation. Prominently, X-shaped intermediates consistent with unresected reversed forks and small-Y shaped intermediates, likely resulting from branch-cleavage reactions of reversed forks, were observed.

The reported persistence of unresected X-shaped reversed forks in *exo1Δ* mutants, argues that Exo1 is the main activity metabolizing these structures. Given its 5'-3' exonucleolytic activity, Exo1 could engage the double stranded extremity of the reversed branch formed by nascent strand annealing or engage the 5' ends of Okazaki fragments at the lagging strand (Figure 47).

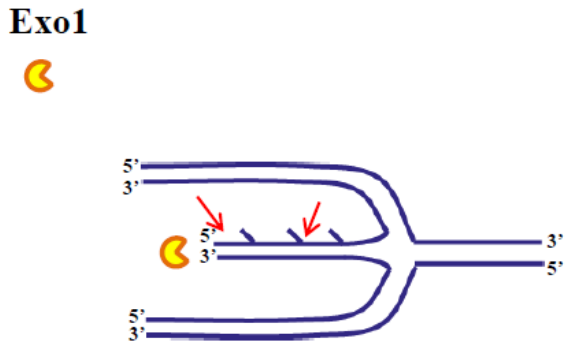

Figure 47. Schematic representation of Exo1 putative substrates at collapsed forks. In checkpoint deficient cells, reversed forks, here depicted in blue, are processed by Exo1 (yellow packman) following 5'-3' polarity. Red arrows indicate

putative substrates suitable for Exo1 nucleolytic activity (i.e. DNA ends and 5' flaps arising during lagging strand replication).

Intermediates consistent with nucleolytic resection are observed in *EXO1* ablated cells, indicating that additional nucleases can process collapsed forks. The data here presented indicate that Sae2 and Dna2 nucleases might resect stalled forks even in cells in which Exo1 is active. The fact that multiple enzymes act on collapsed forks might explain why deletion of *EXO1* does not rescue *rad53* cells viability in the presence of HU (Securado and Diffley, 2008), as additional activities seem to generate aberrant structures precluding fork restart. In this view, genetic inactivation of these enzymes (i.e. Exo1, Sae2 and Dna2) might suppress the lethality of checkpoint cells exposed to HU. This analysis, however, is hampered by the redundant roles played by these enzymes during unperturbed replication.

EXO1 ablation leads to the accumulation of X-shaped reversed forks and small-Y shaped intermediates in *rad53* mutants. Thus, Exo1 likely counteracts reversed fork accumulation by resecting nascent strands. This resection could take place prior to reversion, thus limiting the capacity of nascent strands to base-pair. Alternatively, Exo-1 mediated resection of annealed nascent strands would eventually resolve the four-way junction. Accumulation of Y-shaped intermediates in *rad53exo1Δ* mutants suggests that Exo1-mediated resection counteracts branch cleavage reactions at reversed forks (Figure 48). In this scenario, Exo1-dependent processing might generate intermediate structures bearing ssDNA disrupting the continuity of the DNA joint structure, which might preclude its cleavage by HJ resolvases (Figure 48).

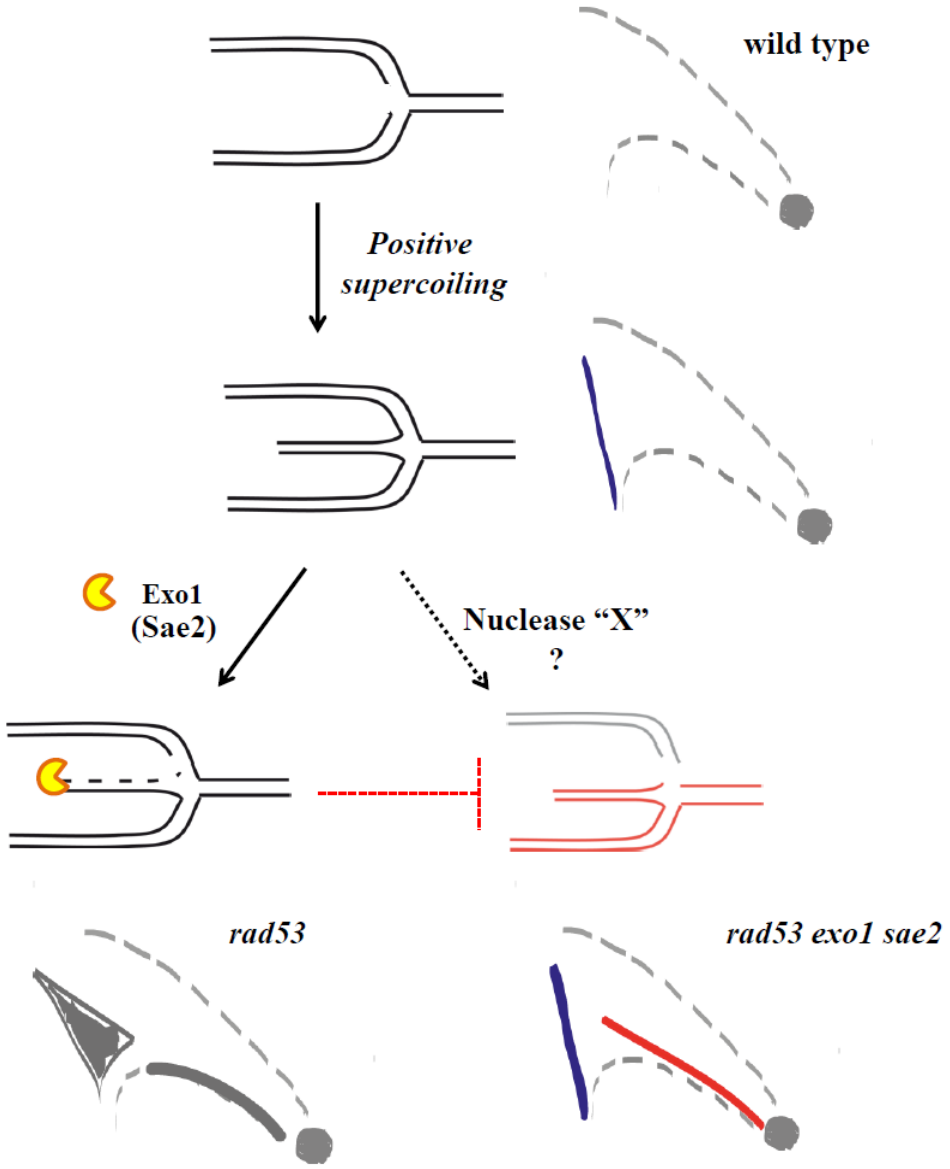

Figure 48. Schematic representation of Exo1 nucleolytic processing of collapsed forks in *rad53* cells and correspondent intermediate of replications observed by 2D gel. In *rad53* mutants topological mediated formation of reversed forks is counteracted by Exo1 – dependent nucleolytic activity, likely through resection of DNA nascent ends. The disruption of the four branched structure continuity so formed might counteract also further nuclease processing. See text for details.

In this work, I could not unmask the identity of the X-nuclease mediating the predicted branched cleavage of reversed forks. Thus, the biological significance of small-Y shaped intermediates formation in *rad53exo1Δ* mutants remains unclear. These intermediates might represent pathological structures that arise in the absence of fork protection and their formation might thus be favored in the absence of Exo1- and Sae2-mediated resection (see below). In this view, these structures might be the consequence of eventual cellular attempts to repair collapsed forks.

Therefore the function of Exo1 at stalled forks remains open. It could be viewed as a "Ying and Yang" role: is Exo1 aberrantly processing intermediates arising at collapsed forks or, alternatively, is it eliminating intermediates that could prime aberrant repair attempts leading to chromosomal rearrangements?. Further work will be necessary to address these non-mutually exclusive hypotheses.

5.5 Sae2: a novel player in replication fork processing.

I found that the Sae2 nuclease contributes to the metabolism of collapsed forks. Deletion of *SAE2* in *rad53* mutants leads to the accumulation of X-shaped reversed forks migrating as a spike signal, on the expense of "cone" signal intermediates. This observation suggests that Sae2 can engage reversed fork structures upon fork collapse. This is a novel role for Sae2, which was previously implicated in early steps in the HR DSBs repair pathway (Mimitou and Symington, 2008). Sae2 is a checkpoint target phosphorylated by Mec1 and Tel1, also during unperturbed cell cycles (Baroni et al., 2004). Sae2, as Exo1, bears a 5'- 3' nuclease activity (Lengsfeld et al., 2007). It is therefore reasonable to think that Sae2 might process the reversed forks extruding branch (Figure 49), which resembles a double stranded chromosome, a substrate engaged by the enzyme during DSBs repair.

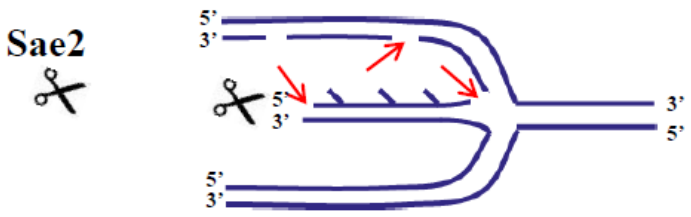

Figure 49. Schematic representation of Sae2 putative substrates at collapsed forks. Reversed forks, here depicted in blue, are processed by Sae2 (black scissors) following 5'-3' polarity. Red arrows indicate putative substrates suitable for Sae2 nucleolytic activity (i.e. DNA ends and small gaps or nicks generated by the enzyme).

2D gel analysis showed that depletion of *SAE2* favors the accumulation of small-Y intermediates. This suggests that this enzyme plays a role in reversed forks resection thus counteracting branch cleavage reactions at collapsed forks. Accumulation of small Y's signal in *sae2Δ* cells was however less evident than in *EXO1* ablated cells, suggesting that Sae2 carries out reversed forks resection less efficiently than Exo1. However, upon deletion of both *SAE2* and *EXO1*, accumulation of branched cleaved small-Y molecules was strikingly increased, suggesting that both enzymes cooperate in reverse fork processing, and that in their absence branch cleave reactions are highly favored. Although other possibilities cannot be excluded, it is reasonable to think that Sae2 generates nicks or short ssDNA gaps thus providing entry points for Exo1 resection (Figure 50). A similar function has been proposed for Sae2 in DSB processing (Nicolette et al., 2010).

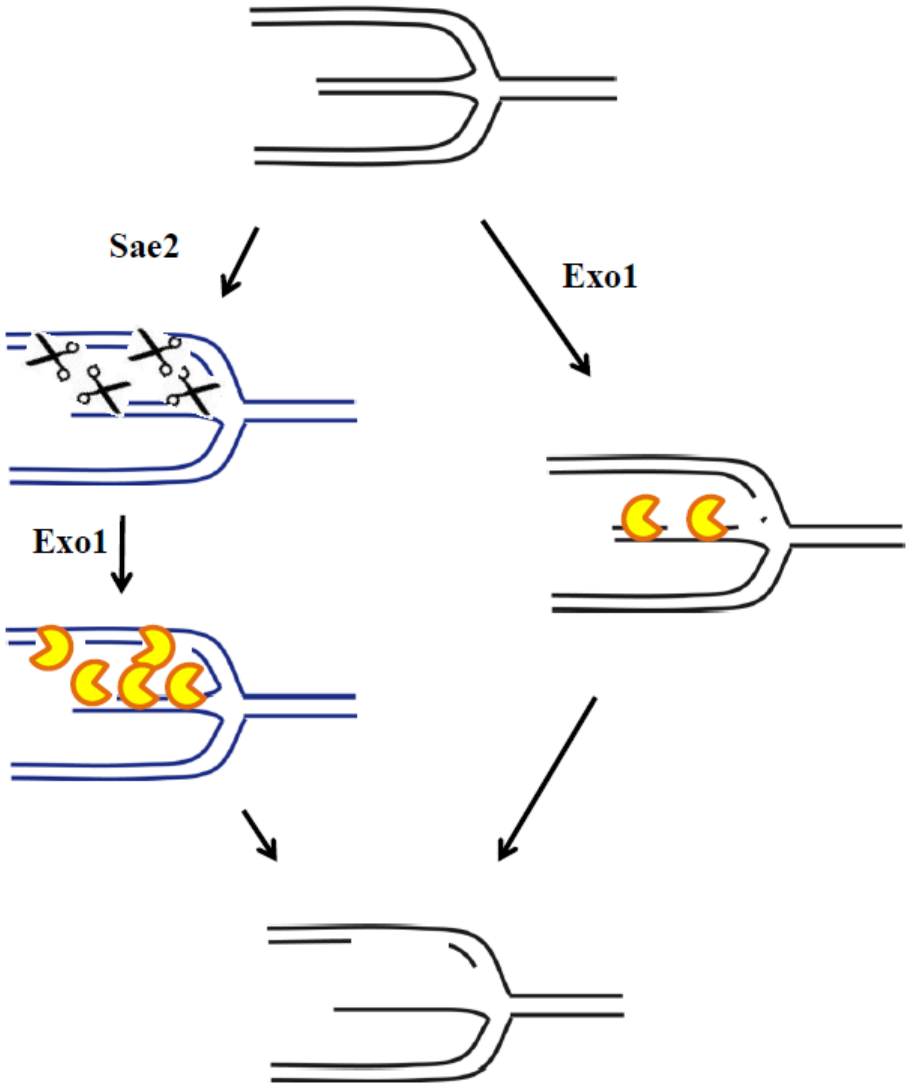

Figure 50. Schematic representation of the cooperative activity of Sae2 and Exo1 at collapsed forks in *rad53* mutants. Reversed forks might be initially processed by Sae2, thus creating intermediates suitable for Exo1 processing. However, Exo1 would catalyze the same process in the absence of Sae2 activity.

Our data indicate that Mre11, which can act as a partner of Sae2 in DSBs processing, is unlikely to play a role in reversed fork resection. This notion is in agreement with previous reports (Cotta-Ramusino et al., 2005). Furthermore, I found that Mre11 is dispensable for branch cleavage reactions at collapsed forks. These data hint at a function of Sae2 in collapsed fork processing

separable from Mre11's. Sae2 and Mre11 cooperation has been extensively characterized in DSB repair and terminal fork protection (Mimitou et al., 2008; Doksany et al., 2009). However, different lines of evidence suggested unrelated roles for these enzymes (Lisby et al., 2004, Baroni et al., 2004). Interestingly, human EXO1 was shown to preferentially bind CtIP, the human homologue of Sae2, but not MRE11, both in unperturbed cells and in cells treated with CPT or HU (Eid et al., 2010). Moreover, concomitant depletion of CtIP and EXO1 in cells treated with CPT leads to chromosomal rearrangements (Eid et al., 2010). It would be therefore very interesting to clarify the possible mechanistic cooperation between the two enzymes in collapsed forks processing.

Intriguingly, it was described that Sae2 and Mre11 cooperate in the stabilization of replication forks approaching DSBs in the template (i.e. terminal forks), in a mechanism also involving the checkpoint kinase Tel1 (Doksany et al., 2009). Upon ablation of either these enzymes, terminal forks show X-shaped intermediates consistent with forks reversal and small Y shaped molecules resembling the proposed branch cleavage intermediates accumulating in *rad53exo1Δ* or *rad53sae2Δ* cells. It was proposed that branch cleavage reactions take place as part of the unrescuable terminal forks dismantling when processing by Sae2/Mre11 cannot occur (Doksany et al., 2009). Based on the observations here reported, it is possible to think that a pathway equivalent to the one acting on terminal forks might attempt the dismantling of collapsed forks, thus avoiding the engagement of reversed forks in further genotoxic events.

Importantly, *sae2Δ* and *exo1Δ* are synthetic for HU sensitivity, suggesting that they share a common role in maintaining the integrity of forks challenged by replication stress in checkpoint proficient cells. These observation suggest that

Exo1 and Sae2 share a role in processing aberrant intermediates arising at stalled forks that if not metabolized by the enzymes would preclude replication re-start. Alternatively, aberrant structures could be stabilized at stalled forks when Exo1 does not take part in Okazaky fragments metabolism that might require Sae2 processing to preserve forks functionality.

An important consideration previously mentioned is that eukaryotic cells, differently from procaryotes, can rescue collapsed forks by the firing of additional origins, and therefore it is reasonable to think that fork dismantling could be favored, as opposed to attempting re-start through HR-mediated mechanisms. In line with this idea, we observed that the endonucleolytic processing of collapsed forks occurs preferentially after long exposure to high HU concentrations, when reversed forks are likely to represent terminal structures. At lower doses of HU, intermediates compatible with reversed forks resection are not observed, suggesting that a more pronounced DNA synthesis inhibition promotes the formation of substrates for deleterious Exo1- and Sae2-mediated and branch cleavage relations.

In conclusion, the data here presented suggest a novel function for Sae2 in fork processing, in addition to the more prominent role exerted by Exo1.

5.6 *DNA2*: an alternative to reversion?

Dna2 acts as nuclease in multiple cellular processes relevant for genome stability, such as DNA synthesis and DSBs processing (Bae et al., 2000; Zhu et al., 2008). During lagging strand maturation Dna2 cuts long RPA-coated 5' flaps (Bae et al., 2001) in coordination with Fen1 and Exo1. Dna2 also contributes to DSBs repair by cooperating in DNA resection downstream of the MRX complex and Sae2, in a pathway that mutually excludes Exo1 (Mimitou and Symington, 2008; Zhu et al., 2008). Additionally, loss of function *DNA2* mutants are sensitive to hydroxyurea and both human and fission yeast Dna2 are involved in the response to replication stress (Hu et al., 2012; Peng et al., 2012).

Dna2 was identified in our educated 2D gel screening as a novel factor processing reversed forks in r*ad53* mutants. Considering the nature of Dna2 *in vitro* substrates, it is reasonable to think that this enzyme could act on nascent strands at "long flaps" forming at Okazaky fragments or at reversed branch double stranded DNA ends upon the action of additional nucleases. Dna2 could cleave nascent strands thus eventually precluding base pairing upon their displacement from the parental strands (Figure 51).

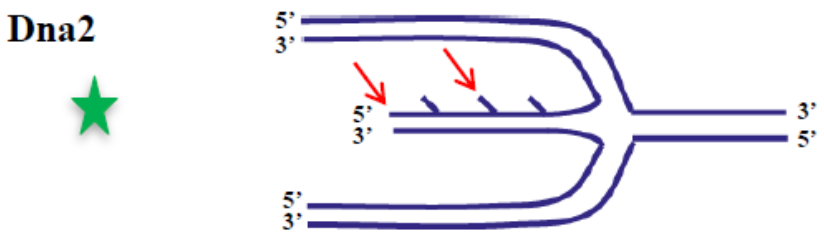

Figure 51. Schematic representation of Dna2 putative substrates at collapsed forks. Reversed forks, here depicted in blue, are counteracted by Dna2 (green star) activity. Red arrows indicate putative substrates suitable for Dna2 (i.e. DNA ends and 5' flaps arising during lagging strand replication).

S. pombe Dna2 was proposed to counteract fork reversal in checkpoint proficient cells experiencing replication stress. SpDna2 cleaves *in vitro* substrates resembling precursors of fork regression and reversed forks were observed by electron microscopy in *dna2* mutants treated with HU (Hu et al., 2012). In contrast, I did not observe reversed forks accumulation in budding yeast *dna2* mutants, suggesting that Dna2 function is dispensable to stabilize stalled forks in this organism. A possible explanation for this apparent discrepancy may reside in the regulation exerted by the DNA damage response in fission yeast. SpDna2 is targeted by the Rad53 homolog Cds1. Dna2 phosphorylation is thought to promote its association to replication forks upon replication stress (Hu et al., 2012). While *S. cerevisiae* Dna2 has been proposed to act as a checkpoint sensor stimulating Mec1 activity (Kumar et al., 2013), regulation of its activity by the DNA damage response has not been reported to date.

A key issue that remains open is which is of Dna2 biochemical activities is relevant in the processing of stalled replication forks, since Dna2 can act both as nuclease and helicase. *S. pombe* Dna2 was suggested to directly counteract reversed fork formation by nucleolytic resection of the nascent strands (Hu et et., 2012). I observed an increase in reversed forks accumulation in HU treated *dna2-1rad53* cells, although I did not discriminate whether the exonucleolytic resection or the helicase unwinding activity is relevant to this function. While *Xenopus laevis* and human Dna2 have been implicated in fork stabilization (Wawrousek et al., 2010; Peng et al., 2012), the *Xenopus* protein helicase activity is not as efficient as the nuclease' one *in vitro* (Liao et al., 2008). Altogether, these evidences suggest that Dna2 nucleolytic, rather than helicase, function might be relevant for stalled replication forks dynamics.

I showed that Dna2 is dispensable for the branch cleavage of reversed forks observed in *rad53exo1Δ* mutants. As in the case of Exo1 and Sae2, it can be argued that Dna2-mediated resection of collapsed forks counteracts branch cleavage by an "endonuclease X". I found that *dna2-1exo1Δ* double mutants exhibit a higher hydroxyurea sensitivity than the corresponding single mutants. Even if *dna2-1exo1Δ* display growth defects in the absence of HU, this observation suggests that Dna2 and Exo1 play independent roles in fork protection upon HU treatment. This situation resembles what occurs in the processing of DSBs, where the two enzymes work in two independent pathways (Mimitou et al., 2009).

5.7 Nucleases: a complicated puzzle.

As mentioned in the introduction, a wide variety of substrate specific nucleases act to preserve genome integrity. Thanks to recent discoveries, their number, partners and functions in different metabolic pathways are increasing every day and to dissect the bundle of pathways cooperating in these networks is like to compose a complicated puzzle.

In summary, the data collected in this work suggest that Exo1 is a major player in reversed forks metabolism. I report that also endonucleases Dna2 and Sae2 counteract forks reversal in checkpoint mutants. This evidence hints at the presence of a novel pathway in which Exo1 and Sae2 might cooperate in stalled replication forks processing. The structural nature and biological significance of small-Y intermediates, predicted to result from branch cleavage, remain elusive as well as the identity of a putative nuclease "X" that would mediate this transition. The data here presented exclude that *S. cerevisiae* HJs resolvases Mus81 and Yen1, as well as the Rad1 and Slx1 nucleases solely contribute to this process. I cannot, however, exclude the possibility that these enzymes act redundantly in mediating this cleavage. Moreover, HJ resolvases are a matter of intense investigation in recent years, and novel factors, perhaps the ones mediating the observed branch cleavage reactions, might be discovered and characterized in the next future.

6. REFERENCES

Achar, Y. J., D. Balogh and L. Haracska (2011). "Coordinated protein and DNA remodeling by human HLTF on stalled replication fork." Proc Natl Acad Sci U S A **108**(34): 14073-14078.

Alcasabas, A. A., A. J. Osborn, J. Bachant, F. Hu, P. J. Werler, K. Bousset, K. Furuya, J. F. Diffley, A. M. Carr and S. J. Elledge (2001). "Mrc1 transduces signals of DNA replication stress to activate Rad53." Nat Cell Biol **3**(11): 958-965.

Aparicio, O. M., D. M. Weinstein and S. P. Bell (1997). "Components and dynamics of DNA replication complexes in S. cerevisiae: redistribution of MCM proteins and Cdc45p during S phase." Cell **91**(1): 59-69.

Ataian, Y. and J. E. Krebs (2006). "Five repair pathways in one context: chromatin modification during DNA repair." Biochem Cell Biol **84**(4): 490-504.

Aze, A., J. C. Zhou, A. Costa and V. Costanzo (2013). "DNA replication and homologous recombination factors: acting together to maintain genome stability." Chromosoma.

Bae, S. H., K. H. Bae, J. A. Kim and Y. S. Seo (2001). "RPA governs endonuclease switching during processing of Okazaki fragments in eukaryotes." Nature **412**(6845): 456-461.

Bae, S. H. and Y. S. Seo (2000). "Characterization of the enzymatic properties of the yeast dna2 Helicase/endonuclease suggests a new model for Okazaki fragment processing." J Biol Chem **275**(48): 38022-38031.

Bardwell, A. J., L. Bardwell, A. E. Tomkinson and E. C. Friedberg (1994). "Specific cleavage of model recombination and repair intermediates by the yeast Rad1-Rad10 DNA endonuclease." Science **265**(5181): 2082-2085.

Baroni, E., V. Viscardi, H. Cartagena-Lirola, G. Lucchini and M. P. Longhese (2004). "The functions of budding yeast Sae2 in the DNA damage response require Mec1- and Tel1-dependent phosphorylation." Mol Cell Biol **24**(10): 4151-4165.

Bell, S. P., R. Kobayashi and B. Stillman (1993). "Yeast origin recognition complex functions in transcription silencing and DNA replication." Science **262**(5141): 1844-1849.

Bell, S. P. and B. Stillman (1992). "ATP-dependent recognition of eukaryotic origins of DNA replication by a multiprotein complex." Nature **357**(6374): 128-134.

Bermejo, R., T. Capra, R. Jossen, A. Colosio, C. Frattini, W. Carotenuto, A. Cocito, Y. Doksani, H. Klein, B. Gomez-Gonzalez, A. Aguilera, Y. Katou, K. Shirahige and M. Foiani (2011). "The replication checkpoint protects fork stability by releasing transcribed genes from nuclear pores." Cell **146**(2): 233-246.

Bermejo, R., Y. Doksani, T. Capra, Y. M. Katou, H. Tanaka, K. Shirahige and M. Foiani (2007). "Top1- and Top2-mediated topological transitions at replication forks ensure fork progression and stability and prevent DNA damage checkpoint activation." Genes Dev **21**(15): 1921-1936.

Bermejo, R., M. S. Lai and M. Foiani (2012). "Preventing replication stress to maintain genome stability: resolving conflicts between replication and transcription." Mol Cell **45**(6): 710-718.

Bianco, P. R., R. B. Tracy and S. C. Kowalczykowski (1998). "DNA strand exchange proteins: a biochemical and physical comparison." Front Biosci **3**: D570-603.

Blanco, M. G., J. Matos, U. Rass, S. C. Ip and S. C. West (2010). "Functional overlap between the structure-specific nucleases Yen1 and Mus81-Mms4 for DNA-damage repair in S. cerevisiae." DNA Repair (Amst) **9**(4): 394-402.

Blastyak, A., L. Pinter, I. Unk, L. Prakash, S. Prakash and L. Haracska (2007). "Yeast Rad5 protein required for postreplication repair has a DNA helicase activity specific for replication fork regression." Mol Cell **28**(1): 167-175.

Boddy, M. N., P. H. Gaillard, W. H. McDonald, P. Shanahan, J. R. Yates, 3rd and P. Russell (2001). "Mus81-Eme1 are essential components of a Holliday junction resolvase." Cell **107**(4): 537-548.

Boddy, M. N., A. Lopez-Girona, P. Shanahan, H. Interthal, W. D. Heyer and P. Russell (2000). "Damage tolerance protein Mus81 associates with the FHA1 domain of checkpoint kinase Cds1." Mol Cell Biol **20**(23): 8758-8766.

Braguglia, D., P. Heun, P. Pasero, B. P. Duncker and S. M. Gasser (1998). "Semi-conservative replication in yeast nuclear extracts requires Dna2 helicase and supercoiled template." J Mol Biol **281**(4): 631-649.

Branzei, D. and M. Foiani (2009). "The checkpoint response to replication stress." DNA Repair (Amst) **8**(9): 1038-1046.

Branzei, D. and M. Foiani (2010). "Maintaining genome stability at the replication fork." Nat Rev Mol Cell Biol **11**(3): 208-219.

Brewer, B. J. and W. L. Fangman (1987). "The localization of replication origins on ARS plasmids in S. cerevisiae." Cell **51**(3): 463-471.

Budd, M. E., W. C. Choe and J. L. Campbell (1995). "DNA2 encodes a DNA helicase essential for replication of eukaryotic chromosomes." J Biol Chem **270**(45): 26766-26769.

Burgers, P. M. (2009). "Polymerase dynamics at the eukaryotic DNA replication fork." J Biol Chem **284**(7): 4041-4045.

Chabes, A., B. Georgieva, V. Domkin, X. Zhao, R. Rothstein and L. Thelander (2003). "Survival of DNA damage in yeast directly depends on increased dNTP levels allowed by relaxed feedback inhibition of ribonucleotide reductase." Cell **112**(3): 391-401.

Champoux, J. J. (2001). "DNA topoisomerases: structure, function, and mechanism." Annu Rev Biochem **70**: 369-413.

Chow, K. H. and J. Courcelle (2004). "RecO acts with RecF and RecR to protect and maintain replication forks blocked by UV-induced DNA damage in Escherichia coli." J Biol Chem **279**(5): 3492-3496.

Cimprich, K. A. and D. Cortez (2008). "ATR: an essential regulator of genome integrity." Nat Rev Mol Cell Biol **9**(8): 616-627.

Clerici, M., D. Mantiero, G. Lucchini and M. P. Longhese (2005). "The Saccharomyces cerevisiae Sae2 protein promotes resection and bridging of double strand break ends." J Biol Chem **280**(46): 38631-38638.

Cobb, J. A., T. Schleker, V. Rojas, L. Bjergbaek, J. A. Tercero and S. M. Gasser (2005). "Replisome instability, fork collapse, and gross chromosomal rearrangements arise synergistically from Mec1 kinase and RecQ helicase mutations." Genes Dev **19**(24): 3055-3069.

Cocker, J. H., S. Piatti, C. Santocanale, K. Nasmyth and J. F. Diffley (1996). "An essential role for the Cdc6 protein in forming the pre-replicative complexes of budding yeast." Nature **379**(6561): 180-182.

Costanzo, V. (2011). "Brca2, Rad51 and Mre11: performing balancing acts on replication forks." DNA Repair (Amst) **10**(10): 1060-1065.

Cotta-Ramusino, C., D. Fachinetti, C. Lucca, Y. Doksani, M. Lopes, J. Sogo and M. Foiani (2005). "Exo1 processes stalled replication forks and counteracts fork reversal in checkpoint-defective cells." Mol Cell **17**(1): 153-159.

Courcelle, J. and P. C. Hanawalt (1999). "RecQ and RecJ process blocked replication forks prior to the resumption of replication in UV-irradiated Escherichia coli." Mol Gen Genet **262**(3): 543-551.

Courcelle, J. and P. C. Hanawalt (2003). "RecA-dependent recovery of arrested DNA replication forks." Annu Rev Genet **37**: 611-646.

D'Amours, D. and S. P. Jackson (2001). "The yeast Xrs2 complex functions in S phase checkpoint regulation." Genes Dev **15**(17): 2238-2249.

Deem, A., A. Keszthelyi, T. Blackgrove, A. Vayl, B. Coffey, R. Mathur, A. Chabes and A. Malkova (2011). "Break-induced replication is highly inaccurate." PLoS Biol **9**(2): e1000594.

Desany, B. A., A. A. Alcasabas, J. B. Bachant and S. J. Elledge (1998). "Recovery from DNA replicational stress is the essential function of the S-phase checkpoint pathway." Genes Dev **12**(18): 2956-2970.

Di Micco, R., M. Fumagalli, A. Cicalese, S. Piccinin, P. Gasparini, C. Luise, C. Schurra, M. Garre, P. G. Nuciforo, A. Bensimon, R. Maestro, P. G. Pelicci and F. d'Adda di Fagagna (2006). "Oncogene-induced senescence is a DNA damage response triggered by DNA hyper-replication." Nature **444**(7119): 638-642.

Diffley, J. F. and K. Labib (2002). "The chromosome replication cycle." J Cell Sci **115**(Pt 5): 869-872.

Doe, C. L., J. S. Ahn, J. Dixon and M. C. Whitby (2002). "Mus81-Eme1 and Rqh1 involvement in processing stalled and collapsed replication forks." J Biol Chem **277**(36): 32753-32759.

Doksani, Y., R. Bermejo, S. Fiorani, J. E. Haber and M. Foiani (2009). "Replicon dynamics, dormant origin firing, and terminal fork integrity after double-strand break formation." Cell **137**(2): 247-258.

Dubey, D. D., S. M. Kim, I. T. Todorov and J. A. Huberman (1996). "Large, complex modular structure of a fission yeast DNA replication origin." Curr Biol **6**(4): 467-473.

Dutta, A. and S. P. Bell (1997). "Initiation of DNA replication in eukaryotic cells." Annu Rev Cell Dev Biol **13**: 293-332.

Eid, W., M. Steger, M. El-Shemerly, L. P. Ferretti, J. Pena-Diaz, C. Konig, E. Valtorta, A. A. Sartori and S. Ferrari (2010). "DNA end resection by CtIP and exonuclease 1 prevents genomic instability." EMBO Rep **11**(12): 962-968.

Elledge, S. J. (1996). "Cell cycle checkpoints: preventing an identity crisis." Science **274**(5293): 1664-1672.

Errico, A. and V. Costanzo (2010). "Differences in the DNA replication of unicellular eukaryotes and metazoans: known unknowns." EMBO Rep **11**(4): 270-278.

Fay, D. S., Z. Sun and D. F. Stern (1997). "Mutations in SPK1/RAD53 that specifically abolish checkpoint but not growth-related functions." Curr Genet **31**(2): 97-105.

Flott, S., C. Alabert, G. W. Toh, R. Toth, N. Sugawara, D. G. Campbell, J. E. Haber, P. Pasero and J. Rouse (2007). "Phosphorylation of Slx4 by Mec1 and Tel1 regulates the single-strand annealing mode of DNA repair in budding yeast." Mol Cell Biol **27**(18): 6433-6445.

Flott, S. and J. Rouse (2005). "Slx4 becomes phosphorylated after DNA damage in a Mec1/Tel1-dependent manner and is required for repair of DNA alkylation damage." Biochem J **391**(Pt 2): 325-333.

Foiani, M., A. Pellicioli, M. Lopes, C. Lucca, M. Ferrari, G. Liberi, M. Muzi Falconi and P. Plevani (2000). "DNA damage checkpoints and DNA replication controls in Saccharomyces cerevisiae." Mutat Res **451**(1-2): 187-196.

Fricke, W. M., S. A. Bastin-Shanower and S. J. Brill (2005). "Substrate specificity of the Saccharomyces cerevisiae Mus81-Mms4 endonuclease." DNA Repair (Amst) **4**(2): 243-251.

Fricke, W. M. and S. J. Brill (2003). "Slx1-Slx4 is a second structure-specific endonuclease functionally redundant with Sgs1-Top3." Genes Dev **17**(14): 1768-1778.

Froget, B., J. Blaisonneau, S. Lambert and G. Baldacci (2008). "Cleavage of stalled forks by fission yeast Mus81/Eme1 in absence of DNA replication checkpoint." Mol Biol Cell **19**(2): 445-456.

Gietz, R. D. and R. H. Schiestl (2007). "High-efficiency yeast transformation using the LiAc/SS carrier DNA/PEG method." Nat Protoc **2**(1): 31-34.

Haber, J. E. and W. D. Heyer (2001). "The fuss about Mus81." Cell **107**(5): 551-554.

Habraken, Y., P. Sung, L. Prakash and S. Prakash (1994). "Holliday junction cleavage by yeast Rad1 protein." Nature **371**(6497): 531-534.

Hanada, K., M. Budzowska, S. L. Davies, E. van Drunen, H. Onizawa, H. B. Beverloo, A. Maas, J. Essers, I. D. Hickson and R. Kanaar (2007). "The structure-specific endonuclease Mus81 contributes to replication restart by generating double-strand DNA breaks." Nat Struct Mol Biol **14**(11): 1096-1104.

Hanada, K., M. Budzowska, M. Modesti, A. Maas, C. Wyman, J. Essers and R. Kanaar (2006). "The structure-specific endonuclease Mus81-Eme1 promotes conversion of interstrand DNA crosslinks into double-strands breaks." EMBO J **25**(20): 4921-4932.

Hartman, J. L. t. and N. P. Tippery (2004). "Systematic quantification of gene interactions by phenotypic array analysis." Genome Biol **5**(7): R49.

Hartwell, L. H. and M. B. Kastan (1994). "Cell cycle control and cancer." Science **266**(5192): 1821-1828.

Hartwell, L. H. and T. A. Weinert (1989). "Checkpoints: controls that ensure the order of cell cycle events." Science **246**(4930): 629-634.

Hashimoto, Y., A. Ray Chaudhuri, M. Lopes and V. Costanzo (2010). "Rad51 protects nascent DNA from Mre11-dependent degradation and promotes continuous DNA synthesis." Nat Struct Mol Biol **17**(11): 1305-1311.

Hu, J., L. Sun, F. Shen, Y. Chen, Y. Hua, Y. Liu, M. Zhang, Y. Hu, Q. Wang, W. Xu, F. Sun, J. Ji, J. M. Murray, A. M. Carr and D. Kong (2012). "The intra-S phase checkpoint targets Dna2 to prevent stalled replication forks from reversing." Cell **149**(6): 1221-1232.

Hubscher, U. and Y. S. Seo (2001). "Replication of the lagging strand: a concert of at least 23 polypeptides." Mol Cells **12**(2): 149-157.

Huertas, P., F. Cortes-Ledesma, A. A. Sartori, A. Aguilera and S. P. Jackson (2008). "CDK targets Sae2 to control DNA-end resection and homologous recombination." Nature **455**(7213): 689-692.

Ip, S. C., U. Rass, M. G. Blanco, H. R. Flynn, J. M. Skehel and S. C. West (2008). "Identification of Holliday junction resolvases from humans and yeast." Nature **456**(7220): 357-361.

Johnson, A. and M. O'Donnell (2005). "Cellular DNA replicases: components and dynamics at the replication fork." Annu Rev Biochem **74**: 283-315.

Kai, M., M. N. Boddy, P. Russell and T. S. Wang (2005). "Replication checkpoint kinase Cds1 regulates Mus81 to preserve genome integrity during replication stress." Genes Dev **19**(8): 919-932.

Kaliraman, V. and S. J. Brill (2002). "Role of SGS1 and SLX4 in maintaining rDNA structure in Saccharomyces cerevisiae." Curr Genet **41**(6): 389-400.

Katou, Y., Y. Kanoh, M. Bando, H. Noguchi, H. Tanaka, T. Ashikari, K. Sugimoto and K. Shirahige (2003). "S-phase checkpoint proteins Tof1 and Mrc1 form a stable replication-pausing complex." Nature **424**(6952): 1078-1083.

Kim, R. A. and J. C. Wang (1989). "Function of DNA topoisomerases as replication swivels in Saccharomyces cerevisiae." J Mol Biol **208**(2): 257-267.

Klein, H. L. (2008). "Molecular biology: DNA endgames." Nature **455**(7214): 740-741.

Kogoma, T. (1997). "Stable DNA replication: interplay between DNA replication, homologous recombination, and transcription." Microbiol Mol Biol Rev **61**(2): 212-238.

Koster, D. A., K. Palle, E. S. Bot, M. A. Bjornsti and N. H. Dekker (2007). "Antitumour drugs impede DNA uncoiling by topoisomerase I." Nature **448**(7150): 213-217.

Kraus, E., W. Y. Leung and J. E. Haber (2001). "Break-induced replication: a review and an example in budding yeast." Proc Natl Acad Sci U S A **98**(15): 8255-8262.

Krishnan, V., S. Nirantar, K. Crasta, A. Y. Cheng and U. Surana (2004). "DNA replication checkpoint prevents precocious chromosome segregation by regulating spindle behavior." Mol Cell **16**(5): 687-700.

Kumar, S. and P. M. Burgers (2013). "Lagging strand maturation factor Dna2 is a component of the replication checkpoint initiation machinery." Genes Dev **27**(3): 313-321.

Kunkel, T. A. and P. M. Burgers (2008). "Dividing the workload at a eukaryotic replication fork." Trends Cell Biol **18**(11): 521-527.

Labib, K. and G. De Piccoli (2011). "Surviving chromosome replication: the many roles of the S-phase checkpoint pathway." Philos Trans R Soc Lond B Biol Sci **366**(1584): 3554-3561.

Lambert, S., B. Froget and A. M. Carr (2007). "Arrested replication fork processing: interplay between checkpoints and recombination." DNA Repair (Amst) **6**(7): 1042-1061.

Lambert, S., K. Mizuno, J. Blaisonneau, S. Martineau, R. Chanet, K. Freon, J. M. Murray, A. M. Carr and G. Baldacci (2010). "Homologous recombination

restarts blocked replication forks at the expense of genome rearrangements by template exchange." Mol Cell **39**(3): 346-359.

Lee, S. E., A. Pellicioli, J. Demeter, M. P. Vaze, A. P. Gasch, A. Malkova, P. O. Brown, D. Botstein, T. Stearns, M. Foiani and J. E. Haber (2000). "Arrest, adaptation, and recovery following a chromosome double-strand break in Saccharomyces cerevisiae." Cold Spring Harb Symp Quant Biol **65**: 303-314.

Lengsfeld, B. M., A. J. Rattray, V. Bhaskara, R. Ghirlando and T. T. Paull (2007). "Sae2 is an endonuclease that processes hairpin DNA cooperatively with the Mre11/Rad50/Xrs2 complex." Mol Cell **28**(4): 638-651.

Liao, S., T. Toczylowski and H. Yan (2008). "Identification of the Xenopus DNA2 protein as a major nuclease for the 5'->3' strand-specific processing of DNA ends." Nucleic Acids Res **36**(19): 6091-6100.

Lisby, M., J. H. Barlow, R. C. Burgess and R. Rothstein (2004). "Choreography of the DNA damage response: spatiotemporal relationships among checkpoint and repair proteins." Cell **118**(6): 699-713.

Lisby, M., R. Rothstein and U. H. Mortensen (2001). "Rad52 forms DNA repair and recombination centers during S phase." Proc Natl Acad Sci U S A **98**(15): 8276-8282.

Liu, L. F. and J. C. Wang (1987). "Supercoiling of the DNA template during transcription." Proc Natl Acad Sci U S A **84**(20): 7024-7027.

Llorente, B., C. E. Smith and L. S. Symington (2008). "Break-induced replication: what is it and what is it for?" Cell Cycle **7**(7): 859-864.

Longhese, M. P., M. Clerici and G. Lucchini (2003). "The S-phase checkpoint and its regulation in Saccharomyces cerevisiae." Mutat Res **532**(1-2): 41-58.

Lopes, M., C. Cotta-Ramusino, G. Liberi and M. Foiani (2003). "Branch migrating sister chromatid junctions form at replication origins through Rad51/Rad52-independent mechanisms." Mol Cell **12**(6): 1499-1510.

Lopes, M., C. Cotta-Ramusino, A. Pellicioli, G. Liberi, P. Plevani, M. Muzi-Falconi, C. S. Newlon and M. Foiani (2001). "The DNA replication checkpoint response stabilizes stalled replication forks." Nature **412**(6846): 557-561.

Lucca, C., F. Vanoli, C. Cotta-Ramusino, A. Pellicioli, G. Liberi, J. Haber and M. Foiani (2004). "Checkpoint-mediated control of replisome-fork association and signalling in response to replication pausing." Oncogene **23**(6): 1206-1213.

Lydeard, J. R., Z. Lipkin-Moore, Y. J. Sheu, B. Stillman, P. M. Burgers and J. E. Haber (2010). "Break-induced replication requires all essential DNA

replication factors except those specific for pre-RC assembly." Genes Dev **24**(11): 1133-1144.

Mazon, G., E. P. Mimitou and L. S. Symington (2010). "SnapShot: Homologous recombination in DNA double-strand break repair." Cell **142**(4): 646, 646 e641.

McGlynn, P. and R. G. Lloyd (2000). "Modulation of RNA polymerase by (p)ppGpp reveals a RecG-dependent mechanism for replication fork progression." Cell **101**(1): 35-45.

McGlynn, P. and R. G. Lloyd (2002). "Recombinational repair and restart of damaged replication forks." Nat Rev Mol Cell Biol **3**(11): 859-870.

Merrill, B. J. and C. Holm (1998). "The RAD52 recombinational repair pathway is essential in pol30 (PCNA) mutants that accumulate small single-stranded DNA fragments during DNA synthesis." Genetics **148**(2): 611-624.

Michel, B., H. Boubakri, Z. Baharoglu, M. LeMasson and R. Lestini (2007). "Recombination proteins and rescue of arrested replication forks." DNA Repair (Amst) **6**(7): 967-980.

Michel, B., G. Grompone, M. J. Flores and V. Bidnenko (2004). "Multiple pathways process stalled replication forks." Proc Natl Acad Sci U S A **101**(35): 12783-12788.

Mimitou, E. P. and L. S. Symington (2008). "Sae2, Exo1 and Sgs1 collaborate in DNA double-strand break processing." Nature **455**(7214): 770-774.

Mimitou, E. P. and L. S. Symington (2009). "DNA end resection: many nucleases make light work." DNA Repair (Amst) **8**(9): 983-995.

Mimura, S. and H. Takisawa (1998). "Xenopus Cdc45-dependent loading of DNA polymerase alpha onto chromatin under the control of S-phase Cdk." EMBO J **17**(19): 5699-5707.

Moore, D. M., J. Karlin, S. Gonzalez-Barrera, A. Mardiros, M. Lisby, A. Doughty, J. Gilley, R. Rothstein, E. C. Friedberg and P. L. Fischhaber (2009). "Rad10 exhibits lesion-dependent genetic requirements for recruitment to DNA double-strand breaks in Saccharomyces cerevisiae." Nucleic Acids Res **37**(19): 6429-6438.

Morin, I., H. P. Ngo, A. Greenall, M. K. Zubko, N. Morrice and D. Lydall (2008). "Checkpoint-dependent phosphorylation of Exo1 modulates the DNA damage response." EMBO J **27**(18): 2400-2410.

Myung, K. and R. D. Kolodner (2002). "Suppression of genome instability by redundant S-phase checkpoint pathways in Saccharomyces cerevisiae." Proc Natl Acad Sci U S A **99**(7): 4500-4507.

Neelsen, K. J., I. M. Zanini, R. Herrador and M. Lopes (2013). "Oncogenes induce genotoxic stress by mitotic processing of unusual replication intermediates." J Cell Biol **200**(6): 699-708.

Nicolette, M. L., K. Lee, Z. Guo, M. Rani, J. M. Chow, S. E. Lee and T. T. Paull (2010). "Mre11-Rad50-Xrs2 and Sae2 promote 5' strand resection of DNA double-strand breaks." Nat Struct Mol Biol **17**(12): 1478-1485.

Nitiss, J. L. (1998). "Investigating the biological functions of DNA topoisomerases in eukaryotic cells." Biochim Biophys Acta **1400**(1-3): 63-81.

Osman, F. and M. C. Whitby (2007). "Exploring the roles of Mus81-Eme1/Mms4 at perturbed replication forks." DNA Repair (Amst) **6**(7): 1004-1017.

Paques, F. and J. E. Haber (1999). "Multiple pathways of recombination induced by double-strand breaks in Saccharomyces cerevisiae." Microbiol Mol Biol Rev **63**(2): 349-404.

Paulovich, A. G. and L. H. Hartwell (1995). "A checkpoint regulates the rate of progression through S phase in S. cerevisiae in response to DNA damage." Cell **82**(5): 841-847.

Pellicioli, A. and M. Foiani (2005). "Signal transduction: how rad53 kinase is activated." Curr Biol **15**(18): R769-771.

Peng, G., H. Dai, W. Zhang, H. J. Hsieh, M. R. Pan, Y. Y. Park, R. Y. Tsai, I. Bedrosian, J. S. Lee, G. Ira and S. Y. Lin (2012). "Human nuclease/helicase DNA2 alleviates replication stress by promoting DNA end resection." Cancer Res **72**(11): 2802-2813.

Perego, P., G. S. Jimenez, L. Gatti, S. B. Howell and F. Zunino (2000). "Yeast mutants as a model system for identification of determinants of chemosensitivity." Pharmacol Rev **52**(4): 477-492.

Petermann, E., M. L. Orta, N. Issaeva, N. Schultz and T. Helleday (2010). "Hydroxyurea-stalled replication forks become progressively inactivated and require two different RAD51-mediated pathways for restart and repair." Mol Cell **37**(4): 492-502.

Pike, B. L., S. Yongkiettrakul, M. D. Tsai and J. Heierhorst (2003). "Diverse but overlapping functions of the two forkhead-associated (FHA) domains in Rad53 checkpoint kinase activation." J Biol Chem **278**(33): 30421-30424.

Postow, L., N. J. Crisona, B. J. Peter, C. D. Hardy and N. R. Cozzarelli (2001). "Topological challenges to DNA replication: conformations at the fork." Proc Natl Acad Sci U S A **98**(15): 8219-8226.

Postow, L., C. Ullsperger, R. W. Keller, C. Bustamante, A. V. Vologodskii and N. R. Cozzarelli (2001). "Positive torsional strain causes the formation of a four-way junction at replication forks." J Biol Chem **276**(4): 2790-2796.

Putnam, C. D., E. J. Jaehnig and R. D. Kolodner (2009). "Perspectives on the DNA damage and replication checkpoint responses in Saccharomyces cerevisiae." DNA Repair (Amst) **8**(9): 974-982.

Raghuraman, M. K., E. A. Winzeler, D. Collingwood, S. Hunt, L. Wodicka, A. Conway, D. J. Lockhart, R. W. Davis, B. J. Brewer and W. L. Fangman (2001). "Replication dynamics of the yeast genome." Science **294**(5540): 115-121.

Ray Chaudhuri, A., Y. Hashimoto, R. Herrador, K. J. Neelsen, D. Fachinetti, R. Bermejo, A. Cocito, V. Costanzo and M. Lopes (2012). "Topoisomerase I poisoning results in PARP-mediated replication fork reversal." Nat Struct Mol Biol **19**(4): 417-423.

Roca, J., J. M. Berger, S. C. Harrison and J. C. Wang (1996). "DNA transport by a type II topoisomerase: direct evidence for a two-gate mechanism." Proc Natl Acad Sci U S A **93**(9): 4057-4062.

Rouse, J. (2009). "Control of genome stability by SLX protein complexes." Biochem Soc Trans **37**(Pt 3): 495-510.

Sandler, S. J. and K. J. Marians (2000). "Role of PriA in replication fork reactivation in Escherichia coli." J Bacteriol **182**(1): 9-13.

Santocanale, C. and J. F. Diffley (1996). "ORC- and Cdc6-dependent complexes at active and inactive chromosomal replication origins in Saccharomyces cerevisiae." EMBO J **15**(23): 6671-6679.

Santocanale, C. and J. F. Diffley (1997). "Genomic footprinting of budding yeast replication origins during the cell cycle." Methods Enzymol **283**: 377-390.

Santocanale, C., K. Sharma and J. F. Diffley (1999). "Activation of dormant origins of DNA replication in budding yeast." Genes Dev **13**(18): 2360-2364.

Schlacher, K., N. Christ, N. Siaud, A. Egashira, H. Wu and M. Jasin (2011). "Double-strand break repair-independent role for BRCA2 in blocking stalled replication fork degradation by MRE11." Cell **145**(4): 529-542.

Schwartz, E. K. and W. D. Heyer (2011). "Processing of joint molecule intermediates by structure-selective endonucleases during homologous recombination in eukaryotes." Chromosoma **120**(2): 109-127.

Segurado, M. and J. F. Diffley (2008). "Separate roles for the DNA damage checkpoint protein kinases in stabilizing DNA replication forks." Genes Dev **22**(13): 1816-1827.

Segurado, M. and J. A. Tercero (2009). "The S-phase checkpoint: targeting the replication fork." Biol Cell **101**(11): 617-627.

Shim, E. Y., W. H. Chung, M. L. Nicolette, Y. Zhang, M. Davis, Z. Zhu, T. T. Paull, G. Ira and S. E. Lee (2010). "Saccharomyces cerevisiae Mre11/Rad50/Xrs2 and Ku proteins regulate association of Exo1 and Dna2 with DNA breaks." EMBO J **29**(19): 3370-3380.

Sirbu, B. M., F. B. Couch, J. T. Feigerle, S. Bhaskara, S. W. Hiebert and D. Cortez (2011). "Analysis of protein dynamics at active, stalled, and collapsed replication forks." Genes Dev **25**(12): 1320-1327.

Smith, S., J. Y. Hwang, S. Banerjee, A. Majeed, A. Gupta and K. Myung (2004). "Mutator genes for suppression of gross chromosomal rearrangements identified by a genome-wide screening in Saccharomyces cerevisiae." Proc Natl Acad Sci U S A **101**(24): 9039-9044.

Smolka, M. B., C. P. Albuquerque, S. H. Chen and H. Zhou (2007). "Proteome-wide identification of in vivo targets of DNA damage checkpoint kinases." Proc Natl Acad Sci U S A **104**(25): 10364-10369.

Sogo, J. M., M. Lopes and M. Foiani (2002). "Fork reversal and ssDNA accumulation at stalled replication forks owing to checkpoint defects." Science **297**(5581): 599-602.

Stewart, L., M. R. Redinbo, X. Qiu, W. G. Hol and J. J. Champoux (1998). "A model for the mechanism of human topoisomerase I." Science **279**(5356): 1534-1541.

Sun, X., D. Thrower, J. Qiu, P. Wu, L. Zheng, M. Zhou, J. Bachant, D. M. Wilson, 3rd and B. Shen (2003). "Complementary functions of the Saccharomyces cerevisiae Rad2 family nucleases in Okazaki fragment

maturation, mutation avoidance, and chromosome stability." DNA Repair (Amst) **2**(8): 925-940.

Symington, L. S. (1998). "Homologous recombination is required for the viability of rad27 mutants." Nucleic Acids Res **26**(24): 5589-5595.

Symington, L. S. and J. Gautier (2011). "Double-strand break end resection and repair pathway choice." Annu Rev Genet **45**: 247-271.

Tay, Y. D. and L. Wu (2010). "Overlapping roles for Yen1 and Mus81 in cellular Holliday junction processing." J Biol Chem **285**(15): 11427-11432.

Tercero, J. A. and J. F. Diffley (2001). "Regulation of DNA replication fork progression through damaged DNA by the Mec1/Rad53 checkpoint." Nature **412**(6846): 553-557.

Tercero, J. A., M. P. Longhese and J. F. Diffley (2003). "A central role for DNA replication forks in checkpoint activation and response." Mol Cell **11**(5): 1323-1336.

Thomas, B. J. and R. Rothstein (1989). "Elevated recombination rates in transcriptionally active DNA." Cell **56**(4): 619-630.

Toh, G. W., N. Sugawara, J. Dong, R. Toth, S. E. Lee, J. E. Haber and J. Rouse (2010). "Mec1/Tel1-dependent phosphorylation of Slx4 stimulates Rad1-Rad10-dependent cleavage of non-homologous DNA tails." DNA Repair (Amst) **9**(6): 718-726.

Trenz, K., E. Smith, S. Smith and V. Costanzo (2006). "ATM and ATR promote Mre11 dependent restart of collapsed replication forks and prevent accumulation of DNA breaks." EMBO J **25**(8): 1764-1774.

Tse, Y. and J. C. Wang (1980). "E. coli and M. luteus DNA topoisomerase I can catalyze catenation of decatenation of double-stranded DNA rings." Cell **22**(1 Pt 1): 269-276.

Wach, A., A. Brachat, R. Pohlmann and P. Philippsen (1994). "New heterologous modules for classical or PCR-based gene disruptions in Saccharomyces cerevisiae." Yeast **10**(13): 1793-1808.

Wang, J. C. (1996). "DNA topoisomerases." Annu Rev Biochem **65**: 635-692.

Wang, J. C. (2002). "Cellular roles of DNA topoisomerases: a molecular perspective." Nat Rev Mol Cell Biol **3**(6): 430-440.

Wawrousek, K. E., B. K. Fortini, P. Polaczek, L. Chen, Q. Liu, W. G. Dunphy and J. L. Campbell (2010). "Xenopus DNA2 is a helicase/nuclease that is

found in complexes with replication proteins And-1/Ctf4 and Mcm10 and DSB response proteins Nbs1 and ATM." Cell Cycle **9**(6): 1156-1166.

Wechsler, T., S. Newman and S. C. West (2011). "Aberrant chromosome morphology in human cells defective for Holliday junction resolution." Nature **471**(7340): 642-646.

Wellinger, R. E. and J. M. Sogo (1998). "In vivo mapping of nucleosomes using psoralen-DNA crosslinking and primer extension." Nucleic Acids Res **26**(6): 1544-1545.

West, S. C. (2003). "Molecular views of recombination proteins and their control." Nat Rev Mol Cell Biol **4**(6): 435-445.

Whitby, M. C., F. Osman and J. Dixon (2003). "Cleavage of model replication forks by fission yeast Mus81-Eme1 and budding yeast Mus81-Mms4." J Biol Chem **278**(9): 6928-6935.

Yao, N. Y. and M. O'Donnell (2010). "SnapShot: The replisome." Cell **141**(6): 1088, 1088 e1081.

Zhao, X., A. Chabes, V. Domkin, L. Thelander and R. Rothstein (2001). "The ribonucleotide reductase inhibitor Sml1 is a new target of the Mec1/Rad53 kinase cascade during growth and in response to DNA damage." EMBO J **20**(13): 3544-3553.

Zhu, Z., W. H. Chung, E. Y. Shim, S. E. Lee and G. Ira (2008). "Sgs1 helicase and two nucleases Dna2 and Exo1 resect DNA double-strand break ends." Cell **134**(6): 981-994.

Zou, L. and S. J. Elledge (2003). "Sensing DNA damage through ATRIP recognition of RPA-ssDNA complexes." Science **300**(5625): 1542-1548.

Zou, L. and B. Stillman (1998). "Formation of a preinitiation complex by S-phase cyclin CDK-dependent loading of Cdc45p onto chromatin." Science **280**(5363): 593-596.

ACKNOLEDGMENTS

Approaching the end of my PhD, I realised that the people I need to acknowledge are really too many!!!!

First of all, I would like to thank my boss, Marco Foiani, for the opportunity he gave me to do this PhD.

I thank my supervisor, Rodrigo Bermejo Moreno, for having been my scientific guide during those years.

I thank Thelma Capra and Camilla Frattini, not only for being great colleagues, but also wonderful friends.

I thank Mong Sing Lai for sharing part of her project with me.

I thank Daniele Piccini and Walter Carotenuto for the technical support and for sharing ideas in the everyday lab life.

I thank all the lab members for having supported me especially in the last two years, inside and outside the lab. This PhD was not only a scientific experience, but also a human experience and for that I am grateful to all the lab members.

I am grateful to the girls, Elisa, Giulia Saredi, Giulia Bastianello, Stefania, Marta, Arta, Silvia and Donika, Gadheer, Joanna, Chiara, Sophie, Mary, Anna and to the guys Giordano, Amit, Michele, Yatish and Pawan for all the help and the great memories together (dancing nights, wonderful retreats .....).

I thank all my family and friends outside the lab for the everyday support and comprehension.

Finally, I thank my internal and external supervisors, Dr. Dana Branzei and Professor Rouse, and my examiners for the time they spend in correcting and reading my work.